

Fall 12-29-2015

Debris Flow Susceptibility Map for Mount Rainier, Washington Based on Debris Flow Initiation Zone Characteristics from the November, 2006 Climate Event in the Cascade Mountains

Kassandra Lindsey
Portland State University

Follow this and additional works at: https://pdxscholar.library.pdx.edu/open_access_etds



Part of the [Geology Commons](#), and the [Geomorphology Commons](#)

Let us know how access to this document benefits you.

Recommended Citation

Lindsey, Kassandra, "Debris Flow Susceptibility Map for Mount Rainier, Washington Based on Debris Flow Initiation Zone Characteristics from the November, 2006 Climate Event in the Cascade Mountains" (2015). *Dissertations and Theses*. Paper 2654.
<https://doi.org/10.15760/etd.2650>

This Thesis is brought to you for free and open access. It has been accepted for inclusion in Dissertations and Theses by an authorized administrator of PDXScholar. Please contact us if we can make this document more accessible: pdxscholar@pdx.edu.

Debris Flow Susceptibility Map for Mount Rainier, Washington Based on Debris Flow
Initiation Zone Characteristics from the November, 2006 Climate Event in the Cascade
Mountains

by

Kassandra Lindsey

A thesis submitted in partial fulfillment of the
requirements for the degree of

Master of Science
in
Geology

Thesis Committee:
Scott Burns, Chair
Andrew Fountain
Paul Kennard
Thomas Pierson

Portland State University
2015

Abstract

In November 2006 a Pineapple Express rainstorm moved through the Pacific Northwest generating record precipitation, 22 to 50 cm in the two-day event on Mt. Rainier. Copeland (2009) and Legg (2013) identified debris flows in seven drainages in 2006; Inter Fork, Kautz, Ohanapecosh, Pyramid, Tahoma, Van Trump, and West Fork of the White River. This study identified seven more drainages: Carbon, Fryingpan, Muddy Fork Cowlitz, North Puyallup, South Mowich, South Puyallup, and White Rivers. Twenty-nine characteristics, or attributes, associated with the drainages around the mountain were collected. Thirteen were used in a regression analysis in order to develop a susceptibility map for debris flows on Mt. Rainier: Percent vegetation, percent steep slopes, gradient, Melton's Ruggedness Number, height, area, percent bedrock, percent surficial, percent glacier, stream has direct connection with a glacier, average annual precipitation, event precipitation, and peak precipitation. All variables used in the regression were measured in the upper basin. Two models, both with 91% accuracy, were generated for the mountain. Model 1 determined gradient of the upper basin, upper basin area, and percent bedrock to be the most significant variables. This model predicted 10 drainages with high potential for failure: Carbon, Fryingpan, Kautz, Nisqually, North Mowich, South Mowich, South Puyallup, Tahoma, West Fork of the White, and White Rivers. Of the remaining drainages 5 are moderate, 10 are low, and 9 are very low. Model 2 found MRN (Melton's Ruggedness Number) and percent bedrock to be the most significant. This model predicted 10 drainages with high potential for failure during future similar events: Fryingpan, Kautz, Nisqually, North Mowich, Pyramid, South

Mowich, South Puyallup, Tahoma, Van Trump, and White Rivers. Of the remaining drainages, 6 are moderate, 9 are low, and 9 are very low. The two models are very similar. Initiation site elevations range from 1442 m to 2448 m. Six of the thirteen initiation sites are above 2000 m. Proglacial gully erosion initiated debris flows seem to occur at all elevations. Those debris flows initiated partially by landslides occur between 1400 and about 1800 m. The combined regression analysis model for the Mt. Rainier, Mt. St. Helens, Mt. Hood, and Mt. Adams raised the predictive accuracy from 69% (Olson, 2012) to 77%. This model determined that percent glacier/ice and percent vegetation were the most significant.

Acknowledgements

The first people I would like to acknowledge and thank are the members of my committee. Dr. Burns has always encouraged me to be the best student and scientist I can be. Without his excellent guidance I would not have been able to do this. Paul Kennard has also been a huge help for my thesis research and has always tried to help me in any way he can. Andrew Fountain and Tom Pierson have also been huge helps along the way, and I appreciate their guidance and contribution to my education.

I would like to thank my field hands, Bryant Ruiz, Heather Hurtado, and Hilary Whitney for keeping me company in the field and helping me hike around the mountain to collect evidence for my thesis. Also a big thank you to my father for lending his help during my more remote trips to the west side of the mountain and offering his equipment for my use.

My family has been a huge support mechanism for this process. Thanks to Adrienne and Jeff for letting me live with them to save money. Thanks to my mom and dad and grandparents for their continued support as well. Also, thanks to my fellow graduate students and friends that I have made while living and working in Portland. With their help and friendship this would have been a much more difficult experience. Thanks to Gabriela Ferreira, Kat Barnard, Kelly Hughes, Joshua Hurtado, Liam Hurtado, Adam Large, and Emily Jenkins for their continued support and encouragement.

Table of Contents

Abstract	i
Acknowledgements	iii
List of Figures	viii
List of Tables	xvii
Chapter 1: Introduction	1
1.1 Aims and Objectives	3
Chapter 2: Background	4
2.1 Geology	4
2.2 Glaciation	4
2.3 Debris Flows	6
2.4 Debris Flows and Lahars on Mt. Rainier	8
2.5 Climate	9
2.6 November 2006 Pineapple Express Storm	9
2.7 Past Work	10
Chapter 3: Methods	12
3.1 Field Reconnaissance	12
3.2 Drainage Basin Attributes	12
3.3 Data Analysis	20
Chapter 4: Results	22
4.1 Basalt Drainage Basin	23
4.2 Boulder Drainage Basin	25
4.3 Carbon Drainage Basin	27

4.4 Cataract and Marmot Drainage Basin.....	30
4.5 Crater Drainage Basin.....	33
4.6 Fish Drainage Basin.....	35
4.7 Fryingpan Drainage Basin	37
4.8 Grant and Spray Drainage Basin.....	43
4.9 Inter Fork Drainage Basin.....	45
4.10 Kautz Drainage Basin	48
4.11 Lee Drainage Basin.....	50
4.12 Lodi Drainage Basin	52
4.13 Muddy Fork Cowlitz Drainage Basin.....	55
4.14 Nisqually Drainage Basin	59
4.15 North Mowich Drainage Basin	62
4.16 North Puyallup Drainage Basin	65
4.17 Ohanapecosh Drainage Basin	70
4.18 Paradise Drainage Basin	72
4.19 Pyramid Drainage Basin	74
4.20 Rushing Water Drainage Basin.....	76
4.21 South Mowich Drainage Basin	79
4.22 South Puyallup Drainage Basin	84
4.23 St. Andrews Drainage Basin.....	89
4.24 Stevens Drainage Basin	92
4.25 Sunbeam Drainage Basin.....	95

4.26 Swift Drainage Basin	97
4.27 Tahoma Drainage Basin.....	100
4.28 Tatoosh Drainage Basin.....	102
4.29 Unicorn Drainage Basin.....	104
4.30 Van Trump Drainage Basin	107
4.31 West Fork of the White Drainage Basin	109
4.32 White Drainage Basin.....	110
4.33 Williwakas Drainage Basin.....	114
4.34 Wright Drainage Basin	117
Summary	119
Chapter 5: Statistics	120
5.1 ANOVA	120
5.2 Mt. Rainier Multiple Regression.....	121
5.3 Model 1	122
5.4 Model 2	123
5.5 Mt. Hood Comparison	125
5.6 Combined Multiple Regression	126
5.6 Limitations, Assumptions, and Sources of Error	128
5.7 Summary.....	129
Chapter 6: Discussion	131
6.1 Attributes.....	131
6.2 Storm Event	131

6.3 MRN	133
6.4 Initiation Sites	133
6.5 Statistical Analysis.....	134
6.6 Glaciers	136
6.7 Susceptibility Map	137
Chapter 7: Conclusions	141
Chapter 8: Future Work	145
References.....	146
Appendix A: Drainage Basin Data	152
Appendix B: ANOVA Results.....	162
Appendix C: Regression Data.....	169
Appendix D: Combined Regression Data.....	177

List of Figures

Figure 1. Major Cascade Range volcanoes (Topinka, 1997).....	2
Figure 2. Map of the glaciers on Mt. Rainier used in this study.....	5
Figure 3. NOAA figure of a typical Pineapple Express system.	10
Figure 4. Map of Mt. Rainier and the 34 drainages examined in this study. Basins are outlined in black, upper basins in dashed black, glaciers in blue, and initiation sites from Copeland (2009) in purple, Legg (2013) in blue, and this study in orange.	22
Figure 5. Basalt Creek Basin outlined in yellow, other basins outlined in black, the upper basin outlined in dashed black, glaciers in blue, and initiation sites from Copeland (2009) in purple, Legg (2013) in blue, and this study in orange. No 2006 debris flow was recorded in this basin.	23
Figure 6. a) Google Earth image of Basalt Creek Drainage in August 2006. b) Google Earth image of Basalt Creek Drainage in September 2009.	24
Figure 7. Boulder Creek basin outlined in yellow, other basins outlined in black, the upper basin outlined in dashed black, glaciers in blue, and initiation sites from Copeland (2009) in purple, Legg (2013) in blue, and this study in orange. No debris flow was recorded in this drainage.	26
Figure 8. a) Google Earth image of Boulder Drainage in August 2006. b) Google Earth image of Boulder Drainage in September 2009.....	27
Figure 9. Carbon River Basin outlined in yellow, other basins outlined in black, the upper basin outlined in dashed black, glaciers in blue, and initiation sites from Copeland (2009) in purple, Legg (2013) in blue, and this study in orange.	28

Figure 10. a) Carbon initiation in 2006.....	29
Figure 11. Cataract and Marmot creek basins outlined in yellow, other basins outlined in black, the upper basin outlined in dashed black, glaciers in blue, and initiation sites from Copeland (2009) in purple, Legg (2013) in blue, and this study in orange. No debris flow was recorded in this basin.....	31
Figure 12. a) Google Earth image of Cataract and Marmot Creek Drainage in August 2006. b) Google Earth image of Cataract and Marmot Creek Drainage in September 2009.....	32
Figure 13. Crater Creek basin outlined in yellow, other basins outlined in black.....	33
Figure 14. a) Google Earth image of Crater Drainage in August 2006. b) Google Earth image of Crater Drainage in September 2009.....	34
Figure 15. Fish Creek basin outlined in yellow, other basins outlined in black.....	36
Figure 16. a) Google Earth image of Fish Drainage in August 2006. b) Google Earth image of Fish Drainage in September 2009.....	37
Figure 17. Fryingpan River basin outlined in yellow, other basins outlined in black, the upper basin outlined in dashed black, glaciers in blue, and initiation sites from Copeland (2009) in purple, Legg (2013) in blue, and this study in orange.....	38
Figure 18. Photographic evidence for Fryingpan.....	39
Figure 19. a) 2006 channel margin. b) Channel margin in 2008. Orange point is the location at which Figure 20 was captured.....	40
Figure 20. a) Dark blue indicates where the channel margin existed in 2006.....	41

Figure 21. Grant and Spray creek basins outlined in yellow, other basins outlined in black, the upper basin outlined in dashed black, glaciers in blue, and initiation sites from Copeland (2009) in purple, Legg (2013) in blue, and this study in orange. No debris flow occurred in this drainage basin.	43
Figure 22. a) Google Earth image of Grant and Spray Drainage in August 2006. b) Google Earth image of Grant and Spray Drainage in September 2009.....	44
Figure 23. Inter Fork River basin outlined in yellow, other basins outlined in black, the upper basin outlined in dashed black, glaciers in blue, and initiation sites from Copeland (2009) in purple, Legg (2013) in blue, and this study in orange.	46
Figure 24. a) Photograph of boulders and mud deposited by the debris flow that buried trees in the upper basin. b) Major erosion in the drainage due to the 2006 event.	47
Figure 25. Kautz Creek basin outlined in yellow, other basins outlined in black, the upper basin outlined in dashed black, glaciers in blue, and initiation sites from Copeland (2009) in purple, Legg (2013) in blue, and this study in orange.	49
Figure 26. Lee Creek basin outlined in yellow, other basins outlined in black.....	51
Figure 27. a) Google Earth image of Lee Drainage in August 2006. b) Google Earth image of Lee Drainage in September 2009.....	52
Figure 28. Lodi Creek basin outlined in yellow, other basins outlined in black.	53
Figure 29. a) Google Earth image of Lodi Drainage in August 2006. b) Google Earth image of Lodi Drainage in September 2009.	54
Figure 30. Muddy Fork Cowlitz basin outlined in yellow, other basins outlined in black, the upper basin outlined in dashed black, glaciers in blue.....	55

Figure 31. a) Initiation site in 2006. b) Initiation site in 2008 along the sidewall of the upper drainage of Muddy Fork Cowlitz River. This was chosen as the initiation site for this drainage. 57

Figure 32. a) Muddy Fork Cowlitz channel in 2006 (blue). b) Muddy Fork Cowlitz channel erosion in the upper channel between 2006 (blue outline) and 2008 (red outline) assumed to be caused by 2006 event. 58

Figure 33. Nisqually Basin outlined in yellow, other basins outlined in black, the upper basin outlined in dashed black, glaciers in blue, and initiation sites from Copeland (2009) in purple, Legg (2013) in blue, and this study in orange. No debris flow occurred in this drainage basin. 60

Figure 34. a) Google Earth image of Lodi Drainage in August 2006. b) Google Earth image of the drainage in September 2009..... 61

Figure 35. North Mowich basin outlined in yellow, other basins outlined in black, the upper basin outlined in dashed black, glaciers in blue, and initiation sites from Copeland (2009) in purple, Legg (2013) in blue, and this study in orange. No debris flow was recorded in this drainage basin. 63

Figure 36. a) Google Earth image of the drainage in August 2006.b) Google Earth image of the drainage in September 2009. 64

Figure 37. North Puyallup basin outlined in yellow, other basins outlined in black, the upper basin outlined in dashed black, glaciers in blue, and initiation sites from Copeland (2009) in purple, Legg (2013) in blue, and this study in orange. 66

Figure 38. a) Google Earth image of the drainage in August 2006. b) Google Earth image of the drainage in September 2009. 67

Figure 39. Both photos are evidence of debris flow levee(s) and new vegetation growth in the upper North Puyallup basin provided by Paul Kennard, Mt. Rainier National Park Geomorphologist..... 68

Figure 40. a) Initiation site in 2008 indicated by blue dot inside of box. b) Initiation site in 2008 indicated by blue dot..... 69

Figure 41. Ohanapecosh River basin outlined in yellow, other basins outlined in black, the upper basin outlined in dashed black, glaciers in blue, and initiation sites from Copeland (2009) in purple, Legg (2013) in blue, and this study in orange. 71

Figure 42. Paradise River basin outlined in yellow, other basins outlined in black, the upper basin outlined in dashed black, glaciers in blue, and initiation sites from Copeland (2009) in purple, Legg (2013) in blue, and this study in orange. No debris flow was recorded in this drainage in 2006. 72

Figure 43. a) Google Earth image of Paradise Drainage in August 2006. b) Google Earth image of Paradise Drainage in September 2009. 73

Figure 44. Pyramid River basin outlined in yellow, other basins outlined in black, the upper basin outlined in dashed black, glaciers in blue, and initiation sites from Copeland (2009) in purple, Legg (2013) in blue, and this study in orange. 75

Figure 45. Rushing Water Creek basin outlined in yellow, other basins outlined in black, the upper basin outlined in dashed black, glaciers in blue, and initiation sites from

Copeland (2009) in purple, Legg (2013) in blue, and this study in orange. No debris flow occurred in this drainage basin in 2006. 77

Figure 46. a) Google Earth image of Rushing Water Drainage in August 2006. b) Google Earth image of Rushing Water Drainage in September 2009..... 78

Figure 47. South Mowich River basin outlined in yellow, other basins outlined in black, the upper basin outlined in dashed black, glaciers in blue..... 79

Figure 48. a) Avulsion channel with young vegetation that likely started growing back after 2006. 80

Figure 49. a) 2006 (blue) showing major erosion in the channel margins assumed to be caused by 2006 event which contributed material to debris flow in South Mowich Drainage..... 82

Figure 50. South Puyallup River basin outlined in yellow, other basins outlined in black, the upper basin outlined in dashed black, glaciers in blue..... 84

Figure 51. Avulsion channel in lower South Puyallup channel with log and boulder jams. 86

Figure 52. a) Google Earth image of South Puyallup Drainage from 2006. 86

Figure 53. a) Imagery from 2006 (blue) and b) from 2008 (red) showing the major erosion from proglacial material with likely contributed to a debris flow, the initiation site for which is shown by the blue dot..... 88

Figure 54. St. Andrews Creek basin outlined in yellow, other basins outlined in black, the upper basin outlined in dashed black, glaciers in blue, and initiation sites from

<p>Copeland (2009) in purple, Legg (2013) in blue, and this study in orange. No debris flow occurred in 2006 in this drainage.</p>	90
<p>Figure 55. a) Google Earth image of St. Andrews Drainage in August 2006. b) Google Earth image of St. Andrews Drainage in September 2009.</p>	91
<p>Figure 56. Stevens Creek basin outlined in solid black, the upper basin outlined in dashed black, and glacier in blue.</p>	92
<p>Figure 57. a) Google Earth image of the drainage in August 2006 b) Google Earth image of the drainage in September 2009.</p>	93
<p>Figure 58. Photograph of the upper reaches of the Stevens Creek. No debris flow levees were noted and bedrock was prominent in the river channel.....</p>	94
<p>Figure 59. Sunbeam Creek basin outlined in yellow, other basins outlined in black, the upper basin outlined in dashed black, glaciers in blue, and initiation sites from Copeland (2009) in purple, Legg (2013) in blue, and this study in orange. No debris flow was recorded in 2006 in this drainage.</p>	95
<p>Figure 60. a) Google Earth image of Sunbeam Drainage in August 2006.</p>	96
<p>Figure 61. Swift Creek basin outlined in yellow, other basins outlined in black, the upper basin outlined in dashed black, glaciers in blue, and initiation sites from Copeland (2009) in purple, Legg (2013) in blue, and this study in orange. No 2006 debris flow was documented in this drainage.</p>	98
<p>Figure 62. a) Google Earth image of Swift Drainage in August 2006. b) Google Earth image of Swift Drainage in September 2009.</p>	99

Figure 63. Tahoma Creek basin outlined in yellow, other basins outlined in black, the upper basin outlined in dashed black, glaciers in blue, and initiation sites from Copeland (2009) in purple, Legg (2013) in blue, and this study in orange. 101

Figure 64. Tatoosh River basin outlined in yellow, other basins outlined in black, the upper basin outlined in dashed black, glaciers in blue..... 103

Figure 65. a) Google Earth image of Tatoosh Drainage in August 2006. 103

Figure 66. Unicorn Creek basin outlined in yellow, other basins outlined in black, the upper basin outlined in dashed black, glaciers in blue..... 105

Figure 67. a) Google Earth image Unicorn Drainage in August 2006. b) Google Earth image Unicorn Drainage in September 2009..... 106

Figure 68. Van Trump Creek basin outlined in yellow, other basins outlined in black, the upper basin outlined in dashed black, glaciers in blue, and initiation sites from Copeland (2009) in purple, Legg (2013) in blue, and this study in orange. 107

Figure 69. West Fork of the White River basin outlined in yellow, other basins outlined in black, the upper basin outlined in dashed black, glaciers in blue, and initiation sites from Copeland (2009) in purple, Legg (2013) in blue, and this study in orange. 109

Figure 70. White River basin outlined in yellow, other basins outlined in black, the upper basin outlined in dashed black, glaciers in blue, and initiation sites from Copeland (2009) in purple, Legg (2013) in blue, and this study in orange. 111

Figure 71. Small levee just below the western edge of the glacier..... 112

Figure 72. a) Imagery from 2006 showing outlines of channel margins in 2006 (blue). b) Imagery from 2008 (red) showing the major erosion from proglacial material with

likely contributed to a debris flow, the initiation site for which is shown by the blue dot.	113
Figure 73. Williwakas Creek basin outlined in yellow, other basins outlined in black, the upper basin outlined in dashed black, glaciers in blue, and initiation sites from Copeland (2009) in purple, Legg (2013) in blue, and this study in orange. No 2006 debris flow was documented in this drainage basin.....	115
Figure 74. a) Google Earth image of Williwakas Drainage in August 2006. b) Google Earth image of Williwakas Drainage in September 2009.....	116
Figure 75. Wright Creek basin outlined in yellow, other basins outlined in black, the upper basin outlined in dashed black, glaciers in blue, and initiation sites from Copeland (2009) in purple, Legg (2013) in blue, and this study in orange. No 2006 debris flow was recorded in this drainage.....	117
Figure 76. a) Google Earth image of Wright Drainage in August 2006. b) Google Earth image of Wright Drainage in September 2009.	118
Figure 77. Colored drainages are drainages that experienced debris flows in 2006. Seven were added by this study and are shown in red. Initiation zones are shown in green.	132
Figure 78. Susceptibility map for drainages on Mt. Rainier based on Model 1 results..	138
Figure 79. Susceptibility map for drainages on Mt. Rainier based on Model 2 results..	139

List of Tables

Table 1. The drainage basin attributes that were used for the regression analysis. Those highlighted were swapped depending on the combination since they could not be run through the regression together.....	121
Table 2. Results of Model 1. The bolded drainages and Y values are drainages that experienced a debris flow. Inter Fork, Nisqually, and North Mowich are highlighted because they were run as "no" but were predicted to have a debris flow.	122
Table 3. Results of Model 2. The bold are the drainages that experienced a debris flow. Basalt, Nisqually, and North Mowich are highlighted because they were run as "no" but were predicted to have a debris flow.	124
Table 4. Drainages that experienced debris flows on Mt. Hood are bolded. A Y above 0.50 indicates a debris flow occurred.	125
Table 5. Drainages that experienced debris flows on Mt. Hood are bolded. A Y above 0.50 indicates a debris flow occurred.	126
Table 6. Basin attributes that were used in the combined multiple regression analysis of Mt. Hood, Mt. Adams, Mt. St. Helens, and Mt. Rainier.....	126
Table 7. Combined regression results from each previous study and this one. The accuracy of each model was reduced from each previous study until this study, where the results increased the accuracy from 69% to 77%.	127
Table 8. Difference between models.	140

Chapter 1: Introduction

Debris flow hazards are a major concern in regions with steeply sloped mountains and volcanoes. Debris flows are channelized slurries of water and volcanic sediment debris that are extremely destructive (Brantley and Power, 1985; Tilling et al., 1990). They can travel over 80 km down drainages commonly reaching speeds between 30 -70 km hr⁻¹ (Myers and Brantley, 1995). Cascade Range volcanoes have proven to be a source of numerous, large debris flows, or lahars, in the past.

Mount Rainier is one of the most well-known stratovolcanoes in the Cascade Range, standing at 4,392 m (14,410 ft) and located southeast of the Seattle metropolitan area (Figure 1). It is particularly dangerous because numerous, large volume lahar deposits are mapped in populated areas. Since events of large magnitude have occurred in the past, there is a possibility for such events to occur in the future. One of the largest lahars in the world was generated at Mt. Rainier. The Osceola Mudflow began as a series of avalanches from the summit and encompassed 3.8 km³ of material which spread over 200 km² of the Puget Sound lowland and into the Puget Sound about 5,600 years ago (Vallance and Scott, 1997). Many other debris and mudflows have occurred since then, some related to volcanic processes and some not, including the well-known Electron, Paradise, Round Pass, and National lahars (Crandell, 1971; Scott and Vallance, 1995; Vallance and Scott, 1997).

In November, 2006 a “Pineapple Express” in the Pacific Northwest dropping record amounts of rain. This system is produced when a jet stream drives a warm moisture plume generated in the eastern Pacific onto the western coast of North America

and into the Cascade Range (NOAA, 2005; Gottschalk et al., 2005). High snow pack can act as a barrier to gully initiated debris flows as the snow will absorb the rainfall. Low snow pack will melt with warm rainfall and increase runoff. Increased precipitation and lack of snow cover to absorb the rain in the Cascades initiated debris flows on at least five volcanoes in 2006: Mount Jefferson (Sobieszczyk et al., 2009), Mount St. Helens (Olson, 2012), Mount Rainier (Copeland, 2009; Legg, 2013), Mount Adams (Williams, 2011), and Mount Hood (Piro, 2010). Studies done by Piro (2010), Williams (2011), and Olson (2012) developed methodologies to determine which drainages are most susceptible to debris flows and develop potential forecasting methods. Copeland (2009) and Legg (2013) looked specifically at recent debris flow history on Mt. Rainier and potential forecasting methods.



Figure 1. Major Cascade Range volcanoes (Topinka, 1997).

1.1 Aims and Objectives

My objective is to combine the methodologies from Pirot (2010), Williams (2011), and Olson (2012) and their findings to develop a susceptibility map for debris flows on Mt. Rainier, initiated by rainstorm events like the 2006 event. There are three major aims for this study:

1. Define major non debris flow and debris flow generating drainages surrounding Mt. Rainier and collect attributes related to glacier coverage, geology, rainfall, vegetation, topography, and debris flows to describe each drainage.
2. Identify which drainage basin attributes are the most significant to debris flow initiation using a regression analysis, test the results against what actually occurred in 2006 to identify accuracy of the model, and use the resulting model to develop a susceptibility map for similar future rainstorm events on Mt. Rainier.

Combine the attributes from this study and those from Pirot (2010), Williams (2011), and Olson (2012), perform a regression analysis on the data and develop a model for these four Cascade Range volcanoes.

Chapter 2: Background

2.1 Geology

There are at least four major formations that help illustrate the history of Mt. Rainier (Sisson and Vallance, 2011; Fiske et al., 1963): About 36 to 28 million years ago, 3,050 m thick andesitic breccias and rock of the Ohanapecosh Formation. The next youngest rock is about 26 million years old, 915 m thick rhyodacite ash flow system of the Stevens Ridge Formation. The second youngest formations are about 26 to 22 million years old, 1520 m thick andesitic and basaltic rocks of the Fifes Peak Formation. The youngest rocks are the 18 to 14 million year old granodiorite Tatoosh Pluton.

Around 10 to 12 million years ago, subduction of the Juan de Fuca plate along the western margin of North America started to build the Cascade Range. There have been multiple growing stages of the Mount Rainier cone; the ancestral growth period occurred between 2 to 1 million years ago with the most recent growing period starting about 500,000 years ago.

There are 26 named glaciers on the flanks of Mount Rainier (Figure 2). Due to advance and recession of glaciers on the mountain, there are numerous glacial deposits on the mountain which have contributed to debris flow initiation in the past. The combination of highly weathered volcanic rock deposited in over-steepened, unbuttressed glacial moraines and water contribution from melting glaciers and storm events creates and debris flow hazard in many drainages.

2.2 Glaciation

This study identifies 26 named glaciers on the flanks of the volcano (Figure 2).

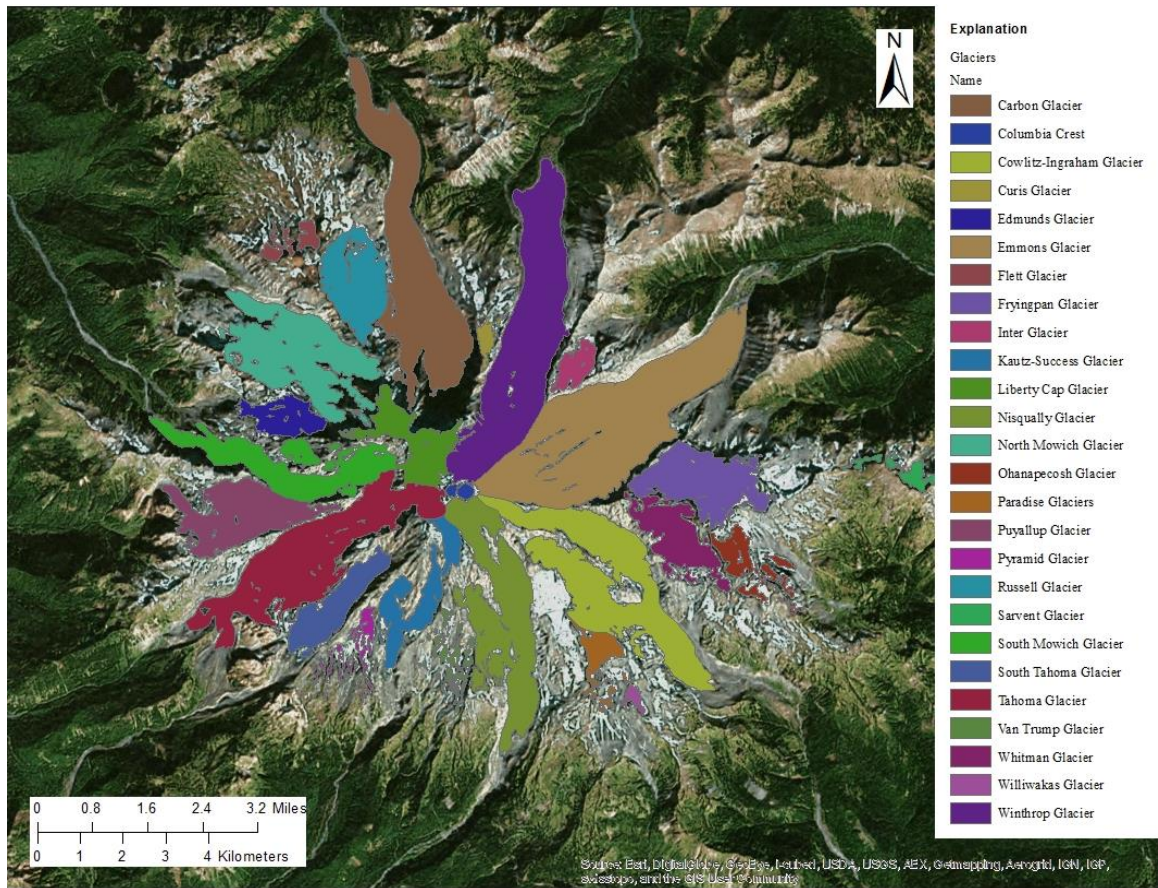


Figure 2. Map of the glaciers on Mt. Rainier used in this study.

According to the U.S. Geological Survey, there have been two major glacial periods affecting Mount Rainier. The first, Hayden Creek Glaciation, occurred 170 thousand to 130 thousand years ago. Glaciers during this period extended down the Cowlitz River Channel 105 km (63 mi) and down the Nisqually River Valley 48 km (30 mi). The second, Evans Creek Glaciation, occurred 22 to 15 thousand years ago. During this time, glaciers were much smaller and confined to valleys on the volcano. These glaciers existed up to 64 km (38 mi) down the Cowlitz Valley, 30 km (19 mi) down the Nisqually Valley, 38 km (24 mi) down the White Valley, and 26 km (16 mi) down the

Puyallup and Mowich valleys. Additionally, there have been many small glaciations since the Evans Creek period, the most recent of which started about 10,000 years ago.

2.3 Debris Flows

2.3.1 Characteristics

Debris flows are fast moving (10s km hr^{-1}) sediment water slurry (like wet concrete) characteristic of debris flows (Iverson, 1997; Pierson, 2005; Vallance et al., 2003). Debris flows are very destructive processes that can transport boulders as large as 10 m in diameter (Iverson, 1997). Peak discharges can be 5 to 40 times greater than normal floods (Wilford et al., 2004). Flow physics are slightly different than other mass wasting processes. They are under the influence of both solid and fluid forces, whereas a normal flood is completely dominated by fluid forces, and rock avalanches are completely dominated by solid forces (Iverson, 1997).

Debris flows leave behind distinctive topographic features including levees, deposits with lobate margins and surfaces that are curved up with large clasts concentrated at the margins and distributed more randomly closer to the center of the flow on the surface (Pierson, 2005; Godt and Coe, 2007). Clasts are matrix supported subangular to angular sands and gravels. Sand and gravel dominate the grain size distribution of these deposits, with a small fraction of clays ($\leq 10\%$) (Iverson, 1997). Deposits can have normal grading or inverse grading (Pierson, 2005).

Debris flows inflict much damage on the riparian vegetation and can erode in the stream channel. Large clasts, typically boulders and cobbles can be found jammed into holes between roots and in cavities in trees and buildings (Pierson, 2005). They tend to

strip bark and erode away wood on trees, especially on the upstream side, and may even remove a tree entirely. Mud coatings collect on surfaces the flow comes in contact with.

2.3.2 Initiation

There are three initiation mechanisms for debris flow, but more commonly debris flows are initiated through a combination of these three mechanisms:

1. Slope failure is the most common mechanism for debris flow initiation (Iverson, 1997; Godt and Coe, 2007). When the material becomes loose on a slope and it fails, it may be able to incorporate enough water in a stream channel to achieve the consistency necessary to be a debris flow (Iverson 1997). A slope failure can be initiated a number of ways; the most common being infiltration from high rainfall or undercutting from increased stream flow (Iverson 1997; Godt and Coe 2007).
2. Outburst floods from glaciers can also cause debris flows (Vallance et al., 2003). High discharges can erode banks and incorporate enough sediment to become debris flows. These types of initiations are less common, but are known to occur in drainages with a large glacier located in the upper basin (Vallance et al., 2003). These types of events are associated with warmer temperatures and increased rainfall (Vallance et al., 2003).
3. Debris flows can also initiate by a process called rilling. Runoff can erode sediment on sidewalls forming rills, the rills coalesce into channels, the channels can erode more from the bed or margins in a process known as bulking up, and the mixture can become a debris flow (Godt and Coe, 2007).

This is referred to as “headless” initiation in Pirot (2010), Williams (2011), and Olson (2012).

2.4 Debris Flows and Lahars on Mt. Rainier

During the past 11,000 years there have been numerous eruptive periods which have produced large lahars and debris flows on Mt. Rainier, the largest of which was the Osceola Mudflow, which occurred at 5,600 years ago (Sisson and Vallance, 2011; Vallance and Scott, 1997). This mudflow began as a water saturated avalanche initiated by eruptions at the summit of the volcano (Vallance and Scott, 1997). It entrained 3.8 km³ of material, flowed down the White River and eventually into the Puget Sound lowland, covering 200 km². The avalanche transformed into a clay-rich lahar within 2 km of the source due to sufficient amounts of water and hydrothermally altered material that was easily incorporated.

The next youngest, notable lahar is the National Lahar (Sisson and Vallance, 2011). It occurred between 2,200 and 500 years ago. The lahar was likely initiated when an eruption rapidly melted snow and ice on the south flank of the mountain. This lahar flowed down the Nisqually River into the Puget Sound.

The Electron Mudflow, which occurred about 500 years ago, was not initiated by a volcanic eruption (Sisson and Vallance, 2011). The western flank of the mountain failed into the Puyallup River Valley, evolved into a debris flow, and flowed 100 km downstream. The trigger for the collapse of the volcano is still under debate. One possibility is a flank collapse when magma inflation destabilized the volcanic flank. Other possibilities include earthquake shaking and slope failure

Within historic times Mount Rainier has had many small debris. These debris flows are commonly unrelated to volcanic activity. More than 40 have occurred within the last few decades, 23 of which have been documented within the Tahoma Creek drainage basin since 1867 (Vallance et al., 2003; Sisson and Vallance, 2011).

In this specific study and environment, lahars are much larger scale, larger volume events which have been mapped to populated areas in the Puget Sound Lowland. Debris flows in this study are much smaller in scale and likely exist as hyperconcentrated flows and floods greater distances down drainage. Debris flows in this study likely only impact park infrastructure and roads closer to the park.

2.5 Climate

According to the Western Regional Climate Center (2013), the Western Cascades receive 1.5-2.5 m or more rainfall annually, most which falls on east-west oriented mountain valleys. Additionally, Mount Rainier also receives 1.3-1.8 m of snowfall in lower elevations and 10.2-15.2 m in higher elevation. The eastern slope of the Cascades receives much less annual rainfall than the western slope; 0.6-2.3 m. Similarly, the snowfall on these slopes is 1.9-10.2 m.

2.6 November 2006 Pineapple Express Storm

In November, 2006 a “Pineapple Express” system moved through the Pacific Northwest, and dropped record amounts of rain. A Pineapple Express system begins around the Hawaiian Islands with a moisture plume. The subtropical jet stream drives the moisture plume towards the West Coast and into the Pacific Northwest (Figure 3) (Gottschalk et al., 2005; NOAA, 2005; NASA Earth Observatory, 2006). The sudden

increased precipitation, in combination with the lack of snow in the Cascades initiated debris flows on Mt. Jefferson (Sobieszczyk et al., 2009), Mt. Hood (Pirot, 2010), Mt. Rainier (Copeland, 2009; Legg, 2013), Mt. Adams (Williams, 2011), and Mt. St. Helens (Olson, 2012).

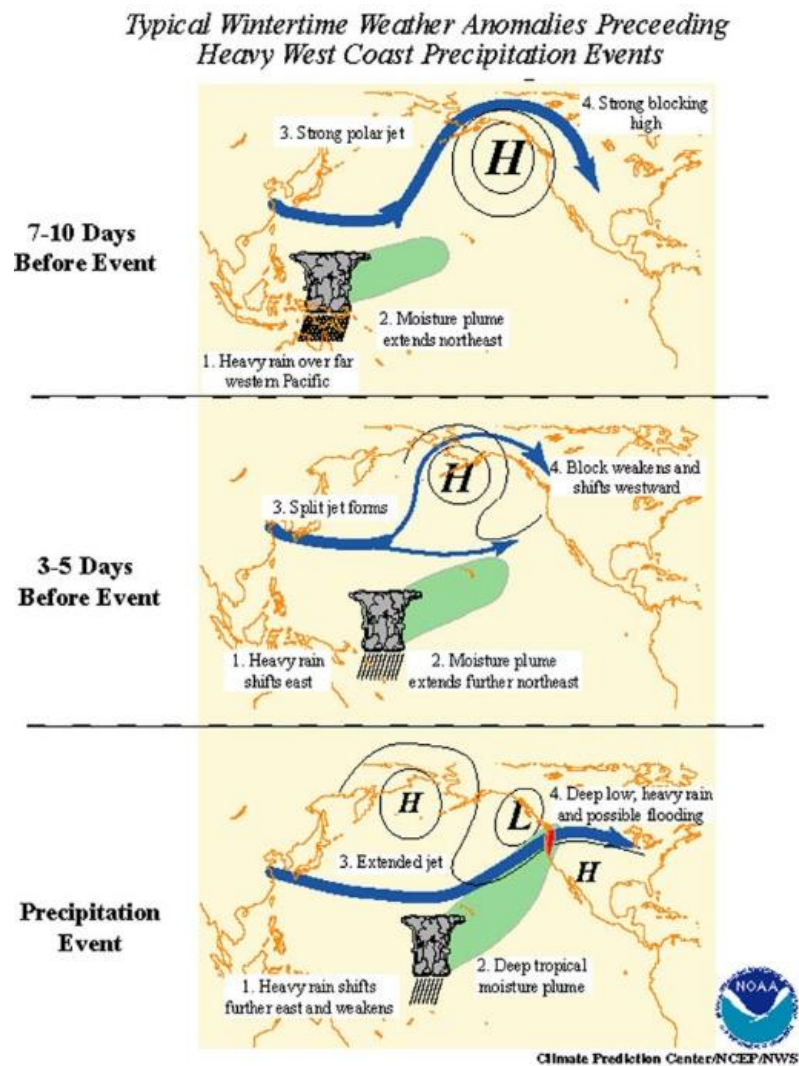


Figure 3. NOAA figure of a typical Pineapple Express system.

2.7 Past Work

Pirot (2010), Williams (2011), and Olson (2012) conducted studies on Mt. Hood, Mt. Adams, and Mt. St. Helens, respectively. Each thesis expanded on the previous to

collect attributes related to the basins draining the volcanoes in an attempt to better refine susceptibility maps for debris flow occurrence. Pirot (2010) found vegetation coverage, gradient, and stream connection with glacier to be the most significant factors correlated with debris flow initiation on Mt. Hood. Williams (2011) found percent ice and average annual precipitation to be the most significant factors on Mt. Adams. Olson (2012) found percent steep slopes, percent unconsolidated material, and average annual precipitation to be the most significant factors on Mt. St. Helens.

Copeland (2009) identified debris flow initiation in 2006 in Van Trump, Pyramid, West Fork of the White, Inter Fork, Tahoma, and Kautz. Legg (2013) added Ohanapecosh to the list. This study seeks to expand on these two. All debris flows identified by Copeland (2009) and Legg (2013) were initiated to some degree, or entirely by channel erosion, or headless initiation. Glacier outburst floods and glacial lake outburst floods played a role in initiation at least partially in Tahoma and West Fork of the White, respectively (Copeland, 2009).

Ellinger (2010) examined the influence of glacial recession on debris flow initiation on Mt. Rainier and Mt. Hood, in an effort to identify the impacts of climate change on mass wasting events. His study identified glacial terminus boundaries between 1987 and 2005. Copeland (2009) identified Inter Fork, Pyramid, and Van Trump had their first historic debris flows in 2006 and Ellinger (2010) found that they initiated within 1987 and 2005 recession boundaries, indicating that glacial recession plays a role in debris flow initiation sites on Mt. Rainier.

Chapter 3: Methods

3.1 Field Reconnaissance

A total of 15 days during the summers of 2013 and 2014 were spent hiking into or attempting to hike into the upper drainages of Carbon, Fryingpan, Inter Fork, North Puyallup, North Mowich, Nisqually, Ohanapecosh, South Puyallup, South Mowich, Stevens, and White rivers, looking for evidence of debris flows. Other drainages had well-established evidence either for debris flow by Copeland (2009) and Legg (2013) or against debris flow by looking at imagery. Photographs taken include evidence of levees, matrix supported deposits with angular clasts, small deposits dammed by logs, sediment coatings on boulders, logs, and trees, and stripped bark and further damage to trees in the channel (Pierson, 2005). Since reconnaissance was conducted in 2013 and 2014, six to seven years following the event, re-growth of vegetation was also documented as evidence in areas like avulsion channels.

3.2 Drainage Basin Attributes

The aim for this research is to figure out what characteristics, or attributes, of each drainage basin are most important in debris flow initiation. Data for 29 attributes were compiled from a combination of Pirot (2010), Williams (2011), and Olson (2012), in addition to selecting or slightly altering a few variables, to suit the unique environment of Mt. Rainier and this study. The attributes were collected by examining aerial imagery from July/August 2006 and August 2009 in Google Earth. I tried to correlate evidence found in the field with aerial imagery, in addition to channel avulsions, major areas of sediment erosion, channel expansion and avulsion, landslide scarps, and large patches of

vegetation removed in or near the channel (Piro, 2010). Changes were digitized by comparing 2006 orthophotos from US Geological Survey Earth Explorer and lidar collected in 2007/2008 (USGS, 2008) in ArcGIS.

1. **Total Basin Area:** Basins were digitized as polygons in ArcMap using watershed data from the DNR and lidar collected from the USGS. A drainage was defined using major ridgelines. The ridgelines were traced starting at the top of the basin and continued down until the stream entered another stream that does not drain the same area. The area was calculated using the *calculate geometry* tool in the attribute table in square meters.
2. **Upper Basin Area:** The upper basin was digitized in the same way as total basin area. The upper basin is defined as the area at the top of the basin, above a region where the basin ridges naturally narrow. It includes the initiation zone for all drainages that experienced debris flows. The area was calculated using the *calculate geometry* tool in the attribute table in square meters.
3. **Average annual precipitation:** Average annual precipitation was collected using PRISM data (PRISM Climate Group, 2007) with 4 km resolution for each month from 1995 to 2005. The PRISM data were converted to contours using the *Contour* tool in the "3D Analyst" toolkit. A contour interval of 50 millimeters was chosen. The contours were then clipped to the extent of each upper drainage basin boundary. The average annual precipitation for each basin was calculated using the following equation (Williams, 2011; Olson, 2012):

$$P = \frac{(\sum_1^n R_n + A_n)}{A_T} \quad (\text{Equation 1})$$

Where:

P = average annual precipitation

R_n = average annual precipitation at the nth contour line

A_n = is the area above the nth contour line

A_T = total area of the upper basin

4. **Stream has Direct Connection with Glacier:** A stream was considered to have a direct connection with a glacier if, on orthophotos, the stream is shown to be fed by a glacier located in its upper basin. In addition, many of the glaciers are documented to feed rivers in Matthes (1928). This attribute is defined as true or false.
5. **Distance of the Stream from a Glacier:** Distance was calculated using the *measurement* tool in ArcGIS. The distance was calculated from the headwaters of the stream to the nearest edge of the glacier. Distance was measured in meters.
6. **Elevation of Initiation Zone:** Elevation was measured using the *identification* tool on DEM rasters.
7. **Gradient of Total Basin:** This was calculated by dividing the change in elevation of the basin, which is the highest elevation minus the elevation of the stream where it leaves the digitized basin boundary, and the length of the basin.
8. **Gradient of Upper Basin:** This was calculated by dividing the change in elevation of the upper basin and the length of the upper basin.
9. **Height of Total Basin:** This was calculated by subtracting the lowest elevation from the highest elevation in the whole basin.

10. **Height of Upper Basin:** This was calculated by subtracting the lowest elevation from the highest elevation in the upper basin.
11. **Highest elevation in Total Basin:** Highest elevation in the whole drainage was calculated using DEM derived data. The DEM was clipped to the drainage using the *mask* tool.
12. **Highest elevation in Upper Basin:** Highest elevation in the upper drainage was calculated using DEM derived data. The DEM was clipped to the upper drainage using the *mask* tool.
13. **Lowest Elevation of Total Basin:** Lowest elevation in the whole drainage was calculated using DEM derived data. The DEM was clipped to the drainage using the *mask* tool.
14. **Lowest Elevation of Upper Basin:** Lowest elevation in the upper drainage was calculated using DEM derived data. The DEM was clipped to the upper drainage using the *mask* tool.
15. **Length of Total Basin:** Length of the total basin was calculated by measuring the horizontal distance from the highest elevation in the whole drainage to the lowest elevation, following the river path.
16. **Length of Upper Basin:** Length of the upper basin was calculated by measuring the horizontal distance from the highest elevation in the upper drainage to the lowest elevation, following the river path.
17. **MRN for Total Basin:** An MRN greater than 0.3 is supposed to be a good indication of a basin's potential to generate a debris flow (Melton, 1965).

Melton's Ruggedness Number (MRN) was calculated using the following equation (Melton, 1965).

$$MRN = \frac{H_T}{\sqrt{A_T}} \quad (\text{Equation 2})$$

Where:

H_T = Basin height

A_T = Basin area

18. **MRN for Upper Basin:** This was calculated the same way as variable 18, only for the upper basin.
19. **Percent Glacier in Upper Basin:** Glacier areas were calculated using a glacier limits shapefile (Fountain et al., 2007). A glacier is defined as a perennial accumulation of ice, snow that moves (Paterson, 1994). All other regular ice and snow was not included in this study. The glacier polygons were divided into basins using the *intersect* tool in ArcGIS. Area was then calculated for each basin using the *calculate geometry* tool in the attribute table in square meters. Those calculated areas were then divided by the upper basin area and then multiplied by 100 to get a percent glacial coverage in the upper basin.
20. **Percent Change in Surface Area of Glacier:** Glacier limit shapefiles produced for 1994 (Nylen, 2004) and 2007/2008 were examined in order to determine the change in surface area of each glacier. The surface area in 2007/2008 was subtracted from the surface area in 1994, and then multiplied by 100.
21. **Percent Steep Slopes in Upper Basin:** Steep slopes are those that are greater than or equal to 33°. Lidar was converted using the *Slope* tool. Then, using the upper basin shapefile, the raster was cut up by drainages, and the cells were

defined as greater than or equal to, or less than 33°. The percent steep slopes were calculated by dividing the number of cells with slopes greater than or equal to 33° by the total number of cells multiplied by 100.

22. **Percent Vegetation in Upper Basin:** Vegetation was digitized by hand using orthophotos from before the storm in 2006. The area was then calculated in ArcGIS using the *calculate geometry* tool in the attribute table. The total vegetation area for a drainage was then divided by the upper basin area of the same drainage then multiplied by 100 to get the percent vegetation cover in the upper basin.
23. **Retreat Distance of Glacier:** This variable was measured using the *measure* tool. Three distances were measured from terminus to a comparable terminus location between glacial extents mapped in 1994 and 2007/2008 (PSU Inventory, personal communication) and averaged.
24. **Peak Precipitation:** Peak precipitation of the two day 2006 event was measured by identifying the max precipitation between the two days (November 6th and 7th) in a basin using PRISM data (PRISM Climate Group, 2007) with 4 km resolution. The PRISM data were clipped to each basin, and the highest value was determined.
25. **Precipitation at the Initiation Zone:** Precipitation was measured using PRISM data and determined using the *Identify* tool in GIS at the location of initiation (PRISM Climate Group, 2007).

26. Sum of Two Day Event Average Precipitation: Event average precipitation was collected using PRISM data with 4km resolution for each month from 1995 to 2005 (PRISM Climate Group, 2007). It is the sum of the average of the two separate days. The PRISM data were converted to contours using the *Contour* tool in the "3D Analyst" toolkit. A contour interval of 5 millimeters was chosen. The contours were then clipped to the extent of each upper drainage basin boundary. The average precipitation for each basin during the 6th and 7th of November was calculated using Equation 1. The results for the two days were calculated for the total precipitation during the storm event.

27. Percent bedrock in Upper Basin: A compilation of hand digitized bedrock and a 100,000 scale geologic map of Washington shapefile from the Washington DNR (2010) was used to calculate the percent bedrock in each drainage. All bedrock that could be seen on orthophotos was digitized and used instead of what was recorded by the DNR. Bedrock looked like consolidated rock that outcropped from evident surficial deposits. They could also be seen on the lidar as consolidated outcrop. In places where the upper drainage was covered in vegetation or snow, and no geology could be seen, what was recorded by the DNR was used. This was done in order to get the most accurate calculations for geology in the upper basin. Bedrock was defined as anything consolidated and given a rock classification like diorite.

28. Percent surficial deposits in Upper Basin: A compilation of hand digitized bedrock and a 100,000 scale geologic map of Washington shapefile from the

DNR was used to calculate the percent surficial deposits in each drainage. All surficial deposits that could be seen on orthophotos were digitized and used instead of what was recorded by the DNR. These deposits looked like talus or alluvium on the slopes or in/near the drainage channels. In places where the upper drainage was covered in vegetation or snow, and no geology could be seen, what was recorded by the DNR was used. This was done in order to get the most accurate calculations for geology in the upper basin.

29. Distance of Initiation Zone from a Glacier: Distance was calculated using the *measurements* tool in ArcGIS. The distance was calculated from the initiation zone to the nearest edge of the glacier. Distance was measured in meters.

Attributes used in Pirot (2010), Williams (2011), and Olson (2012), not used in this study are azimuth of the upper basin, area above initiation zone, grain size analysis of deposits at the initiation site, bedrock and surficial deposits geology of the entire basin. They were not used because previous studies showed they would not provide any unique data to the analysis here.

PRISM data was used instead of individual rain stations because data for only four stations could be used for the whole mountain, three of which are located on the south side of the mountain. PRISM datasets were modeled using DEMs and station weather gauge information. Compared to applying the four stations across the entire mountain for the precipitation attributes, using the PRISM data seems more accurate. Additionally, Olson (2012) used this method and his study is the most recent study done

prior to this one. The station data and PRSIM data are presented in a comparative table in Appendix A for the two data event.

3.3 Data Analysis

3.3.1 ANOVA

A one-way analysis of variance was done between the group of basins that had debris flows and the group that did not. This was done in Excel, using the ANOVA: Single Factor test in the Analysis Toolkit. The groups are deemed statistically different if the resulting p value is less than a significance level of 0.05 (Davis, 2002).

3.3.2 Multiple Regression

A multiple regression analysis was used to determine most significant variables for debris flow initiation. The variables and their corresponding coefficients can then be used to develop a susceptibility map for debris flow initiation on Mt. Rainier using (Equation 3). This regression was conducted very similar to those conducted in Pirot (2010), Williams (2011), and Olson (2012), with some variation.

$$Y = \frac{e^{(\alpha + \beta_1 X_1 + \beta_2 X_2 + \dots + \beta_n X_n)}}{1 + e^{(\alpha + \beta_1 X_1 + \beta_2 X_2 + \dots + \beta_n X_n)}} \quad (\text{Equation 3})$$

Where:

- Y = Probability of occurrence
- α = Intercept of the best fitting equation
- X = Measured variable
- β = Corresponding coefficient

The first step in conducting the analysis is to convert all the data to be used to standard normal form. This is done because each set of variables is measured in different units and

has different magnitudes, so it makes it much easier to conduct the analysis when data are normalized. Equation 4 was used to convert the data.

$$Z_i = \frac{X_i - x}{s} \quad (\text{Equation 4})$$

Where:

X_i = The initial value

x = The mean of that variable set

S = The standard deviation of that variable set

The regression tool in the Analysis Toolkit in Excel was used to calculate the coefficients for each variable. The Wald Test was used to determine which variables are the least and most significant (Equation 5). The reduction of the regression was done in a backward, stepwise procedure. This means that the regression was reduced until all variables are significant and account for the majority of the variance in the analysis (Kachigan, 1991). The R square value was monitored after each regression. Once there was a significant change in value from one regression to another, the remaining variables are the most significant (Kachigan, 1991). The probability for the resulting set of variables and coefficients were calculated. Next, the variables that were previously removed were added back individually, one by one, to test their significance. If any more significant variables were identified through this process, those variable and coefficient combinations were also applied to the probability equation. The best fitting model was then picked.

$$W = \left(\frac{\beta}{SE_{\beta}} \right)^2 \quad (\text{Equation 5})$$

Where:

β = The coefficient calculated from the regression

SE_{β} = The standard error associated with the variable calculated from the regression

Chapter 4: Results

Each major drainage was investigated by hiking into the basin in the field looking for evidence and/or using orthophoto and lidar comparison to identify potential evidence.

Figure 4 shows the 34 drainages used in the analysis. All basin attribute data are presented in Appendix A.

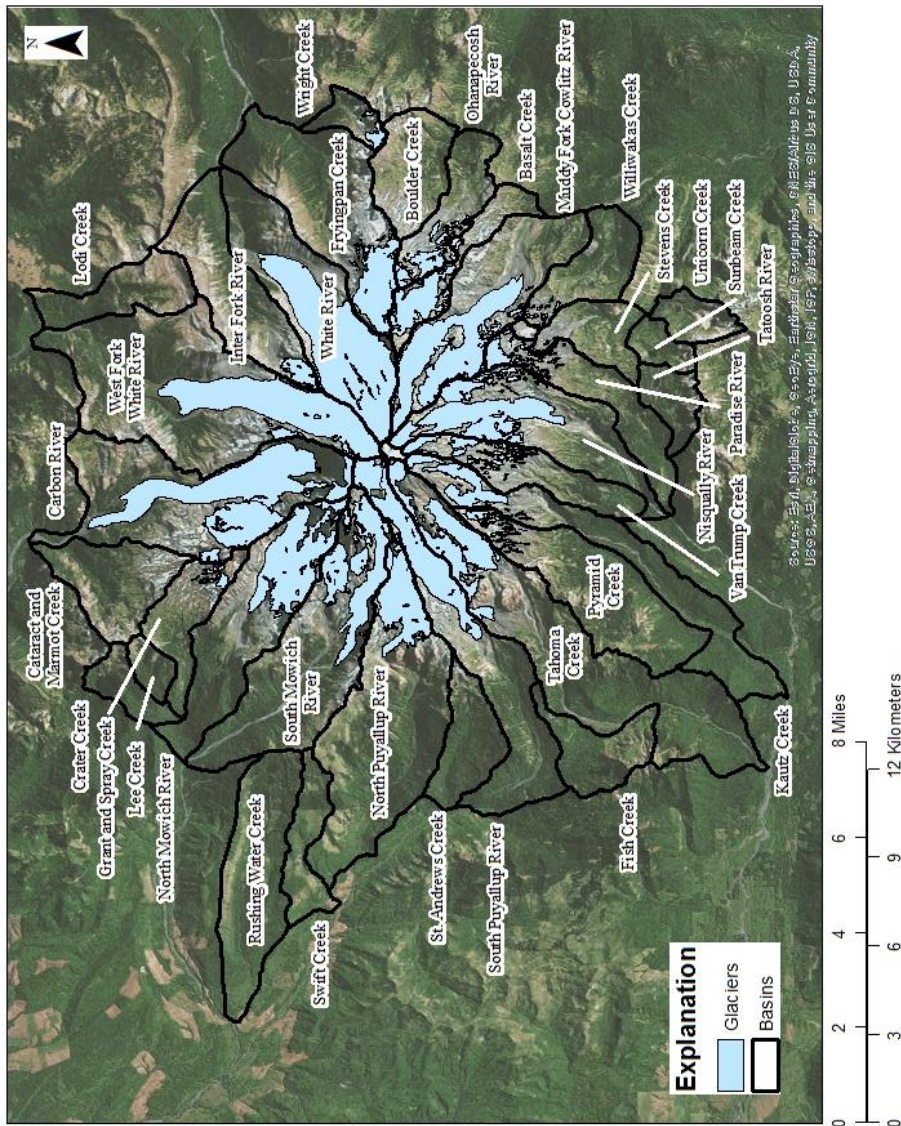


Figure 4. Map of Mt. Rainier and the 34 drainages examined in this study. Basins are outlined in black, upper basins in dashed black, glaciers in blue, and initiation sites from Copeland (2009) in purple, Legg (2013) in blue, and this study in orange.

4.1 Basalt Drainage Basin

4.1.1 Introduction

Basalt Creek Basin is located on the southeast side of the mountain, between Muddy Fork Cowlitz Drainage to the southwest and White River, Fryingspan, and Ohanapecosh drainages to the north and northeast (Figure 4 and Figure 5). The drainage is fairly well-defined by ridges on all sides and 8.7 km long. Its highest elevation is 3395 m and lowest elevation is 1176 m where Basalt Creek meets the Muddy Fork Cowlitz River. It is not easily accessed by maintained trails or roads.

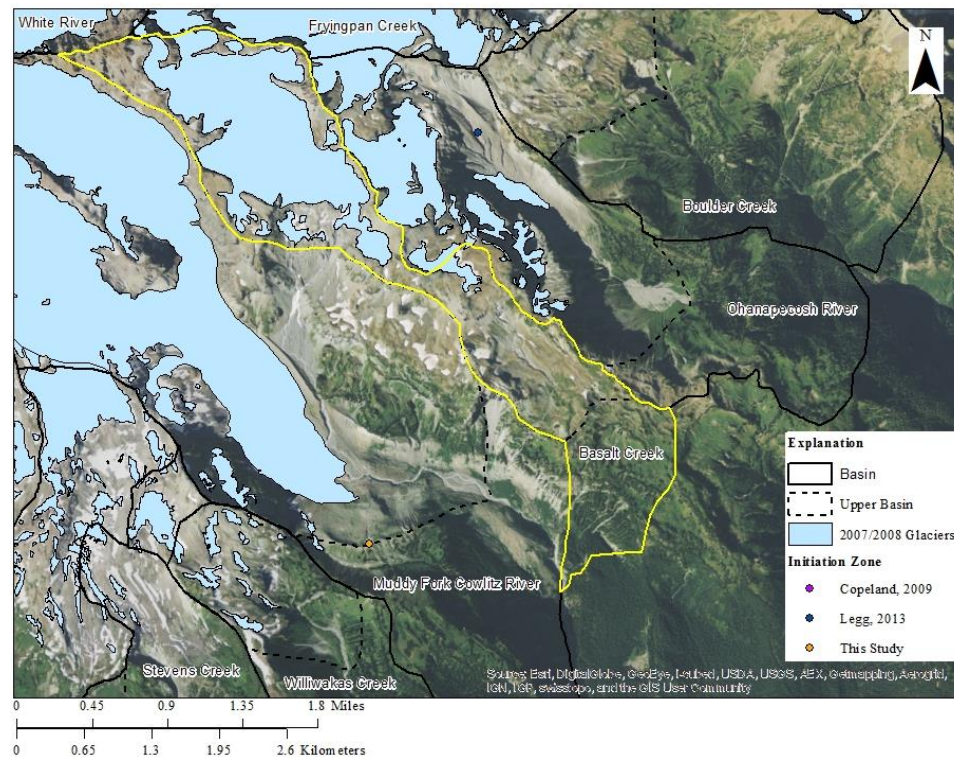


Figure 5. Basalt Creek Basin outlined in yellow, other basins outlined in black, the upper basin outlined in dashed black, glaciers in blue, and initiation sites from Copeland (2009) in purple, Legg (2013) in blue, and this study in orange. No 2006 debris flow was recorded in this basin.

4.1.2 2006 Event

This drainage did not have any evidence of a debris flow on Google Earth (Figure 6a and b). This drainage was not investigated in the field since strong evidence against debris flow was collected using imagery.

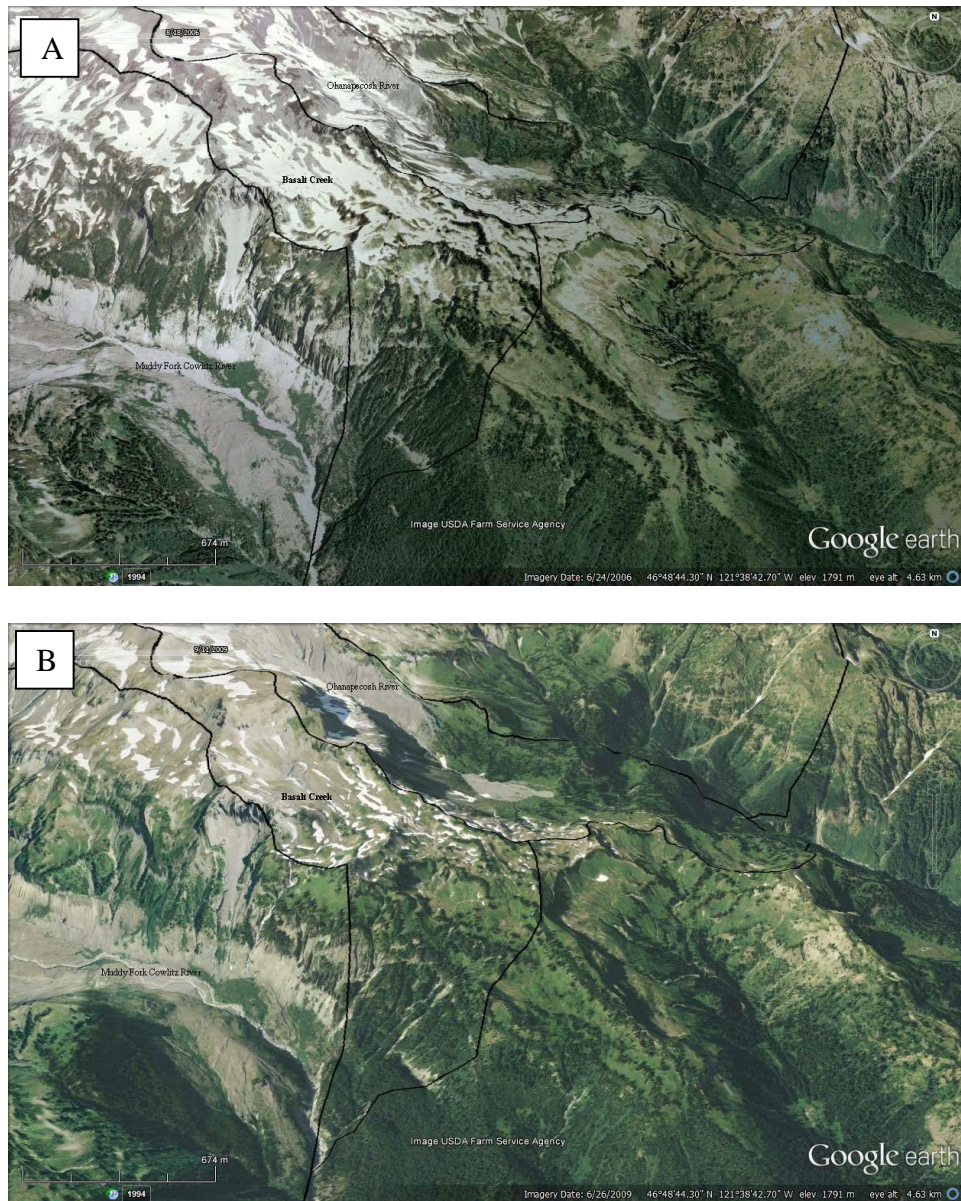


Figure 6. a) Google Earth image of Basalt Creek Drainage in August 2006. b) Google Earth image of Basalt Creek Drainage in September 2009.

4.1.3 Basin Attributes

The total basin area for this drainage is 6.46 km², while the upper basin area is 5.11 km². In the upper basin, 74% of slopes are steeper than 33°. The gradient of the upper basin is slightly less than the gradient of the entire basin, at 24%. Whitman Glacier feeds this drainage and has an area of 2.23 km² which covers about 44% of the upper basin. The glacier retreated a distance of 67.9 m and reduced by 7% in surface area between 1994 and 2007/2008. There is very little vegetation in the upper basin, covering only 1%. The geology is predominantly bedrock, at 51%. Little to no surficial deposits were mapped in the upper basin of this drainage. During the 2006 event, the upper basin received an average sum of 29.6 cm of rain.

4.2 Boulder Drainage Basin

4.2.1 Introduction

Boulder Creek Basin is located on the east side of the mountain, between Ohanapecosh Basin to the southwest and Fryingpan and Wright basins to the north and northeast (Figure 4 and Figure 7). The drainage is fairly well-defined by ridges on all sides and is 5.1 km long. Its highest elevation is 2335 m and lowest elevation is 1167 m where Boulder Creek meets with the Ohanapecosh River. The basin is easily accessed by the Wonderland Trail, which crosses straight through the upper basin.

4.2.2 2006 Event

This drainage did not have any evidence of debris flow on Google Earth (Figure 8a and b). This drainage was not investigated in the field since strong evidence against debris flow was collected using imagery.

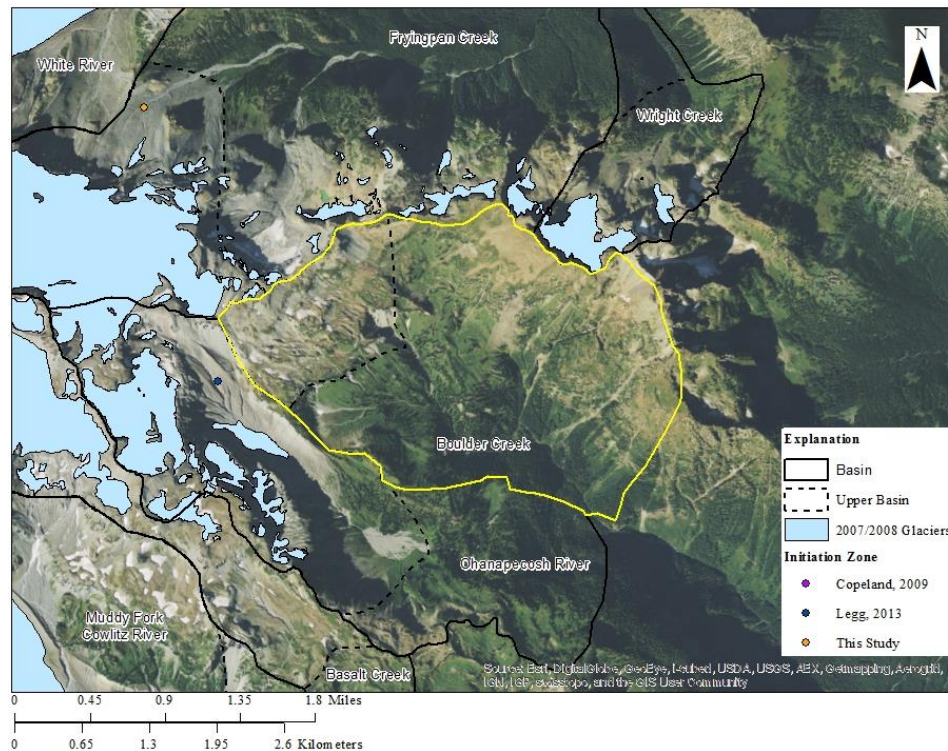


Figure 7. Boulder Creek basin outlined in yellow, other basins outlined in black, the upper basin outlined in dashed black, glaciers in blue, and initiation sites from Copeland (2009) in purple, Legg (2013) in blue, and this study in orange. No debris flow was recorded in this drainage.

4.2.3 Basin Attributes

The total basin area for this drainage is 8.90 km², while the upper basin is 1.85 km². In the upper basin, 78% of slopes are steeper than 33°. The gradient of the upper basin is 30% while the gradient of the whole basin is 23%. Boulder Creek is not fed by a glacier. There is some vegetation in the upper basin covering about 5%. The geology is entirely bedrock. During the 2006 event, the upper basin received an average sum of 20.9 cm.



Figure 8. a) Google Earth image of Boulder Drainage in August 2006. b) Google Earth image of Boulder Drainage in September 2009.

4.3 Carbon Drainage Basin

4.3.1 Introduction

Carbon River Basin is located on the north side of the mountain, between Cataract and Marmot, Grant and Spray, and North Mowich basins to the west, and West Fork of

the White Basin to the east (Figure 4 and Figure 9). The basin is well-defined by ridges on most sides and is 11.5 km long. Its highest elevation is 4304 m and the lowest elevation is 873 m where Spukwush Creek flows into the Carbon River. The lower drainage, not examined in this study, is easily accessed by the hiking or biking the Carbon River Road to Ipsut Creek Campground. From the campground, the Wonderland Trail can be hiked to the toe of the glacier, and the initiation zone can be accessed by hiking the east moraine up next to the glacier.

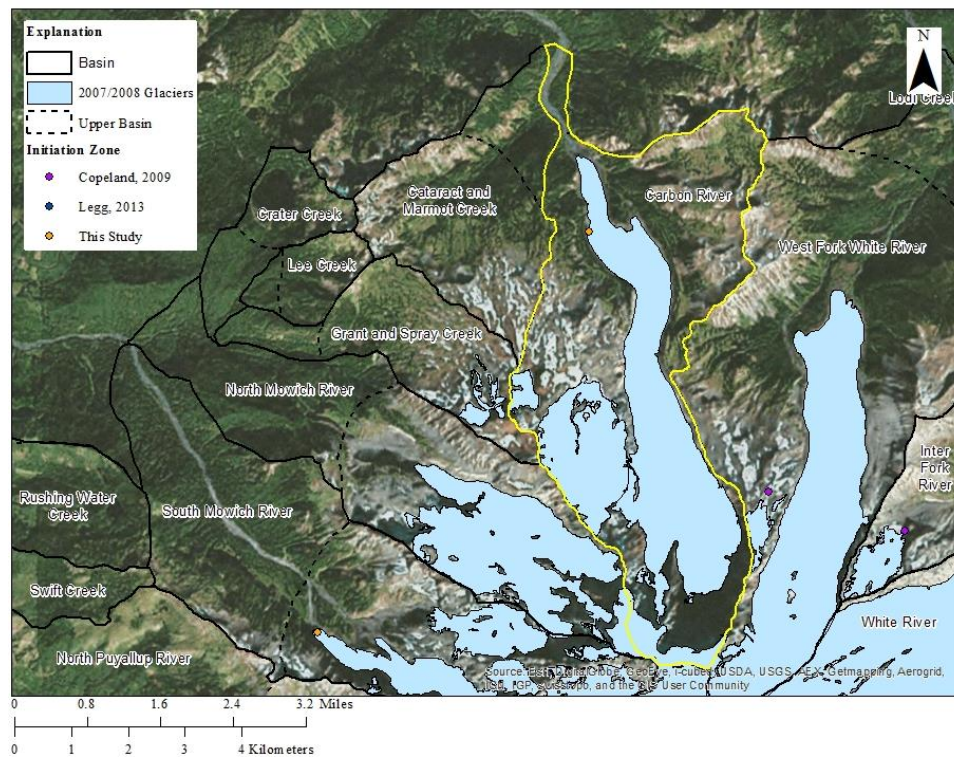


Figure 9. Carbon River Basin outlined in yellow, other basins outlined in black, the upper basin outlined in dashed black, glaciers in blue, and initiation sites from Copeland (2009) in purple, Legg (2013) in blue, and this study in orange.

Carbon River has shown evidence of debris flow in recent history. Czuba et al. (2012) reports that the upper reaches of the drainages, near the glacier terminus, show

evidence of past debris flows, which have traveled at least 2 km downstream. Debris flow levees are evidence of these events. They occur within 300 m of the glacier.

4.3.2 2006 Event

Copeland (2009) had documented this event as a flood. However, the basin has shown evidence of debris flow and during the summer of 2013 the initiation site was identified by Mount Rainier National Park Geomorphologist, Paul Kennard (written comm.; Figure 10a and b). A portion of the moraine failed into the drainage adjacent to the glacier at about 1484 m elevation. The initiation site received a total of 32.7 cm of rain during the two-day event.



Figure 10. a) Carbon initiation in 2006



Figure 10. b) Carbon initiation in 2008. The initiation site is a small debris slope and failed into the drainage on the west side of the drainage.

4.3.3 Basin Attributes

The total basin area for this drainage is 27.9 km², while the upper basin is 27.3 km². In the upper basin, 42% of slopes are steeper than 33°. The gradient of the upper basin is 33.9% while the gradient of the whole basin is 30%. The Carbon River flows directly out of Carbon Glacier, which occupies 41% of the upper basin. The glacier retreated a distance of 92.3 m and reduced by 9% in surface area between 1994 and 2007/2008. The upper basin is 20% covered with vegetation. The geology is 22% bedrock and 36% surficial deposits. During the rainstorm event, the upper basin received 30.3 cm of rain.

4.4 Cataract and Marmot Drainage Basin

4.4.1 Introduction

Cataract and Marmot basins are located on the north side of the mountain, with Crater, Lee, and Grant and Spray basins to the east, and Carbon Basin to the west (Figure

4 and Figure 11). Cataract and Marmot creeks were combined into one drainage because the two drainages do not have a significant ridgeline separating the creeks. It is 5.2 km long. Its highest elevation is 2205 m and the lowest elevation is 885 m where Cataract Creek flows into the Carbon River. The basin is easily accessed by the Spray Park trail, which comes off of the Wonderland Trail at Carbon River Campground to the east or Mowich Lake to the west.

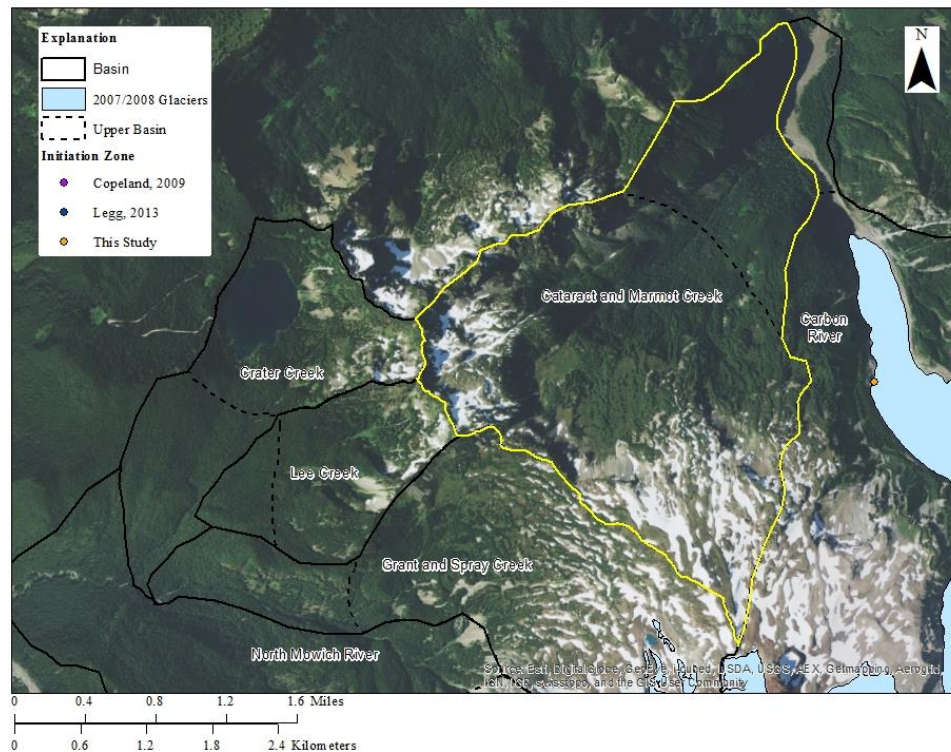


Figure 11. Cataract and Marmot creek basins outlined in yellow, other basins outlined in black, the upper basin outlined in dashed black, glaciers in blue, and initiation sites from Copeland (2009) in purple, Legg (2013) in blue, and this study in orange. No debris flow was recorded in this basin.

4.4.2 2006 Event

This drainage did not have any evidence of debris flow on Google Earth (Figure 12a and b). This drainage was not investigated in the field since strong evidence against debris flow was collected using imagery.



Figure 12. a) Google Earth image of Cataract and Marmot Creek Drainage in August 2006. b) Google Earth image of Cataract and Marmot Creek Drainage in September 2009.

4.4.3 Basin Attributes

The total basin area for this drainage is 10.3 km², while the upper basin is 8.1 km². In the upper basin, 51% of slopes are steeper than 33°. The gradient of the upper basin is 27% while the gradient of the whole basin is 26%. Neither Cataract nor Marmot creeks are fed by a glacier. Almost half of the upper basin is covered by vegetation, at

46%. The geology is 48% bedrock and 52% surficial deposits. During the 2006 event, the upper basin received an average sum of 29.9 cm.

4.5 Crater Drainage Basin

4.5.1 Introduction

Crater Creek Basin is located on the north side of the mountain, with Lee and Grant, Spray, and North Mowich basins to the south and southeast (Figure 4 and Figure 13). The drainage is well-defined by ridges on most sides and is 4.1 km long. Its highest elevation is 1993 m and the lowest elevation is 862 m where Crater Creek flows into the North Mowich River. The basin is easily accessed by the Wonderland Trail.

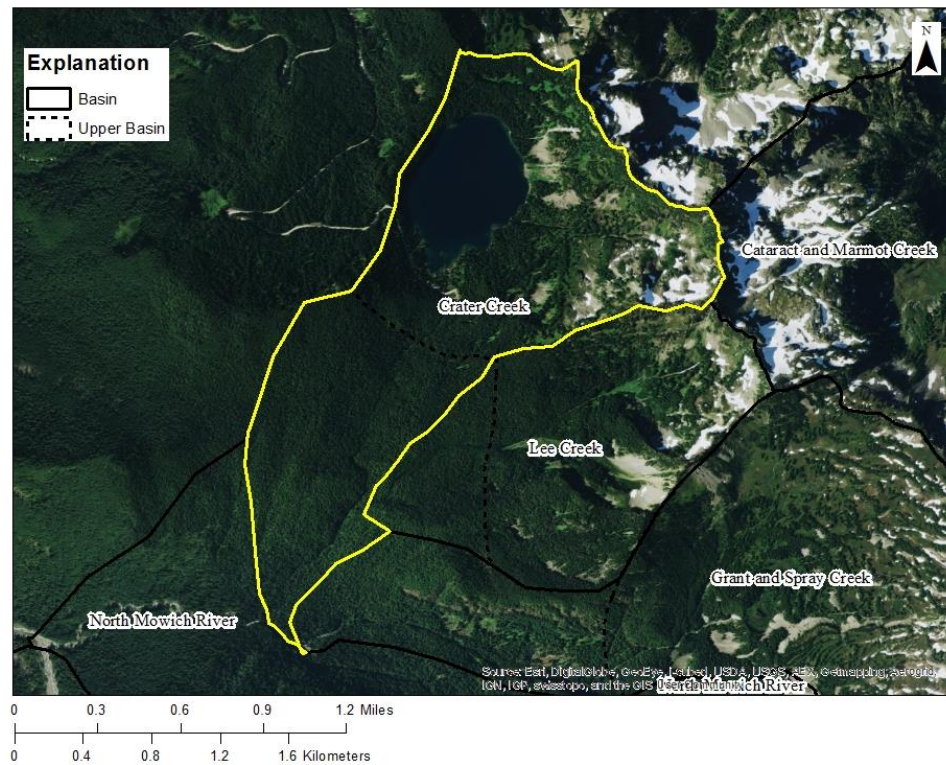


Figure 13. Crater Creek basin outlined in yellow, other basins outlined in black.

4.5.2 2006 Event

This drainage did not have any evidence of debris flow on Google Earth (Figure 14a and b). This drainage was not investigated in the field since strong evidence against debris flow was collected using imagery.

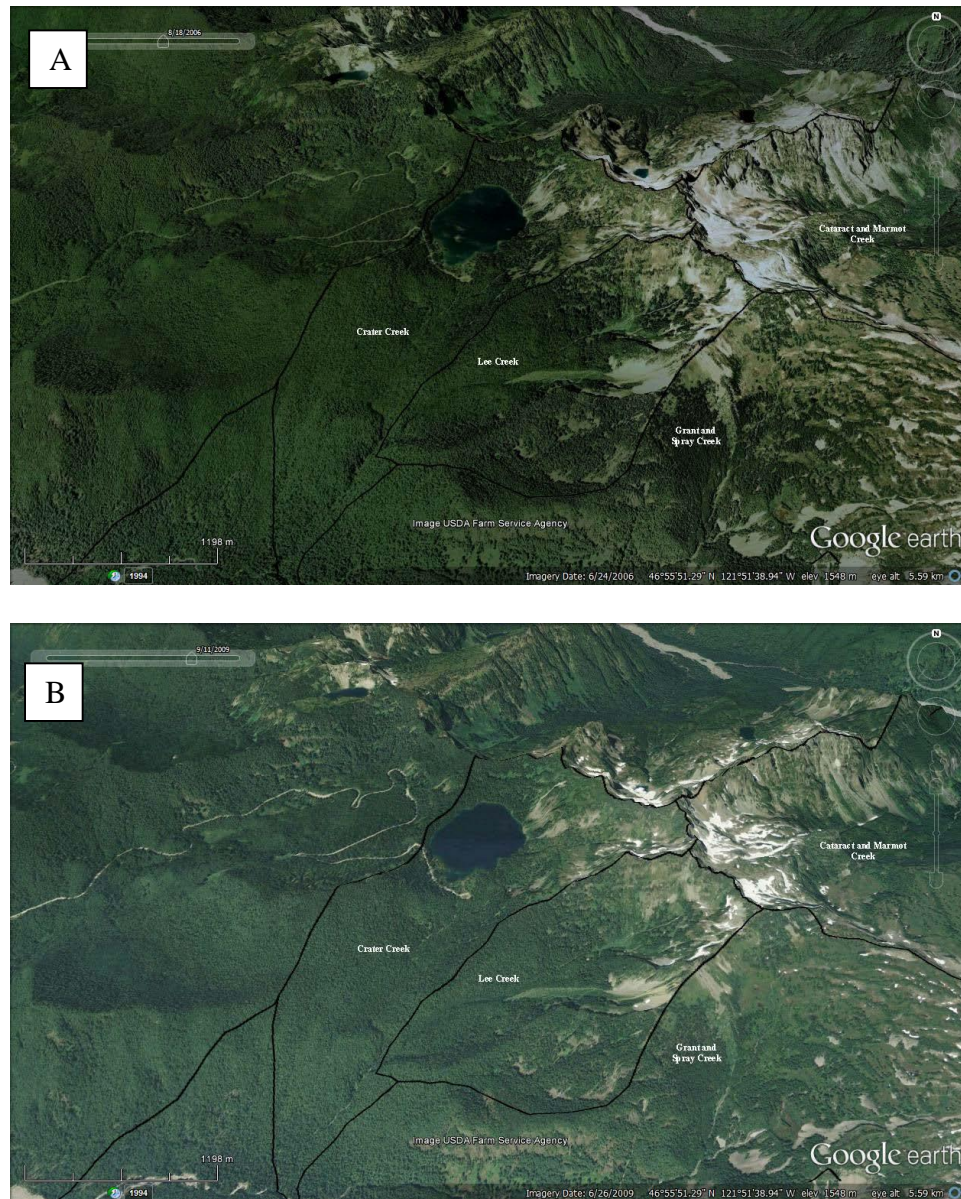


Figure 14. a) Google Earth image of Crater Drainage in August 2006. b) Google Earth image of Crater Drainage in September 2009.

4.5.3 Basin Attributes

The total basin area for this drainage is 3.8 km², while the upper basin is 2.4 km². In the upper basin, 14% of slopes are steeper than 33°. The gradient of the upper basin is 30% while the gradient of the whole basin is 28%. No glaciers are located in this basin. Over half of the upper basin is covered by vegetation, at 65%. The geology is 64% bedrock and 18% surficial deposits. Water covers the remaining percentage of the upper basin. During the 2006 event, the upper basin received an average sum of 26.5 cm.

4.6 Fish Drainage Basin

4.6.1 Introduction

Fish Creek Basin is located on the west side of the mountain, with South Puyallup Basin to the north and Tahoma Basin to the south (Figure 4 and Figure 15). The drainage is well-defined by ridges on most sides and is 4.3 km long. Its highest elevation is 1843 m and the lowest elevation is 790 m where Fish Creek flows into the Tahoma River. The basin is easily accessed by hiking the West Side Road.

4.6.2 2006 Event

This drainage did not have any evidence of debris flow on Google Earth (Figure 16a and b). This drainage was not investigated in the field since strong evidence against debris flow was collected using imagery.

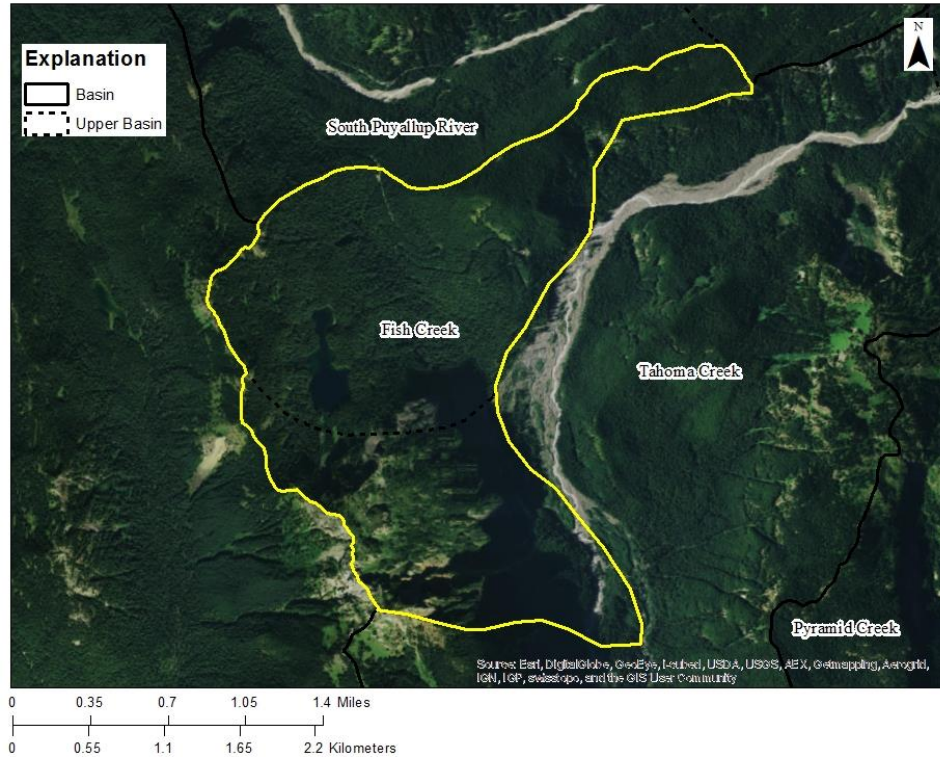


Figure 15. Fish Creek basin outlined in yellow, other basins outlined in black.

4.6.3 Basin Attributes

The total basin area for this drainage is 7.4 km², while the upper basin is 4.6 km². In the upper basin, 49% of slopes are steeper than 33°. The gradient of the upper basin is 36% while the gradient of the whole basin is 24%. No glaciers are located in this basin. Almost the entire upper basin is covered by vegetation, at 96%. The geology is 90% bedrock and 7% surficial deposits. During the 2006 event, the upper basin received an average sum of 27 cm.

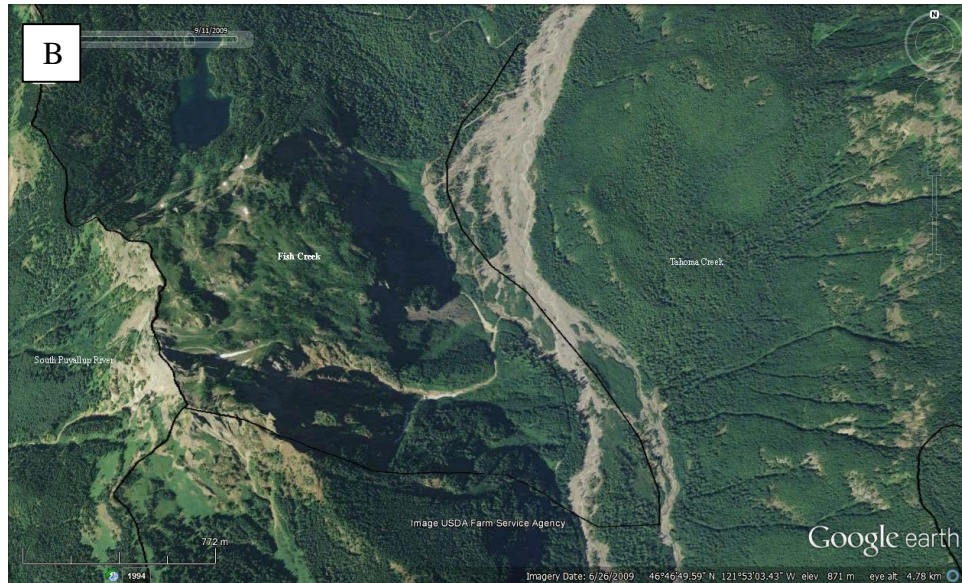


Figure 16. a) Google Earth image of Fish Drainage in August 2006. b) Google Earth image of Fish Drainage in September 2009.

4.7 Fryirpan Drainage Basin

4.7.1 Introduction

Fryirpan River Basin is located on the northeast side of the mountain, between White River Basin to the north, and Wright, Boulder, Ohanapecosh, and Basalt basins to

the south (Figure 4 and Figure 17). The basin is well-defined by ridges on most sides and 10.5 km long. Its highest elevation is 3216 m and the lowest elevation is 113 m where Fryingpan River flows into the White River. The drainage is easily accessed by the Wonderland Trail. Little debris flow activity has been recorded in this drainage in recent history.

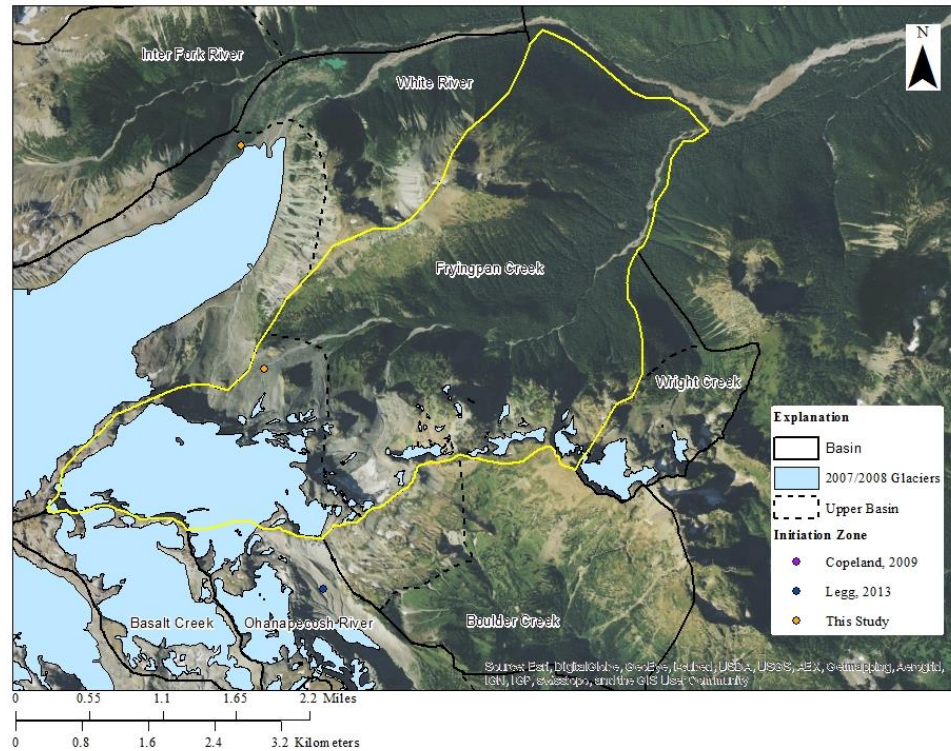


Figure 17. Fryingpan River basin outlined in yellow, other basins outlined in black, the upper basin outlined in dashed black, glaciers in blue, and initiation sites from Copeland (2009) in purple, Legg (2013) in blue, and this study in orange.

4.7.2 2006 Event

The basin had shown evidence of debris flow and during the summer of 2013. Photographs were taken to show evidence of debris flow (Figure 18), in addition to some evidence identified by park employees (Paul Kennard, written communication). The evidence collected in the field is not substantial. There are some major eroded cut banks,

with trees that had fallen into the channel and had bark subsequently removed (Figure 18). Aerial photography and lidar were also used to collect some evidence, including verifying that the cut banks had occurred due to the storm (Figure 19a and b). Major sections of the stream experienced avulsion between 2006 and 2009. Additionally, many large cut banks appear, and large sections of vegetation are removed between 2006 and 2009, which are assumed to be result of the 2006 event (Figure 19a and b).



Figure 18. Photographic evidence for Fryingpan.

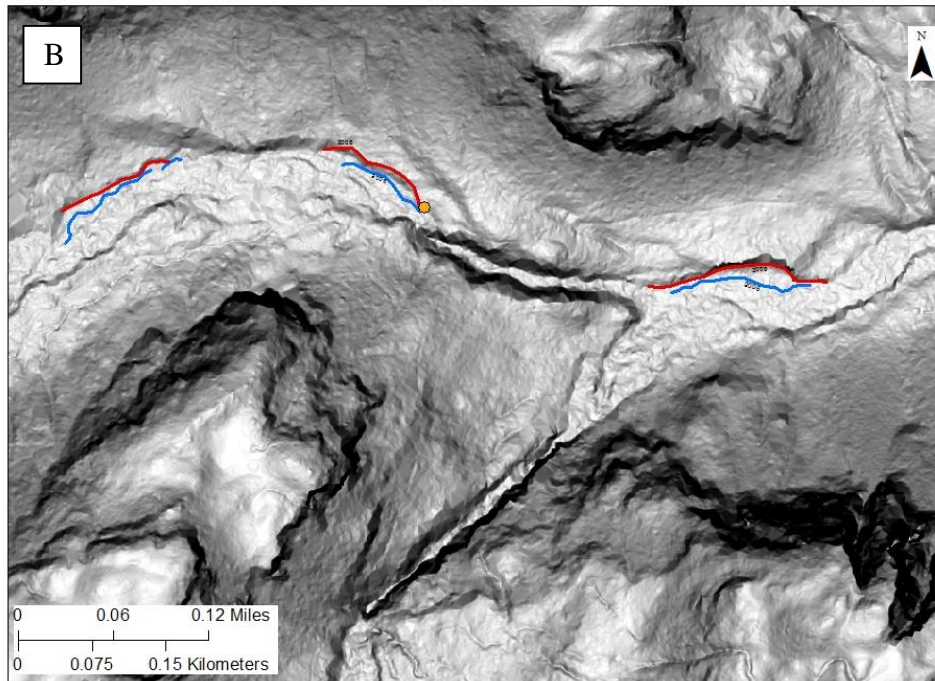


Figure 19. a) 2006 channel margin. b) Channel margin in 2008. Orange point is the location at which Figure 20 was captured.

Due to insufficient field evidence, I ran this drainage as both a "yes" and a "no" through the regression analysis in order to determine which results yielded the most accurate predictive model. I placed the initiation zone for this drainage just below where the stream runs out of snow cover. There doesn't seem to be much gully expansion, nor landslide formation in the sidewalls. However, there does seem to be quite a lot of erosion along margins of the stream channel, which may have contributed to the bulking up of a debris flow (Figure 18a and b). It occurs above some evident erosion and channel avulsion in the upper drainage (Figure 20a and b). It occurs at 1898 m elevation and received a total of 25.3 cm of rain during the two-day event.

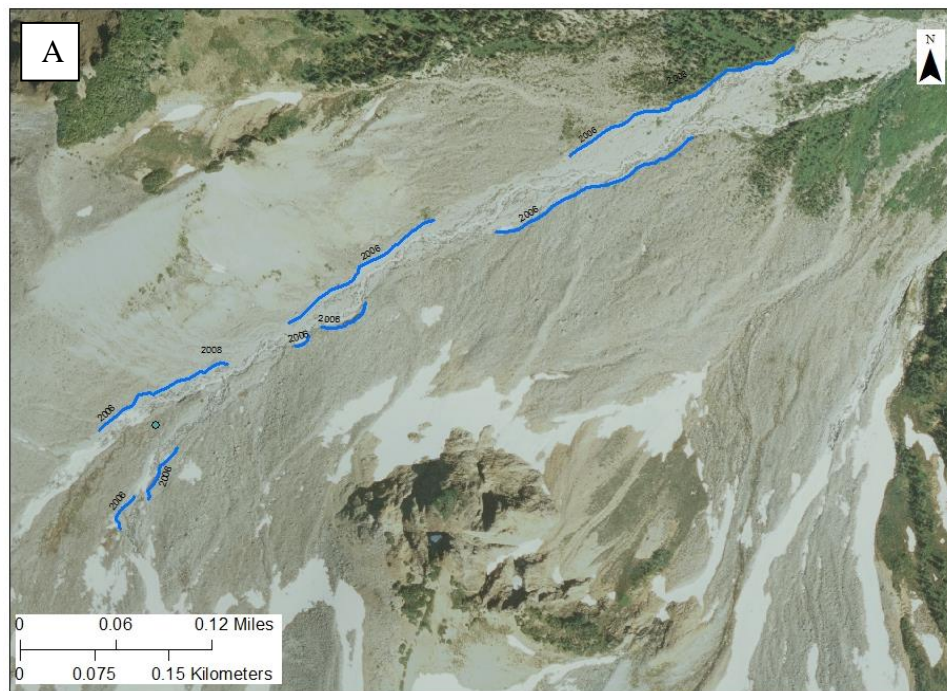


Figure 20. a) Dark blue indicates where the channel margin existed in 2006.

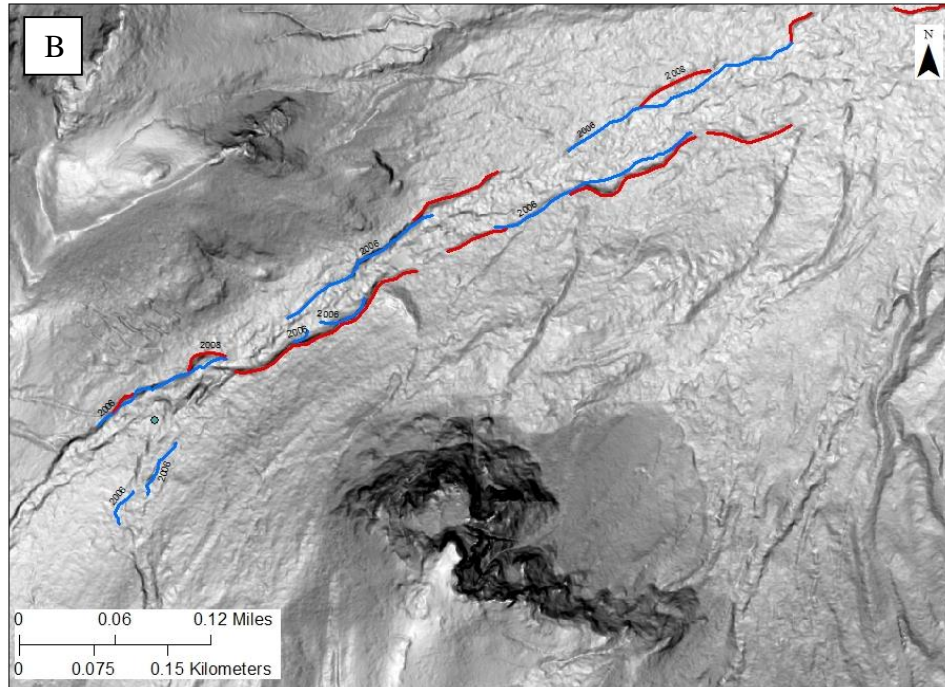


Figure 20. b) Dark blue indicates where the channel margin existed in 2006 while the red line indicates the new channel margin in 2009. This material was likely removed by and contributed to the debris flow in 2006

4.7.3 Basin Attributes

The total basin area for this drainage is 21.3 km², while the upper basin is 5.3 km². In the upper basin, 79% of slopes are steeper than 33°. The gradient of the upper basin is 39% while the gradient of the whole basin is 20%. Part of the Whitman Glacier and most of the Fryingpan Glacier supply the Fryingpan River. Collectively these glaciers occupy 60% of the upper basin. The glacier retreated a distance of 79.1 m and reduced by 20% in surface area between 1994 and 2007/2008. There is very little vegetation in the upper basin, covering about 1%. The geology is 16% bedrock and 24% surficial deposits. During the rainstorm event, the upper basin received 27.8 cm of rain.

4.8 Grant and Spray Drainage Basin

4.8.1 Introduction

Grant and Spray basins are located on the northwest side of the mountain, with Carbon, Cataract and Marmot, Lee, and Crater basins to the east and north, and North Mowich Basin to the south (Figure 4 and Figure 21). Grant and Spray creeks were combined into one drainage because the two drainages do not have a significant ridgeline separating the creeks. It is 6.7 km long. Its highest elevation is 2626 m and the lowest elevation is 879 m where Spray Creek flows into the North Mowich River. The lower basin is easily accessed by hiking the West Side Road.

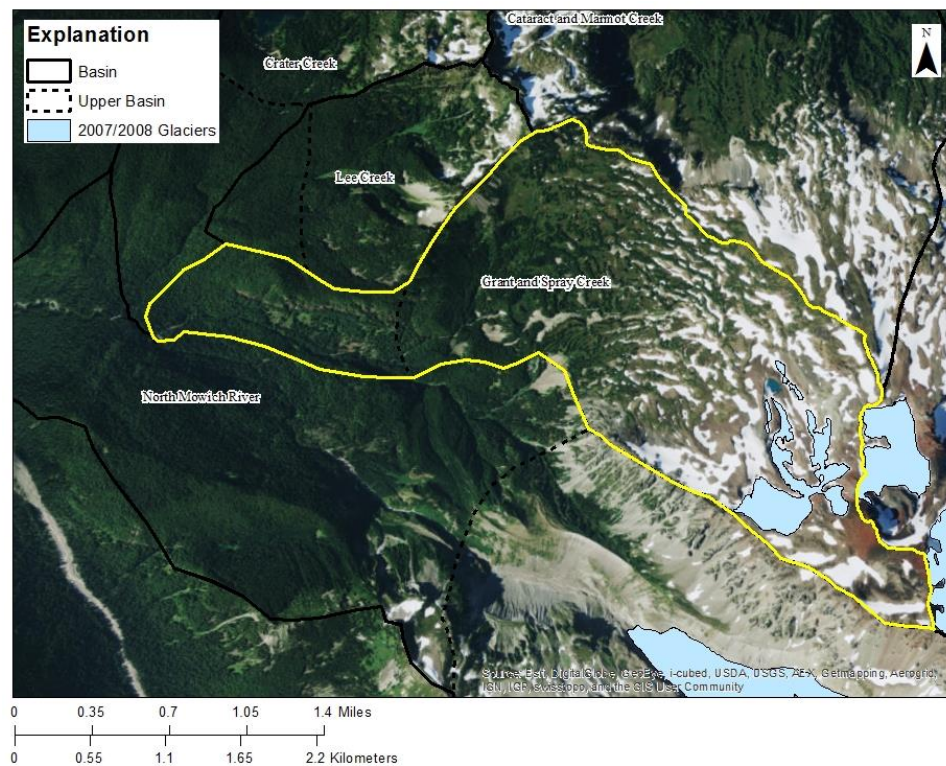


Figure 21. Grant and Spray creek basins outlined in yellow, other basins outlined in black, the upper basin outlined in dashed black, glaciers in blue, and initiation sites from Copeland (2009) in purple, Legg (2013) in blue, and this study in orange. No debris flow occurred in this drainage basin.

4.8.2 2006 Event

This drainage did not have any evidence of debris flow on Google Earth (Figure 22a and b). This drainage was not investigated in the field since strong evidence against debris flow was collected using imagery.

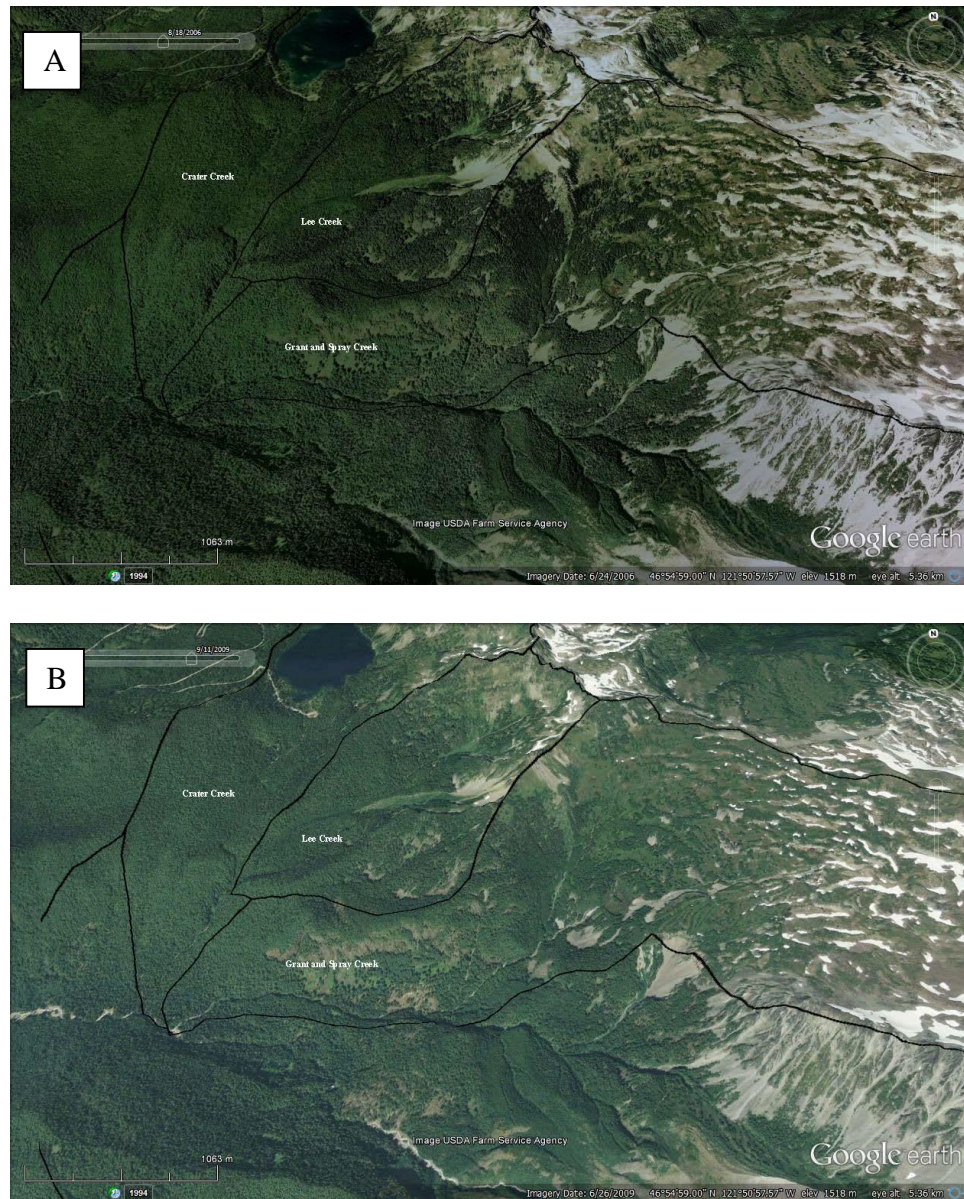


Figure 22. a) Google Earth image of Grant and Spray Drainage in August 2006. b) Google Earth image of Grant and Spray Drainage in September 2009.

4.8.3 Basin Attributes

The total basin area for this drainage is 7.4 km², while the upper basin is 6.3 km². In the upper basin, 34% of slopes are steeper than 33°. The gradient of the upper basin is 30% while the gradient of the whole basin is 26%. Flett Glacier is located in the upper basin but does not directly feed Grant or Spray creeks. It covers about 5% of the upper basin. About a third of the upper basin is covered with vegetation, at 35%. The geology is 48% bedrock and 47% surficial deposits. During the 2006 event, the upper basin received an average sum of 32.1 cm.

4.9 Inter Fork Drainage Basin

4.9.1 Introduction

Inter Fork River Basin is located on the northeast side of the mountain, between West Fork of the White River and Lodi basins to the west and northwest, and White River Basin to the southeast (Figure 23). The basin is well-defined by ridges on most sides and 8.5 km long. Its highest elevation is 2961 m and the lowest elevation is 1253 m where Inter Fork River meets the White River. The drainage is easily accessed by the Glacier Basin Trail, which comes off of the Wonderland Trail at the bottom of the basin, near the White River/Inter Fork River confluence.

Very little evidence exists for recent debris flow history in this drainage. Copeland (2009) documents that this is the first known debris flow in this drainage in recorded history. Remnants of the Osceola Mudflow can be found in the Inter Fork drainage (Vallance and Scott, 1997).

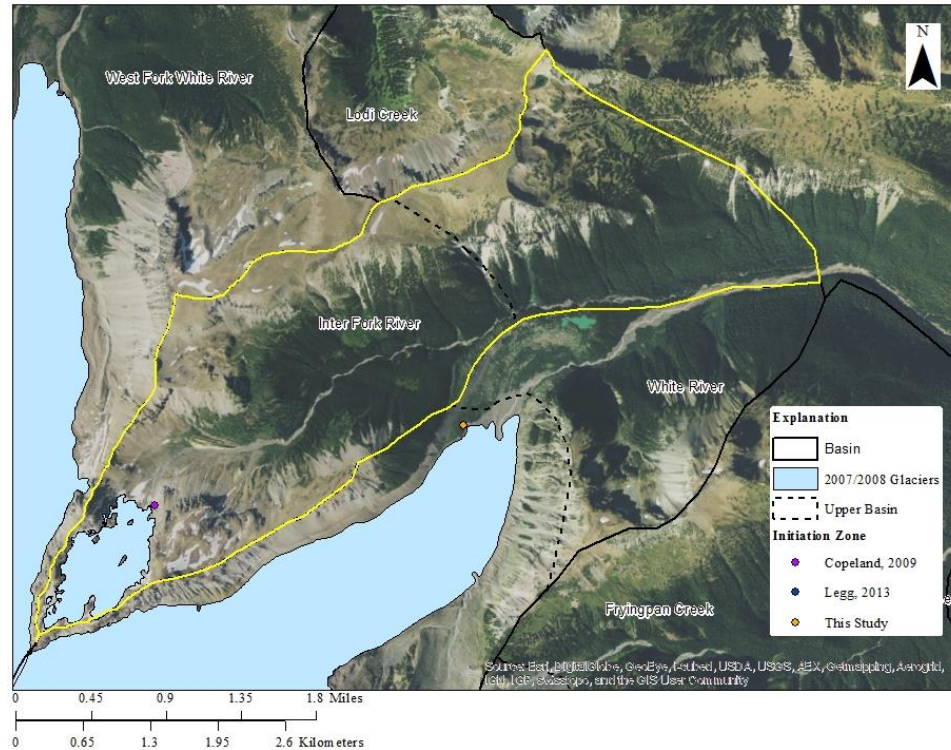


Figure 23. Inter Fork River basin outlined in yellow, other basins outlined in black, the upper basin outlined in dashed black, glaciers in blue, and initiation sites from Copeland (2009) in purple, Legg (2013) in blue, and this study in orange.

4.9.2 2006 Event

Copeland (2009) documented a debris flow in the basin during the 2006 rainstorm event. Brief reconnaissance was conducted during the summer of 2013 to collect photographs showing major erosional features from the debris flow and deposits of boulders in forested areas (Figure 24a and b). The initiation site occurs at 2210 m elevation, just to the north of the end of the glacier and received a total of 28.9 cm of rain during the two-day event (Figure 23).



Figure 24. a) Photograph of boulders and mud deposited by the debris flow that buried trees in the upper basin. b) Major erosion in the drainage due to the 2006 event.

4.9.3 Basin Attributes

The total basin area for this drainage is 14.1 km², while the upper basin is 8.8 km². In the upper basin, 55% of slopes are steeper than 33°. The gradient of the upper basin is 24% while the gradient of the whole basin is 20%. Most of the Inter Glacier is contained in the upper basin, which directly supplies the Inter Fork River. It occupies 8% of the upper basin. The glacier retreated a distance of 108.3 m and reduced by 16% in surface area between 1994 and 2007/2008. Slightly less than half of the upper basin is covered by vegetation, at 42%. The geology is 39% bedrock and 52% surficial deposits. During the rainstorm event, the upper basin received 27.8 cm of rain.

4.10 Kautz Drainage Basin

4.10.1 Introduction

Kautz Creek Basin is located on the south side of the mountain, between Pyramid and Tahoma basins to the west, and Van Trump Falls Basin to the east (Figure 4 and Figure 25). The basin is well-defined by ridges on the east side, but runs adjacent to Pyramid Creek to the east most of the distance to their confluence. The basin is 16.6 km long. Its highest elevation is 4311 m and the lowest elevation is 673 m where Kautz Creek meets Pyramid Creek. The lower drainage is easily accessed by the Wonderland Trail.

There have been at least 12 debris flows initiated in this drainage since 1650 (Legg, 2013). Grater (1947) documents a debris flow event, which initiated through heavy rainfall. The pulses of the debris flow were documented as pulses which were a result of the temporary damming at Box Canyon. This debris flow mobilized 40 million

m³ of material (Crandell, 1971). Another debris flow was documented by Legg (2013), which occurred a year later. It initiated by Kautz Glacier and crossed the drainage divide into Van Trump drainage. More recently, a debris flow was documented in 2005 by Copeland (2009), which initiated from Pyramid Glacier and flowed into Kautz drainage.

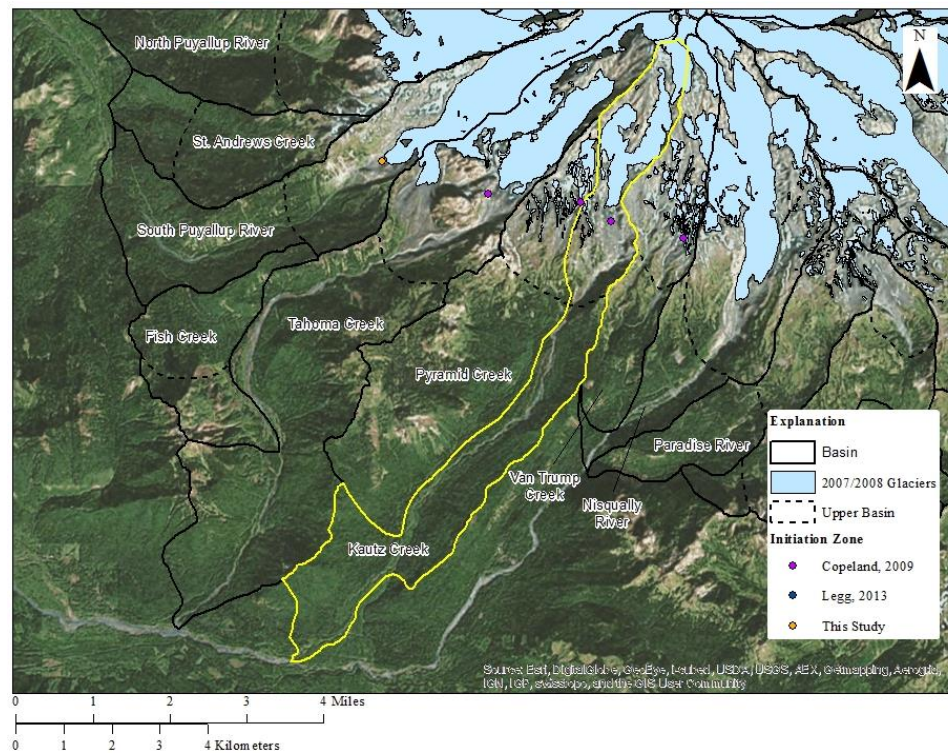


Figure 25. Kautz Creek basin outlined in yellow, other basins outlined in black, the upper basin outlined in dashed black, glaciers in blue, and initiation sites from Copeland (2009) in purple, Legg (2013) in blue, and this study in orange.

4.10.2 2006 Event

Copeland (2009) documented a debris flow in the basin during the 2006 rainstorm event. No reconnaissance was conducted in this drainage as the upper basin is a little more difficult to access, and efforts were better spent elsewhere. The initiation site was documented by Copeland (2009). It occurs at 1960 m elevation, just south of the glacier

in proglacial material, and received a total of 32.5 cm of rain during the two-day event. (Figure 25).

4.10.3 Basin Attributes

The total basin area for this drainage is 17.2 km², while the upper basin is 6.1 km². In the upper basin, 30% of slopes are steeper than 33°. The gradient of the upper basin is 49% while the gradient of the whole basin is 22%. Most of the Kautz-Success Glacier is contained in the upper drainage, in addition to parts of the Pyramid and Nisqually glaciers. Collectively, they occupy 33% of the upper basin. The glacier retreated a distance of 62.8 m and reduced by 3% in surface area between 1994 and 2007/2008. There is very little vegetation in the upper basin, covering at 8%. The geology is 34% bedrock and 33% surficial deposits. During the rainstorm event, the upper basin received 33.1 cm of rain.

4.11 Lee Drainage Basin

4.11.1 Introduction

Lee Creek Basin is located on the northwest side of the mountain, with Crater Creek to the northwest and west, Cataract and Marmot basins to the east, and Grant and Spray basins to the south (Figure 4 and Figure 26). The drainage is fairly well-defined by ridges on most sides and is 2.6 km long. Its highest elevation is 1985 m and the lowest elevation is 1181 m where Lee Creek flows into Crater Creek. The basin is easily accessed by hiking the Spray Park Trail from Mowich Lake.

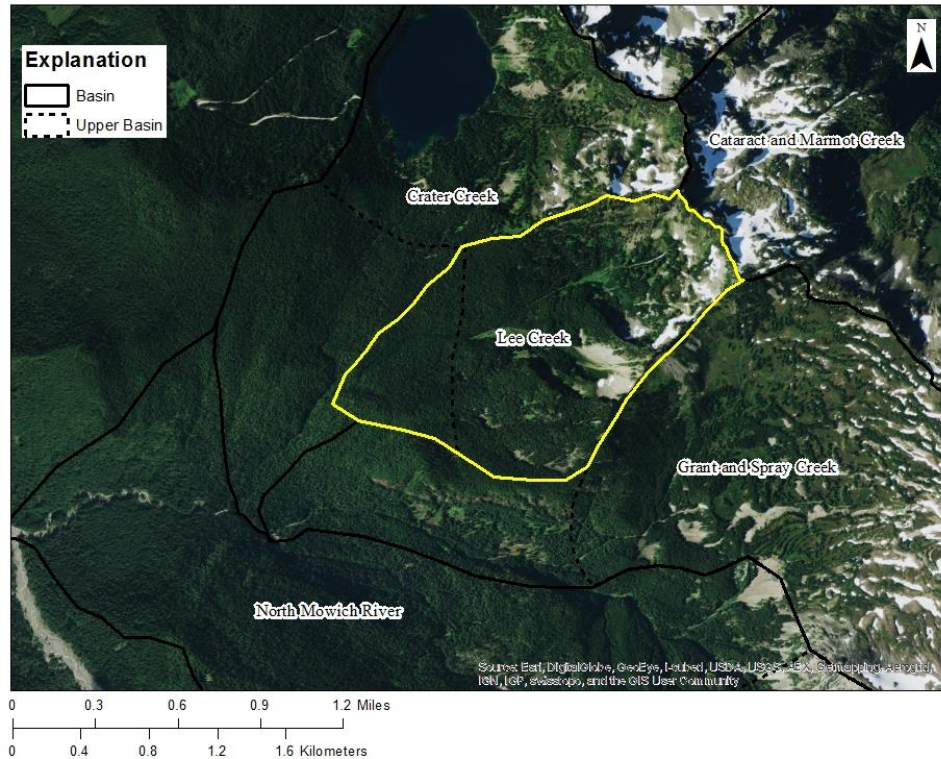


Figure 26. Lee Creek basin outlined in yellow, other basins outlined in black.

4.11.2 2006 Event

This drainage did not have any evidence of debris flow on Google Earth (Figure 27a and b). This drainage was not investigated in the field since strong evidence against debris flow was collected using imagery.

4.11.3 Basin Attributes

The total basin area for this drainage is 2.3 km², while the upper basin is 1.9 km². In the upper basin, 31% of slopes are steeper than 33°. The gradient of the upper basin is 35% while the gradient of the whole basin is 31%. No glaciers are located in this basin. More than three quarters of the upper basin is covered by vegetation, at 81%. The geology is 78% bedrock and 23% surficial deposits. During the 2006 event, the upper basin received an average sum of 28.3 cm.

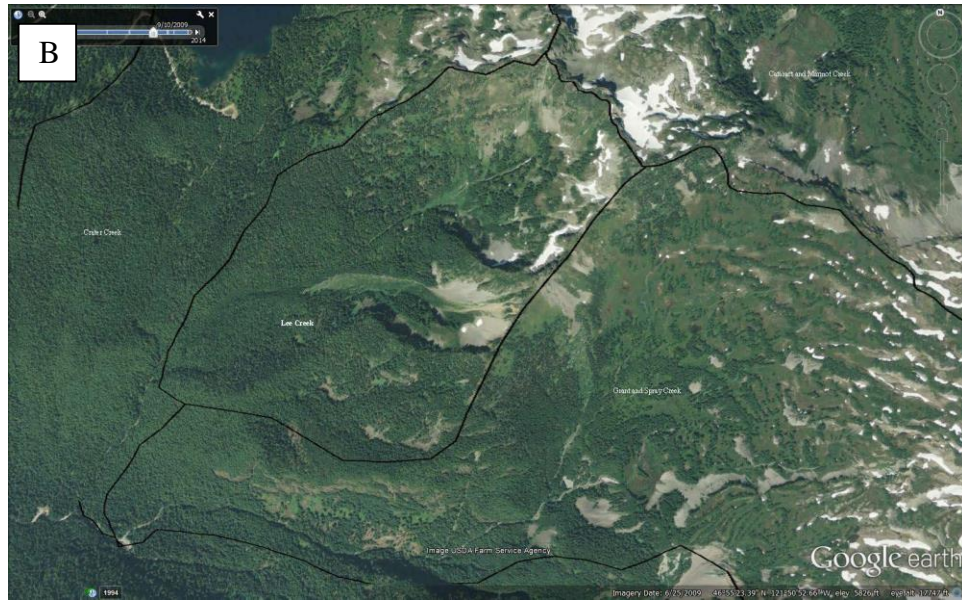


Figure 27. a) Google Earth image of Lee Drainage in August 2006. b) Google Earth image of Lee Drainage in September 2009.

4.12 Lodi Drainage Basin

4.12.1 Introduction

Lodi Creek Basin is located on the northeast side of the mountain, with West Fork of the White Basin to the west, and Inter Fork Basin to the south (Figure 4 and Figure

28). The drainage is fairly well-defined by ridges on most sides and is 6.2 km long. Its highest elevation is 2249 m and the lowest elevation is 1061 m just above where Lodi Creek flows into West Fork of the White River. The basin is easily accessed by hiking the Northern Loop Trail.

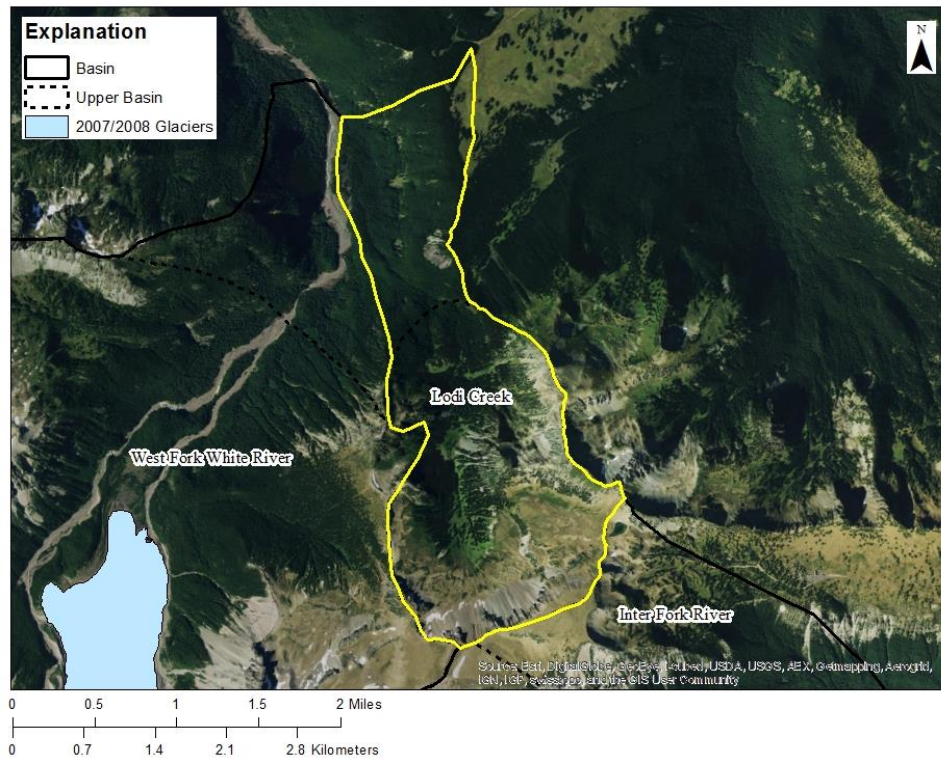


Figure 28. Lodi Creek basin outlined in yellow, other basins outlined in black.

4.12.2 2006 Event

This drainage did not have any evidence of a debris flow on Google Earth (Figure 29a and b). This drainage was not investigated in the field since strong evidence against debris flow was collected using imagery.

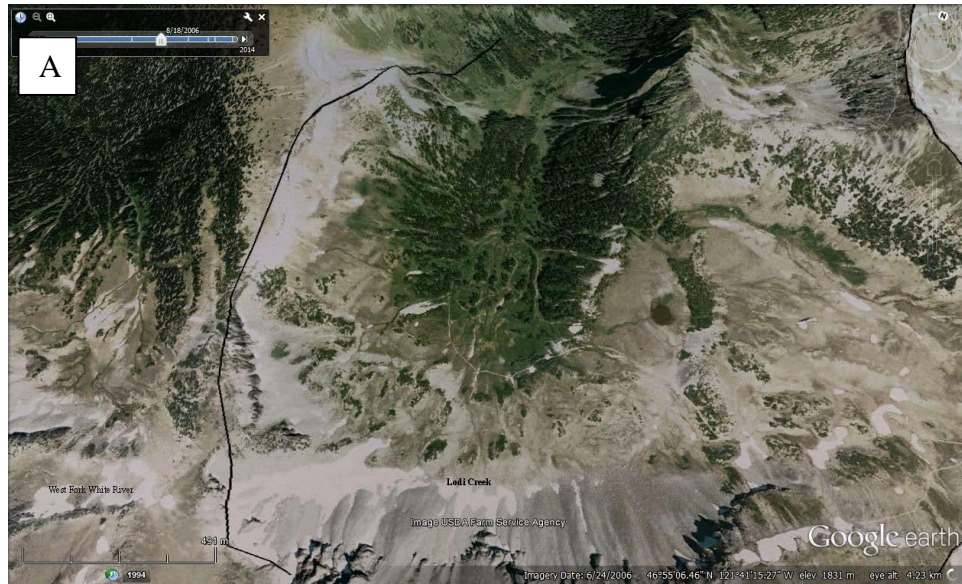


Figure 29. a) Google Earth image of Lodi Drainage in August 2006. b) Google Earth image of Lodi Drainage in September 2009.

4.12.3 Basin Attributes

The total basin area for this drainage is 7.9 km², while the upper basin is 5.4 km². In the upper basin, 49% of slopes are steeper than 33°. The gradient of the upper basin is 19% while the gradient of the whole basin is 19%. No glaciers are located in this basin. A little less than half the upper basin is covered by vegetation, at 49%. The geology is 33%

bedrock and 67% surficial deposits. During the 2006 event, the upper basin received an average sum of 21.7 cm.

4.13 Muddy Fork Cowlitz Drainage Basin

4.13.1 Introduction

Muddy Fork Cowlitz River Basin is located on the southeast side of the mountain, with White River Basin to the north, Basalt Basin to the northeast, and Nisqually, Paradise, and Williwakas basins to the southwest (Figure 4 and Figure 30). The drainage is somewhat well-defined by ridges on most sides and is 9.7 km long. Its highest elevation is 4280 m and the lowest elevation is 1105 m just above where Basalt Creek flows into the Muddy Fork Cowlitz River. No trails come close to the drainage, but it may be accessed by hiking up the channel.

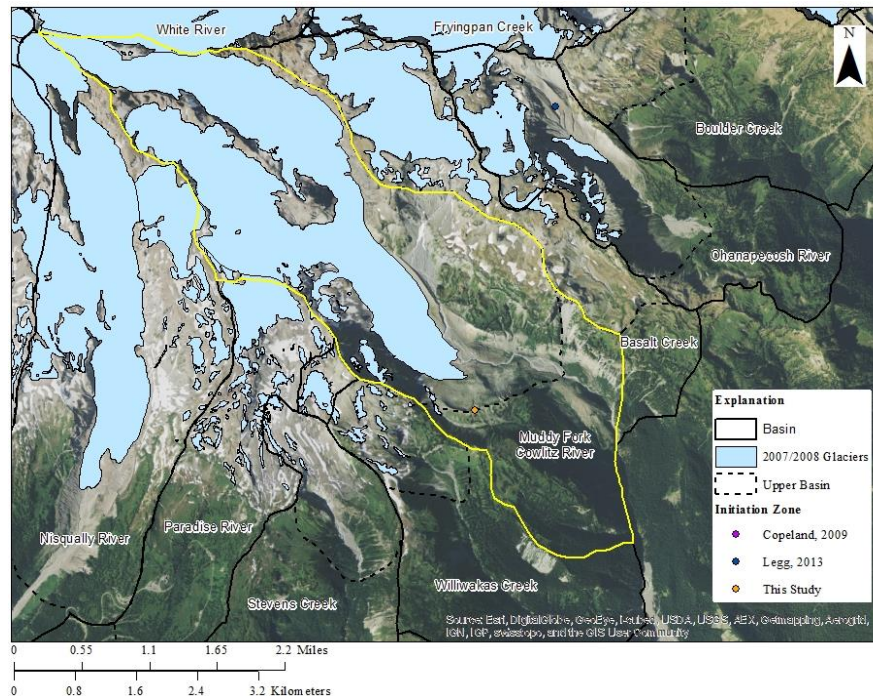


Figure 30. Muddy Fork Cowlitz basin outlined in yellow, other basins outlined in black, the upper basin outlined in dashed black, glaciers in blue.

The Muddy Fork Cowlitz River has long reaches that are controlled by bedrock (Czuba et al., 2012). It shows little evidence of recent or previous debris flow activity (Czuba et al., 2012).

4.13.2 2006 Event

I was unable to get into this drainage during my field reconnaissance, as it is more remote than some of the other drainages. I relied entirely on aerial photography and lidar. There was evidence of landslides along the south sidewall of the upper drainage between 2006 and 2009 imagery, which was assumed to have initiated due to the 2006 event (Figure 31a and b). I chose this location as the initiation site. It occurs at 1697.5 m and received 28.7 cm of rain during the event. Below this, some vegetation has been removed and some small channels have formed in the sidewall, which may have contributed sediment to a debris flow (Figure 32a and b). Slightly lower down in the drainage, the main channel avulsed and wiped out a section of vegetation.

Since all evidence was collected using aerial photographs and lidar, I ran this drainage as a "yes" and a "no" through the regression analysis in order to determine which results yielded the most accurate predictive model.

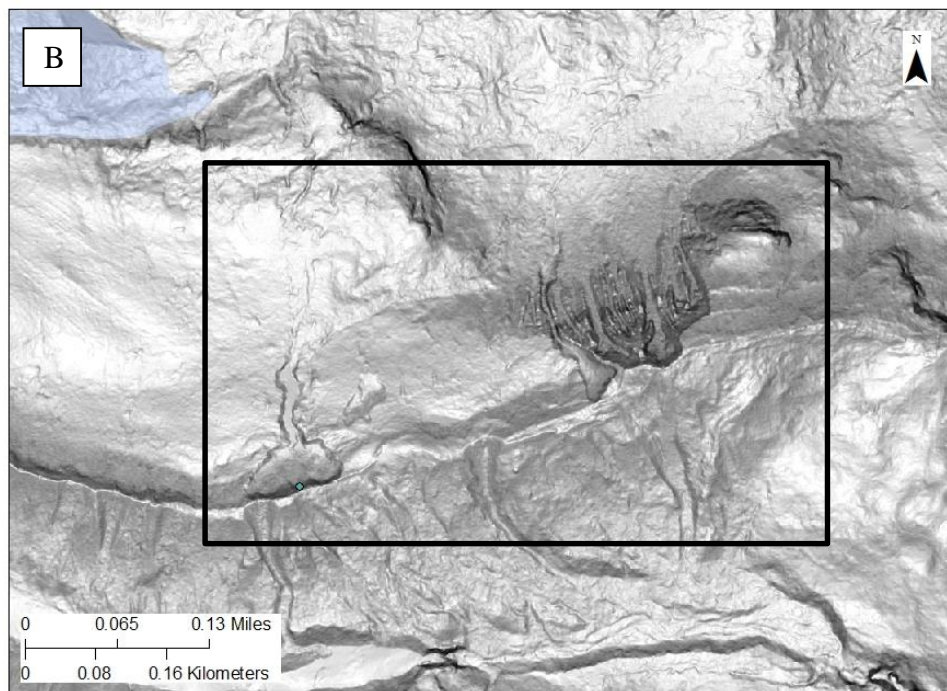
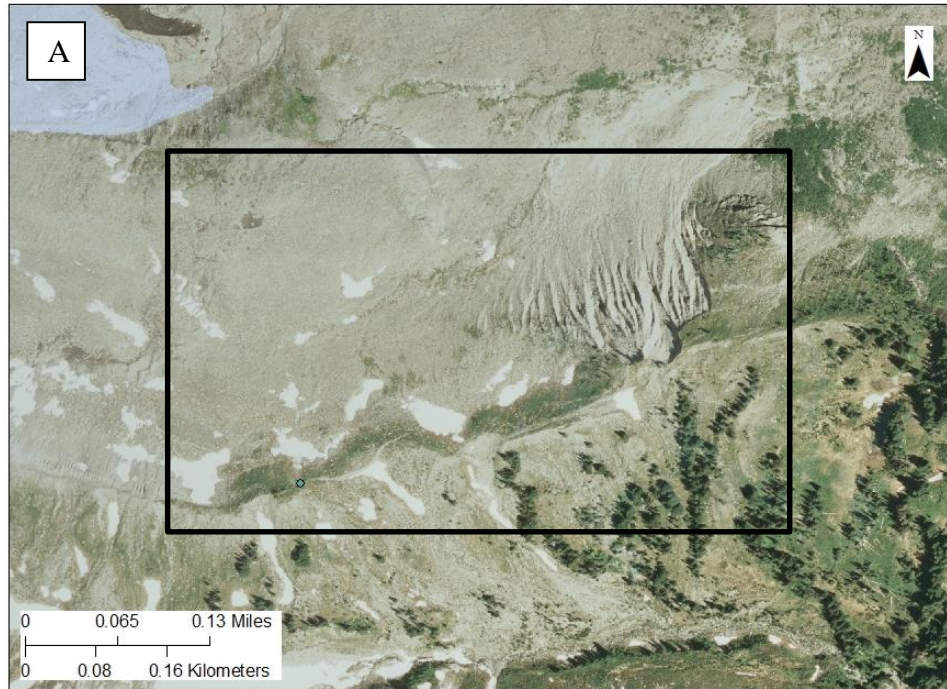


Figure 31. a) Initiation site in 2006. b) Initiation site in 2008 along the sidewall of the upper drainage of Muddy Fork Cowlitz River. This was chosen as the initiation site for this drainage.

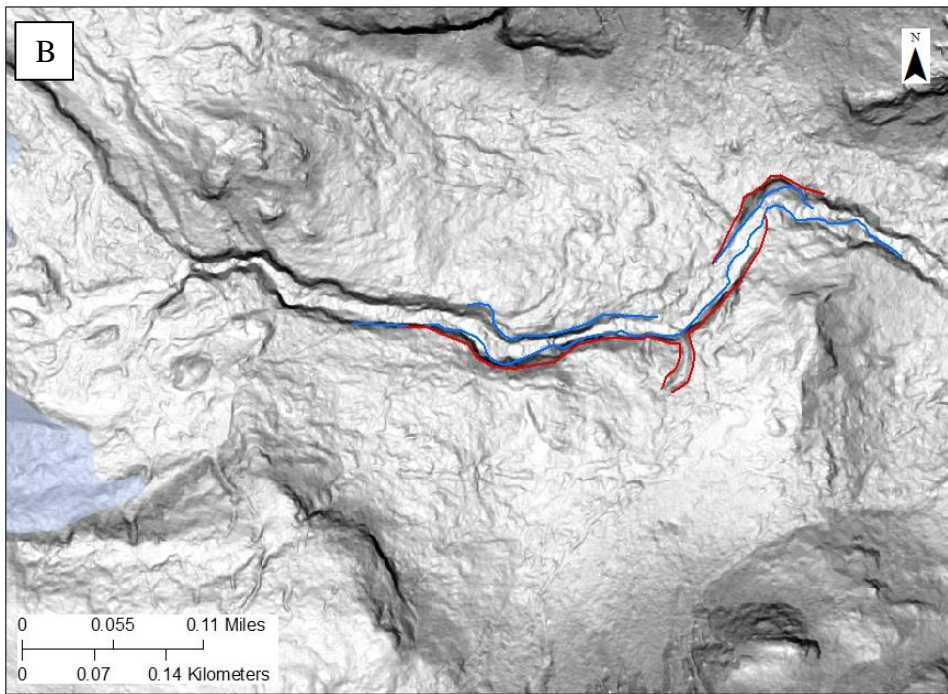


Figure 32. a) Muddy Fork Cowlitz channel in 2006 (blue). b) Muddy Fork Cowlitz channel erosion in the upper channel between 2006 (blue outline) and 2008 (red outline) assumed to be caused by 2006 event.

4.13.3 Basin Attributes

The total basin area for this drainage is 19 km², while the upper basin is 14.6 km². In the upper basin, 58% of slopes are steeper than 33°. The gradient of the upper basin is 34% while the gradient of the whole basin is 33%. Most of the Cowlitz-Ingraham Glacier is contained within the upper basin, which directly supplies the Muddy Fork Cowlitz River. Small sections of the Paradise, Nisqually, and Emmons glaciers are also contained in the upper basin. Collectively, the glaciers occupy 51% of the upper basin. The glacier retreated a distance 212.8 m and reduced by 4% in surface area between 1994 and 2007/2008. A small percentage of the upper basin is covered in vegetation, at 4%. The geology is 33% bedrock and 12% surficial deposits. During the rainstorm event, the upper basin received 31.2 cm of rain.

4.14 Nisqually Drainage Basin

4.14.1 Introduction

Nisqually River Basin located on the south side of the mountain, with Van Trump Basin to the west and Muddy Fork and Paradise basins to the west (Figure 4 and Figure 33). The drainage is well-defined by ridges on most sides and is 10.9 km long. Its highest elevation is 4331 m while the lowest is 959 m where the Paradise River flows into the Nisqually. Many trails occur along the east ridge and the lower basin is easily seen and accessed by road.

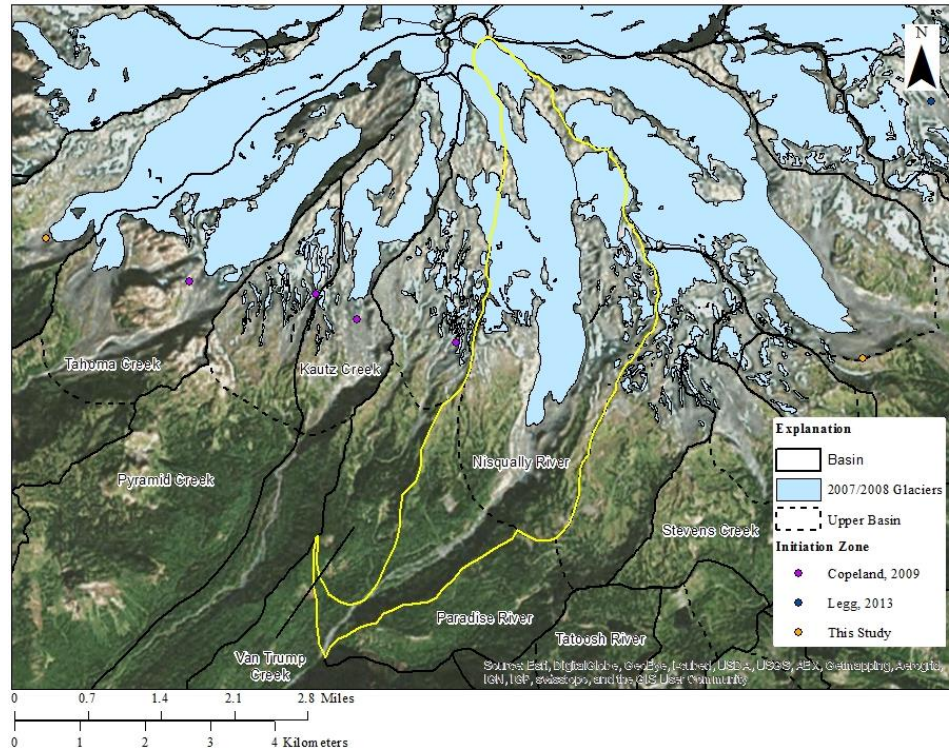


Figure 33. Nisqually Basin outlined in yellow, other basins outlined in black, the upper basin outlined in dashed black, glaciers in blue, and initiation sites from Copeland (2009) in purple, Legg (2013) in blue, and this study in orange. No debris flow occurred in this drainage basin.

4.14.2 2006 Event

There was some vegetation removal from slightly lower regions of the drainage, but the upper drainage shows some evidence of debris flow activity, however, Paul Kennard, Mount Rainier National Park geomorphologist reports that there was no debris flow activity in the upper basin (Figure 34a and b). It is possible there was a debris flow earlier in the event and subsequent erosion from flooding or hyperconcentrated flows removed any evidence of a debris flow.

While Nisqually may not have produce a debris flow in 2006, it has produced debris flows on multiple occasions in recent history. The Cascade Volcano Observatory (2014) has reported that debris flows have destroyed bridges spanning the river at least

four times between 1926 and 1955. Additionally, debris flows have also initiated in the Van Trump drainage and reached the confluence with Nisqually in the past. In prehistoric times, the National Lahar flowed down Nisqually drainage about 2,200 to 2,300 years ago (Cascade Volcano Observatory, 2014).



Figure 34. a) Google Earth image of Lodi Drainage in August 2006. b) Google Earth image of the drainage in September 2009.

4.14.3 Basin Attributes

The total basin area for this drainage is 17.7 km², while the upper basin is 14 km². In the upper basin, 51% of slopes are steeper than 33°. The gradient of the upper basin is 42% while the gradient of the whole basin is 31%. Most of the Nisqually Glacier is contained within the upper basin, which directly supplies the Nisqually River. Small sections of the Van Trump and Cowlitz-Ingraham glaciers are also contained in the upper basin. Collectively, the glaciers occupy 35% of the upper basin. The glacier retreated a distance 168.5 m and reduced by 20% in surface area between 1994 and 2007/2008. A small percentage of the upper basin is covered in vegetation, at 16%. The geology is 32% bedrock and 23% surficial deposits. The overall sum of glacier, bedrock, and surficial deposits make about 90% when they should occupy 100% of the basin. The discrepancy occurs in this basin because there is bedrock that outcrops within the body of the glacier that was unaccounted for in both the DNR and my visual mapping. During the rainstorm event, the upper basin received 33 cm of rain.

4.15 North Mowich Drainage Basin

4.15.1 Introduction

North Mowich River Basin is located on the northwest side of the mountain, with Carbon, Grant and Spray basins, and Crater Basin to the north and northeast, and South Mowich Basin to the south (Figure 4 and Figure 35). The drainage is well-defined by ridges on most sides and is 10.5 km long. Its highest elevation is 4223 m while the lowest is 790 m at the confluence of North and South Mowich. The basin is not easily accessed by any trail, and hiking up from the lower drainage is difficult.

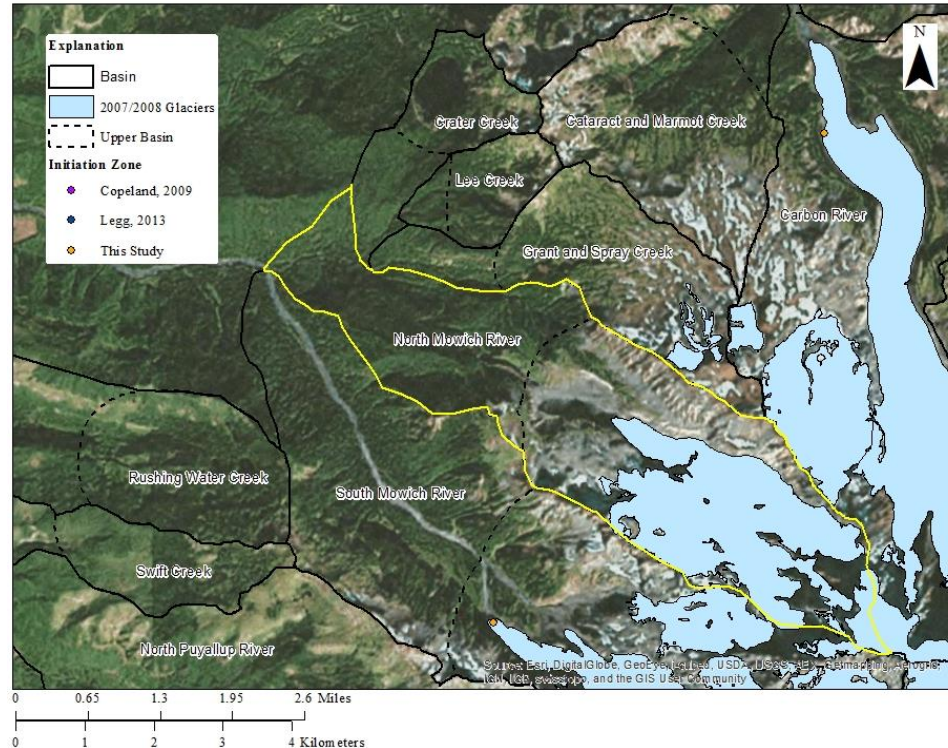


Figure 35. North Mowich basin outlined in yellow, other basins outlined in black, the upper basin outlined in dashed black, glaciers in blue, and initiation sites from Copeland (2009) in purple, Legg (2013) in blue, and this study in orange. No debris flow was recorded in this drainage basin.

4.15.2 2006 Event

Lidar and aerial photos showed little evidence of debris flow activity (Figure 36a and b). The upper basin was extremely difficult to get to from the lower basin, as there was too much tree blow down to hike from that direction. The upper basin is accessed by other off-trail routes, but I was unable to access the upper basin due to time constraints. Since evidence showing debris flow activity on aerial photos was minimal, I concluded that there was no 2006 debris flow, and I spent time on other drainages in the field. Little debris flow activity has been recorded in this drainage in recent history.

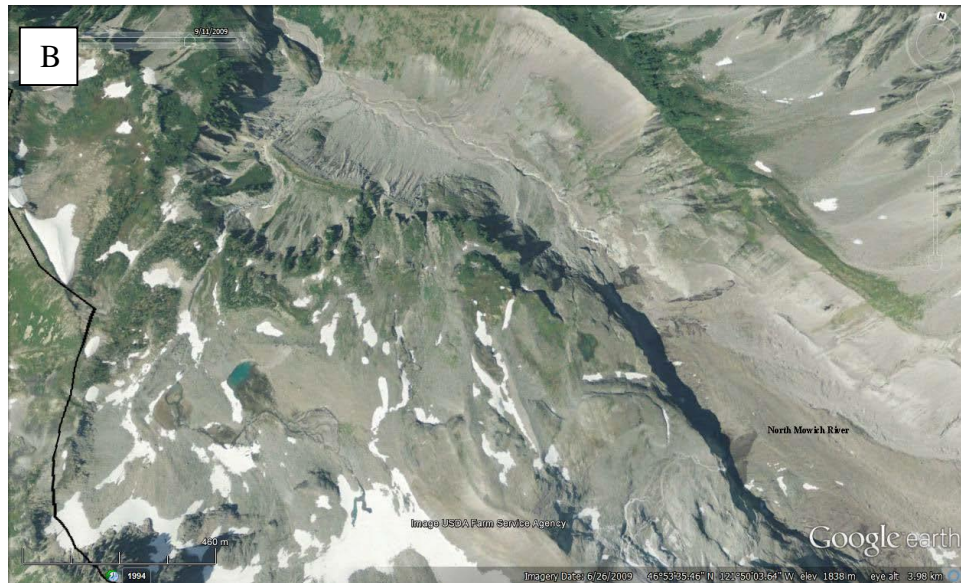
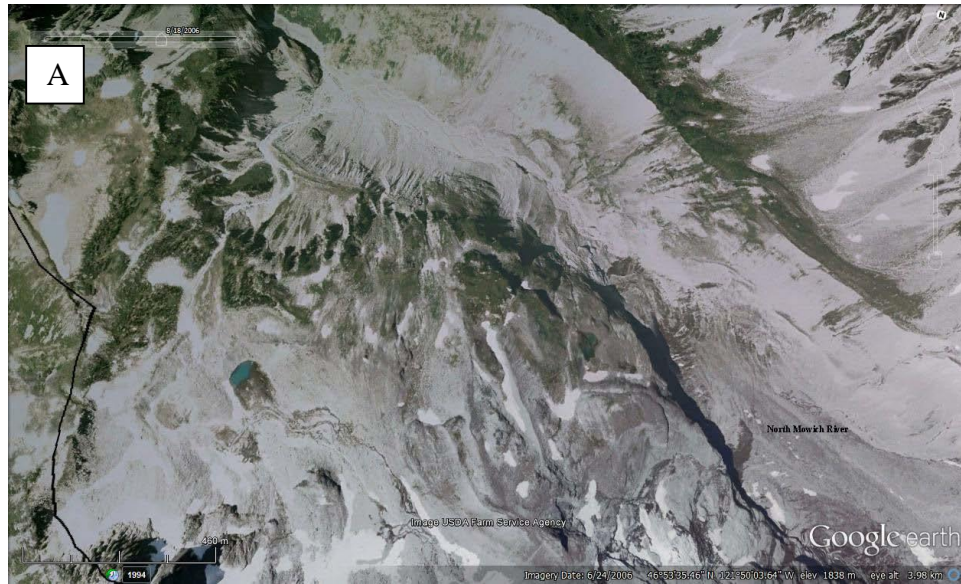


Figure 36. a) Google Earth image of the drainage in August 2006. b) Google Earth image of the drainage in September 2009.

4.15.3 Basin Attributes

The total basin area for this drainage is 19.3 km², while the upper basin is 12.6 km². In the upper basin, 64% of slopes are steeper than 33°. The gradient of the upper basin is 37% while the gradient of the whole basin is 33%. Most of the North Mowich Glacier is contained within the upper basin, which directly supplies the North Mowich

River. Small sections of the Edmunds, Russell, and Liberty Cap glaciers are also contained in the upper basin. Collectively, the glaciers occupy 43% of the upper basin. The glacier retreated 262.9 m and reduced by 11% in surface area between 1994 and 2007/2008. A small percentage of the upper basin is covered in vegetation, at 6%. The geology is 20% bedrock and 40% surficial deposits. During the rainstorm event, the upper basin received 33.7 cm of rain.

4.16 North Puyallup Drainage Basin

4.16.1 Introduction

North Puyallup River Basin is located on the west side of the mountain, South Mowich Basin to the north, and St. Andrews and South Puyallup basins to the south (Figure 4 and Figure 37). The drainage is well-defined by ridges on most sides and is 11.9 km long. Its highest elevation is 3167 m while the lowest is 709 m just above the confluence of North and South Puyallup rivers. The basin is easily accessed by hiking the West Side Road and North Puyallup Trail. Little debris flow activity has been recorded in this drainage in recent history.

4.16.2 2006 Event

During initial field reconnaissance, it was difficult to determine if there had been a debris flow. Post reconnaissance, I examined aerial photos more closely and noticed there was a significant amount of vegetation removed from the upper basin (Figure 38a and b). During the summer of 2014, Paul Kennard conducted field reconnaissance and found evidence of debris flow (Figure 39).

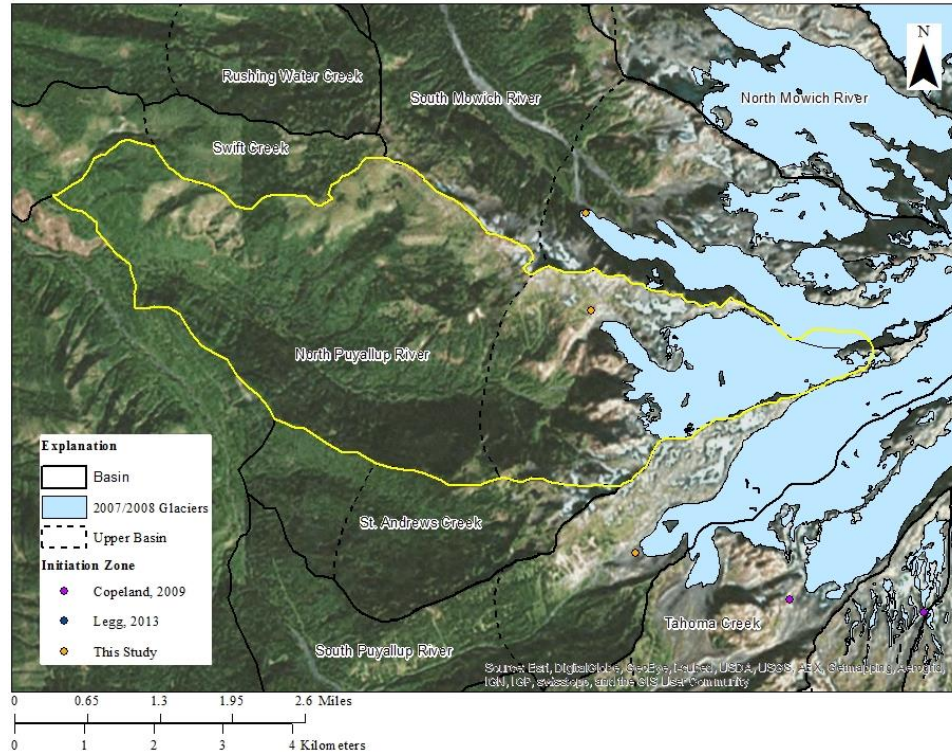


Figure 37. North Puyallup basin outlined in yellow, other basins outlined in black, the upper basin outlined in dashed black, glaciers in blue, and initiation sites from Copeland (2009) in purple, Legg (2013) in blue, and this study in orange.

There looks like a small failure on a sidewall adjacent to the glacier (Figure 40a and b). It is highly possible that there was a significant part of entrainment before the debris flow reached the patches of vegetation that were removed. Additionally, Paul Kennard suspects there may have been a debris flow initiated from the center drainage as well, but no failure was noted, and it was difficult to examine that drainage on aerial photos. It occurs at 1812.6 m elevation and received a total of 36 cm during the two-day event.



Figure 38. a) Google Earth image of the drainage in August 2006. b) Google Earth image of the drainage in September 2009.



Figure 39. Both photos are evidence of debris flow levee(s) and new vegetation growth in the upper North Puyallup basin provided by Paul Kennard, Mt. Rainier National Park Geomorphologist.

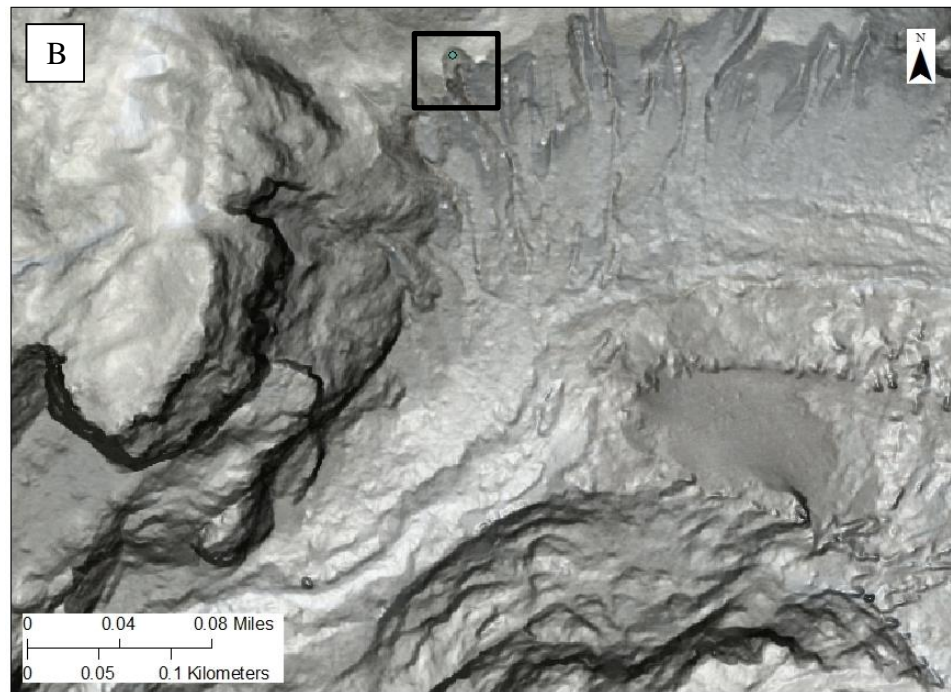
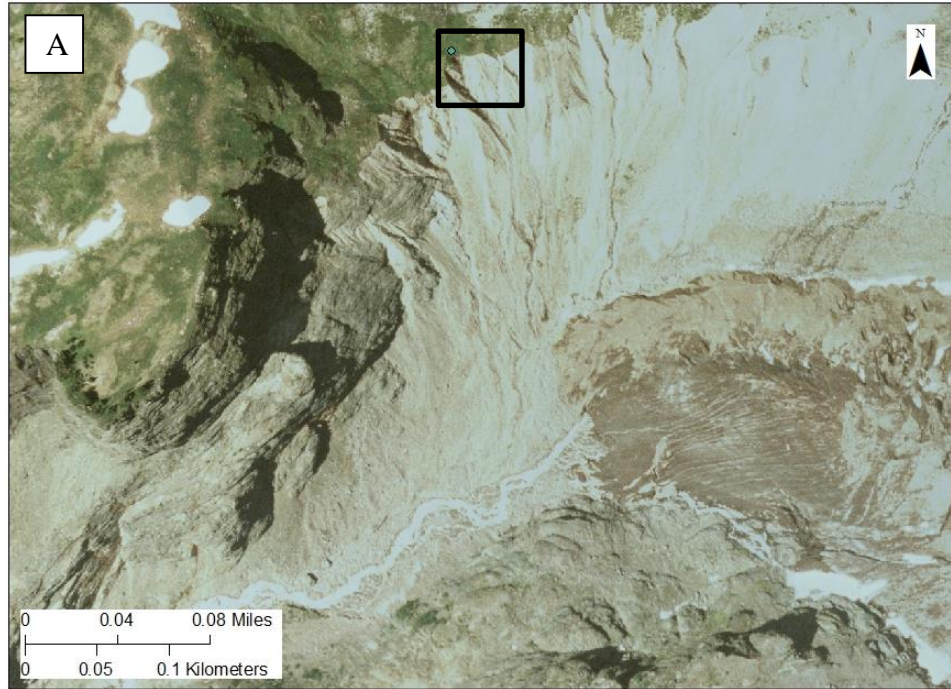


Figure 40. a) Initiation site in 2008 indicated by blue dot inside of box. b) Initiation site in 2008 indicated by blue dot.

4.16.3 Basin Attributes

The total basin area for this drainage is 29.5 km², while the upper basin is 10.8 km². In the upper basin, 66% of slopes are steeper than 33°. The gradient of the upper basin is 37% while the gradient of the whole basin is 21%. Part of the South Mowich Glacier is also contained in the upper basin. Collectively, the glaciers occupy 34% of the upper basin. The glacier retreated 135.1 m and reduced by 11% in surface area between 1994 and 2007/2008. A small percentage of the upper basin is covered in vegetation, at 11%. The geology is 43% bedrock and 24% surficial deposits. During the rainstorm event, the upper basin received 33.3 cm of rain.

4.17 Ohanapecosh Drainage Basin

4.17.1 Introduction

Ohanapecosh River Basin is located on the northeast side of the mountain, between Boulder and Fryingpan basins to the north and northwest, and Basalt Creek Basin to the southeast (Figure 4 and Figure 41). The basin is well-defined by ridges on most sides and 6.7 km long. Its highest elevation is 2836 m and the lowest elevation is 1140 m where Ohanapecosh River and Boulder Creek meet. The upper basin is easily accessed by the Wonderland Trail. Little debris flow activity has been recorded in this drainage in recent history.

4.17.2 2006 Event

Legg (2013) documented a debris flow and identified the initiation site in the basin during the 2006 rainstorm event. The initiation site was identified using aerial

imagery. It occurred in a proglacial gully which expanded between 2006 and 2008. Other evidence includes deposits outside the existing channel. The initiation site occurs at 2058 m elevation. The site received a total of 27.7 cm of rain during the two-day event.

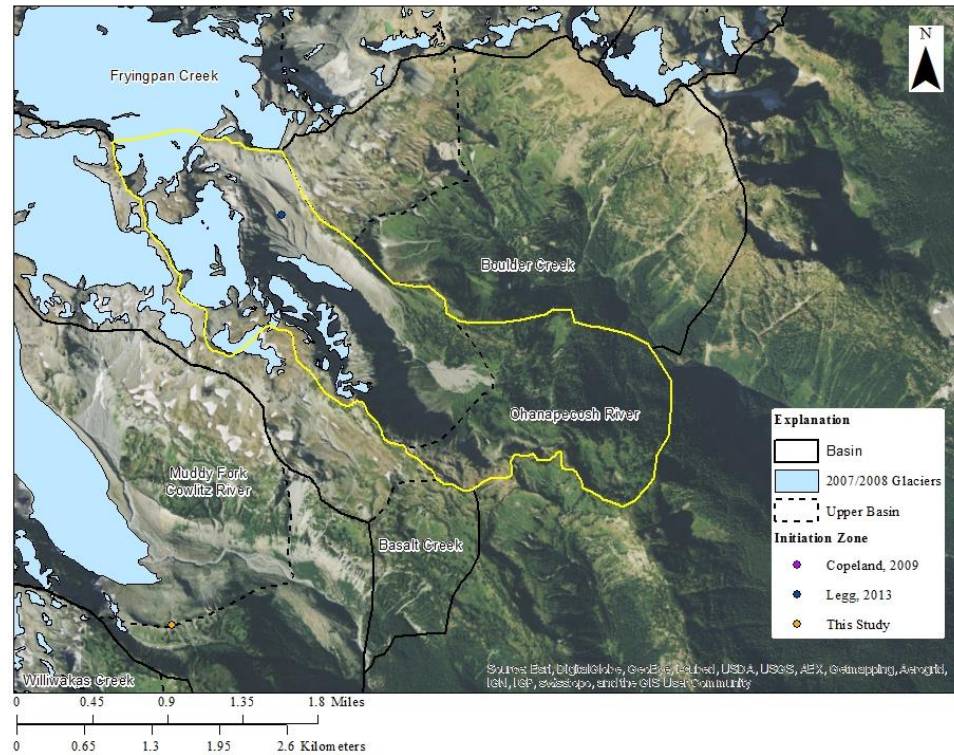


Figure 41. Ohanapeosh River basin outlined in yellow, other basins outlined in black, the upper basin outlined in dashed black, glaciers in blue, and initiation sites from Copeland (2009) in purple, Legg (2013) in blue, and this study in orange.

4.17.3 Basin Attributes

The total basin area for this drainage is 8.0 km², while the upper basin is 5.1 km². In the upper basin, 65% of slopes are steeper than 33°. The gradient of the upper basin is 23% while the gradient of the whole basin is 26%. Most of the Ohanapeosh Glacier is contained in the upper basin, which directly supplies the Ohanapeosh River. It occupies 27% of the upper basin. The glacier retreated a distance of 35.7 m and reduced by 11% in surface area between 1994 and 2007/2008. Some of the upper basin is covered by

vegetation, at 12%. The geology is 28% bedrock and 40% surficial deposits. During the rainstorm event, the upper basin received 27.7 cm of rain.

4.18 Paradise Drainage Basin

4.18.1 Introduction

Paradise River Basin is located on the south side of the mountain, with Nisqually Basin to the west, Tatoosh and Stevens basins to the south and east, and Muddy Fork Cowlitz Basin to the north (Figure 4 and Figure 42). The drainage is fairly well-defined by ridges on most sides and is 10.7 km long. Its highest elevation is 2583 m and lowest elevation is 953 m where it flows into Nisqually River. The basin is easily accessed by numerous hiking trails.

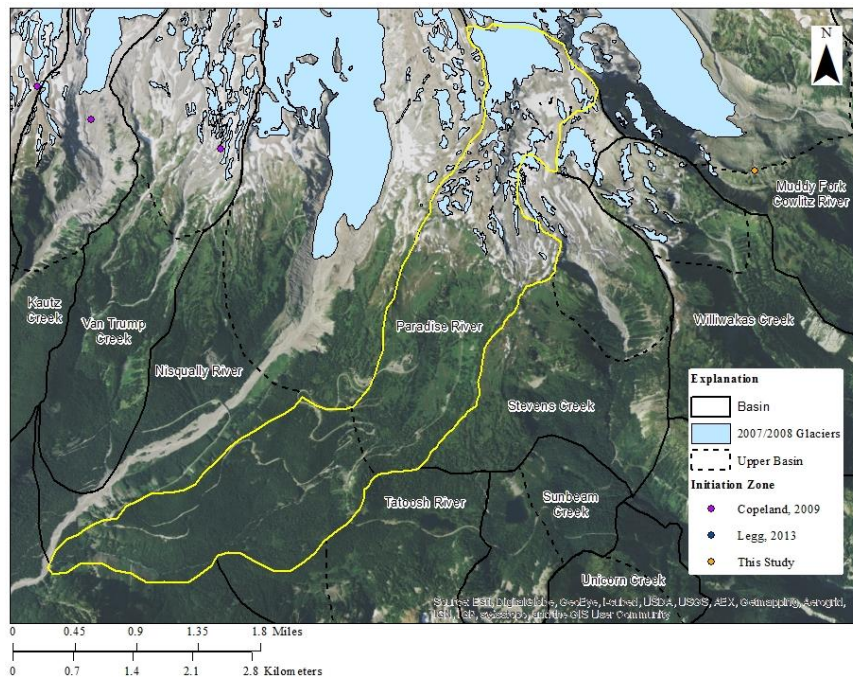


Figure 42. Paradise River basin outlined in yellow, other basins outlined in black, the upper basin outlined in dashed black, glaciers in blue, and initiation sites from Copeland (2009) in purple, Legg (2013) in blue, and this study in orange. No debris flow was recorded in this drainage in 2006.

4.18.2 2006 Event

This drainage did not have any evidence of debris flow on orthophoto or lidar (Figure 43a and b). This drainage was not investigated in the field since strong evidence against debris flow was collected using imagery.



Figure 43. a) Google Earth image of Paradise Drainage in August 2006. b) Google Earth image of Paradise Drainage in September 2009.

4.18.3 Basin Attributes

The total basin area for this drainage is 10.4 km², while the upper basin is 6.3 km². In the upper basin, 23% of slopes are steeper than 33°. The gradient of the upper basin is 18% while the gradient of the whole basin is 15%. Most of Paradise Glacier occurs in this basin, occupying 12% of the upper basin. The glacier retreated a distance of 67 m and reduced by 32% in surface area between 1994 and 2007/2008. About a third of the upper basin is covered with vegetation, at 37%. The geology is 59% bedrock and 23% surficial deposits. During the 2006 event, the upper basin received an average sum of 32.5 cm.

4.19 Pyramid Drainage Basin

4.19.1 Introduction

Pyramid Creek Basin is located on the southwest side of the mountain, with Tahoma Basin to the northwest, and Kautz Basin to the southeast (Figure 4 and Figure 44). The drainage is somewhat well-defined by ridges on the west side but runs adjacent to Kautz Creek to the west most of the distance to their confluence and is 10.7 km long. Its highest elevation is 3140 m and the lowest elevation is 858 m just above its confluence with Kautz Creek. The lower basin is easily accessed by the Wonderland Trail.

The first documented debris flow in this drainage occurred in 2005. It was initiated in a proglacial gully. This site initiated two debris flows historically, one of which flowed into Kautz and the other into another drainage. The debris flows destroyed a backcountry campground.

4.19.2 2006 Event

Copeland (2009) documented a debris flow initiation in this drainage during the 2006 rainstorm event. The same gully that initiated debris flows in 2005 is documented as the initiation site for this event. Copeland (2009) measured the gully between 2006 and 2008 imagery and reports that the gully widened by 0.7 m on average. Slumping in the upper drainage was also identified and likely contributed to initiation in 2006 and previous debris flows. Since debris flows in Kautz and Pyramid interact, it is difficult to distinguish between the two drainages. This debris flow destroyed the same backcountry site as the 2005 debris flow. It has since been relocated. The site occurs at 2243.6 m and received 36.1 cm of rain during the event (Figure 44).

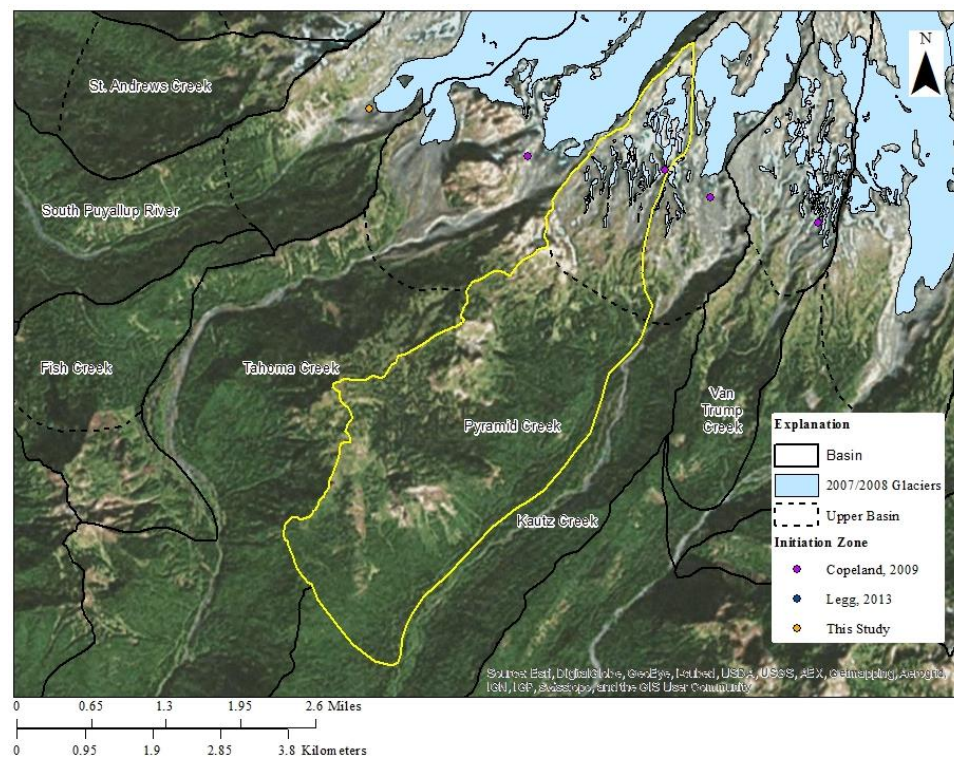


Figure 44. Pyramid River basin outlined in yellow, other basins outlined in black, the upper basin outlined in dashed black, glaciers in blue, and initiation sites from Copeland (2009) in purple, Legg (2013) in blue, and this study in orange.

4.19.3 Basin Attributes

The total basin area for this drainage is 17.5 km², while the upper basin is 3.8 km². In the upper basin, 53% of slopes are steeper than 33°. The gradient of the upper basin is 42% while the gradient of the whole basin is 20%. Most of Pyramid Glacier occurs in this basin, occupying 13% of the upper basin. Some of the upper basin is covered with vegetation, at 15%. The geology is 38% bedrock and 41% surficial deposits. There are discrepancies in the percent glacier, bedrock, and surficial deposit coverage in the upper basin for similar reasons as Nisqually Drainage. During the 2006 event, the upper basin received an average sum of 50.4 cm.

4.20 Rushing Water Drainage Basin

4.20.1 Introduction

Rushing Water Creek Basin is located on the west side of the mountain, with Swift Basin to the south, and South Mowich Basin to the west (Figure 4 and Figure 45). The drainage is fairly well-defined by ridges on most sides and is 10.9 km long. Its highest elevation is 1713 m while the lowest elevation is 546 m where Rushing Water Creek flows into the Mowich River. The Wonderland Trail passes through the upper basin.

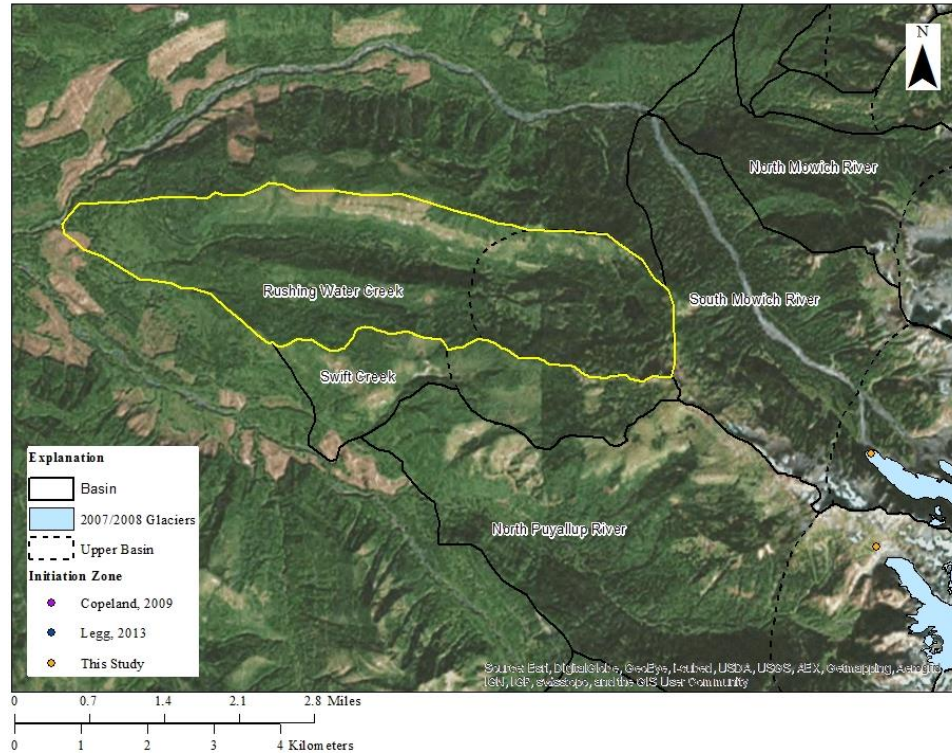


Figure 45. Rushing Water Creek basin outlined in yellow, other basins outlined in black, the upper basin outlined in dashed black, glaciers in blue, and initiation sites from Copeland (2009) in purple, Legg (2013) in blue, and this study in orange. No debris flow occurred in this drainage basin in 2006.

4.20.2 2006 Event

This drainage did not have any evidence of debris flow on orthophoto or lidar (Figure 46a and b). This drainage was not investigated in the field since strong evidence against debris flow was collected using imagery.

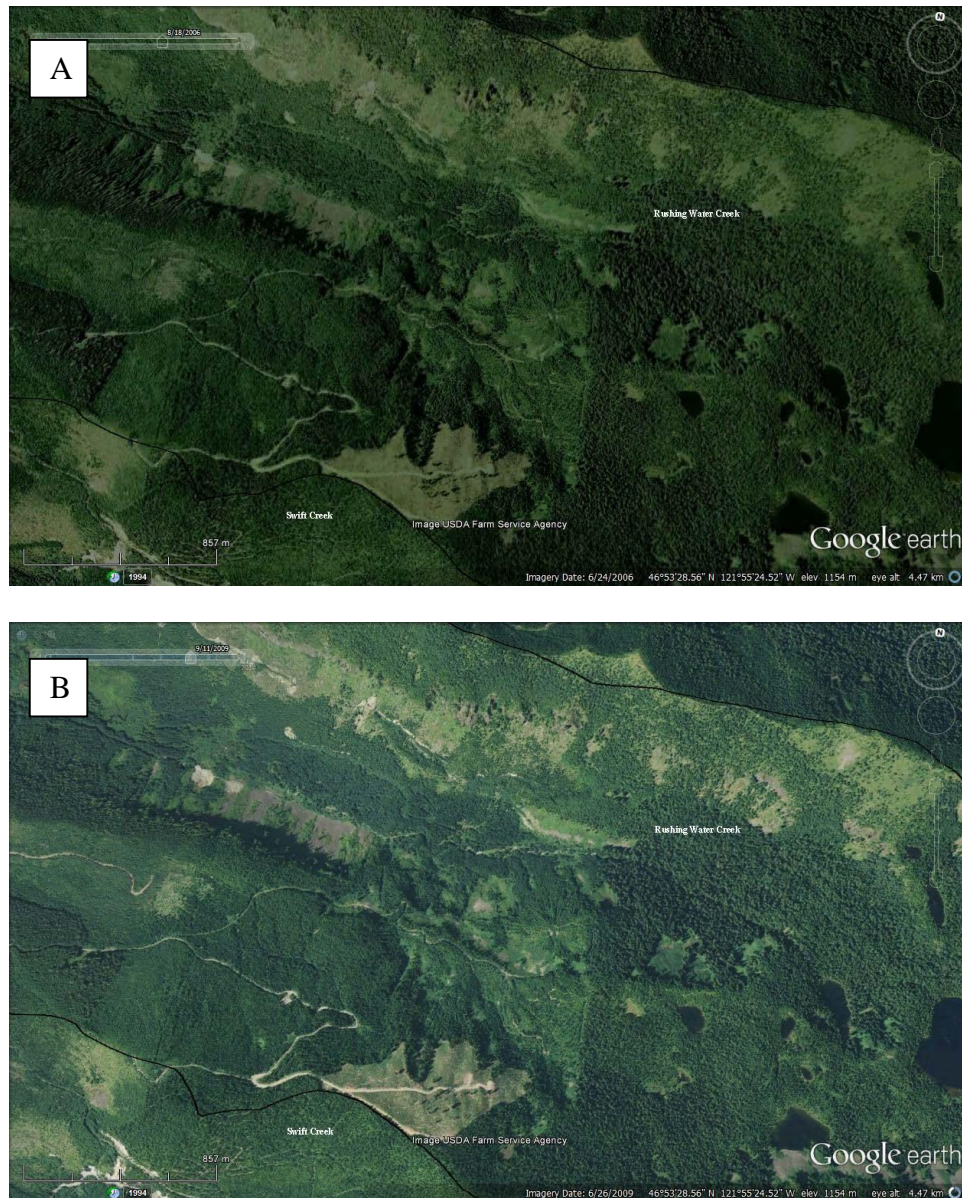


Figure 46. a) Google Earth image of Rushing Water Drainage in August 2006. b) Google Earth image of Rushing Water Drainage in September 2009.

4.20.3 Basin Attributes

The total basin area for this drainage is 16.3 km², while the upper basin is 5.5 km². In the upper basin, 77% of slopes are steeper than 33°. The gradient of the upper basin is 21% while the gradient of the whole basin is 11%. No glaciers are located in this basin. Almost the entire upper basin is covered with vegetation, at 92%. The geology is

95% bedrock and 3% surficial deposits. There is a discrepancy in the total percentage of geology coverage because a lake occupies a small portion of the upper basin. During the 2006 event, the upper basin received an average sum of 23 cm.

4.21 South Mowich Drainage Basin

4.21.1 Introduction

South Mowich River Basin is located on the west side of the mountain, with North Mowich Drainage to the north and North Puyallup Drainage to the south (Figure 4 and Figure 47). The drainage is well-defined by ridges on most sides and is 12.5 km long. Its highest elevation is 4304 m while the lowest elevation is 790 m at the North Mowich and South Mowich confluence. The lower basin is easily accessed by the Wonderland Trail, and it's very easy to hike up the channel from there. Little debris flow activity has been recorded in this drainage in recent history.

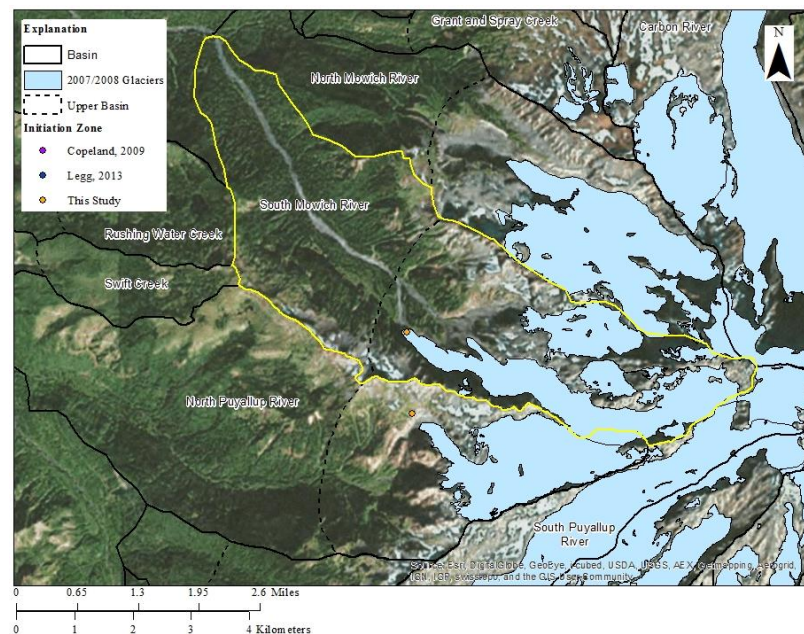


Figure 47. South Mowich River basin outlined in yellow, other basins outlined in black, the upper basin outlined in dashed black, glaciers in blue.

4.21.2 2006 Event

South Mowich showed evidence of debris flow activity on aerial photos. Field reconnaissance was conducted during the summer of 2013. I hiked part way up the drainage. One avulsion channel was noted and photographed (Figure 48a). In this avulsion channel there are log jams and stripped bark as well (Figure 48a). The trees in these photos are also buried in mud and sand (Figure 48b).



Figure 48. a) Avulsion channel with young vegetation that likely started growing back after 2006.



Figure 48. b) trees buried in mud and sand.

Between 2006 and 2008, both channels show evidence of major erosion along the channel margins (Figure 49a and b). The initiation site was identified where it looks like the glacier terminus has receded and major erosion in proglacial material, and material adjacent to the glacier was subsequently eroded. The initiation occurs at 1442.2 m, and it received 28.4 cm of rain during the event. There may have been an initiation in the north channel as well, but no large failure could be identified on aerial photography.



Figure 49. a) 2006 (blue) showing major erosion in the channel margins assumed to be caused by 2006 event which contributed material to debris flow in South Mowich Drainage.

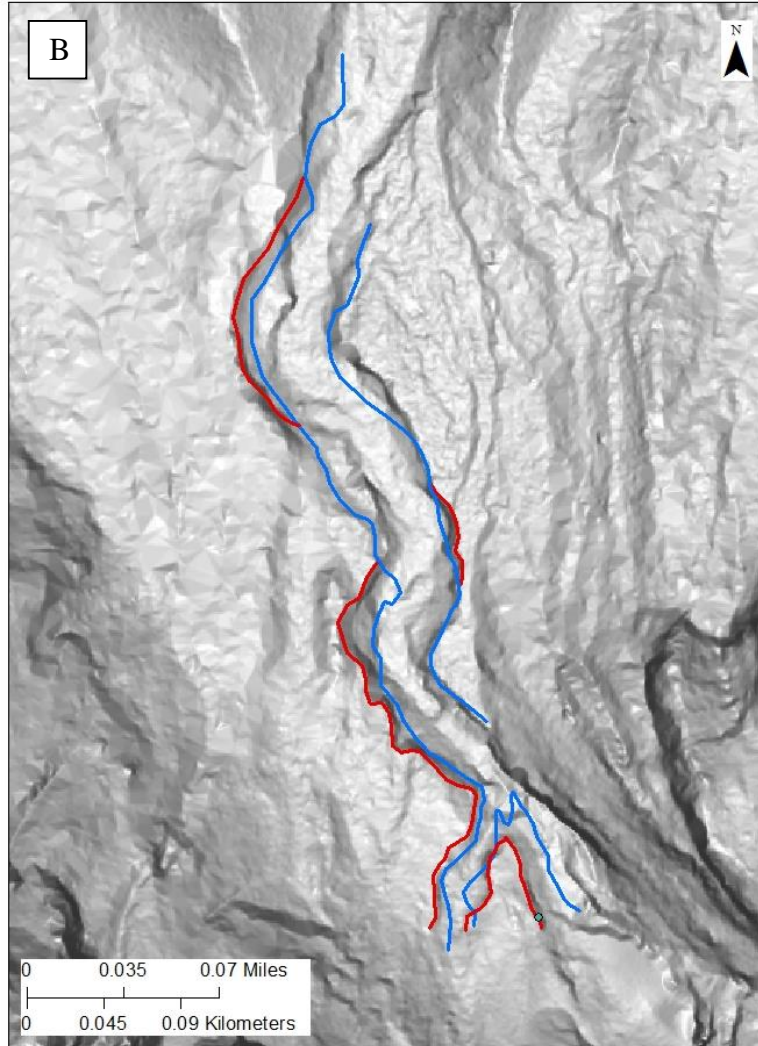


Figure 49. b) 2008 (red) showing major erosion in the channel margins assumed to be caused by 2006 event which contributed material to debris flow in South Mowich Drainage.

4.21.3 Basin Attributes

The total basin area for this drainage is 23.5 km², while the upper basin is 13.5 km². In the upper basin, 55% of slopes are steeper than 33°. The gradient of the upper basin is 45% while the gradient of the whole basin is 28%. Most of South Mowich Glacier and Edmunds Glacier are contained in the upper basin. Parts of Tahoma, Puyallup, Liberty Cap, and North Mowich glaciers also occur in the upper basin.

Collectively they occupy 38% of the upper basin. Very little of the upper basin is covered with vegetation, at 12%. The geology is 34% bedrock and 31% surficial deposits. During the 2006 event, the upper basin received an average sum of 34.3 cm.

4.22 South Puyallup Drainage Basin

4.22.1 Introduction

South Puyallup River Basin is located on the southwest side of the mountain, with St. Andrews, North Puyallup, and South Mowich basins to the north and Tahoma and Fish basins to the south (Figure 4 and Figure 50). The drainage is well-defined by ridges on the most sides and is 14.4 km long. Its highest elevation is 4385 m while the lowest elevation is 843 m just above the confluence with St. Andrews. The lower and upper basins are easily accessed by the Wonderland Trail.

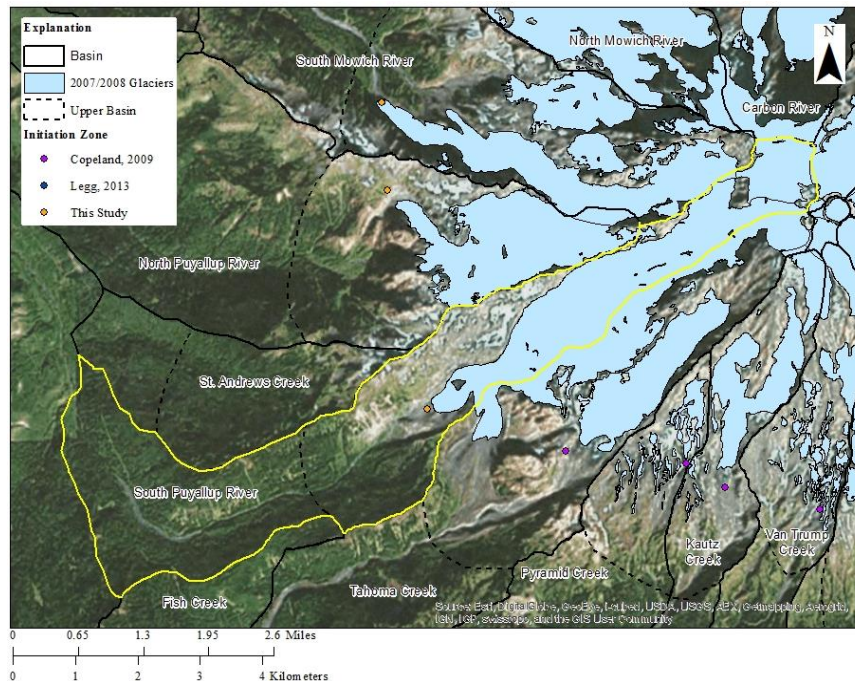


Figure 50. South Puyallup River basin outlined in yellow, other basins outlined in black, the upper basin outlined in dashed black, glaciers in blue.

Crandell and Mullineaux (1967) report that there is some evidence of prehistoric debris flows in South Puyallup drainage. They found charcoal in a debris flow deposit, and dated it to 2,350 radiocarbon years. The charcoal is indicative of volcanic influence. There is also evidence of mudflows younger than 3,500 years that temporarily filled Tahoma Creek and South Puyallup drainages. Crandell and Mullineaux (1967) report that the mudflow initiated in one valley and flowed over Round Pass into the adjacent valley. A similar initiation to that of the Osceola Mudflow is speculated because of the size of the event. The Electron Mudflow, which is another of three very large mudflows, was also initiated in the Puyallup River drainage and has been mapped as far as Sumner, Washington.

4.22.2 2006 Event

South Puyallup showed some evidence of 2006 debris flow activity on aerial photographs. Field reconnaissance was conducted during the summer of 2013. I hiked into parts of the lower drainage and noticed an abandoned avulsion channel (Figure 51). After looking at aerial photographs, the avulsion channel formed between 2006 and 2009 and is assumed to be a result of the 2006 event (Figure 52a and b). In the channel, there are log and boulder jams. This stretch of channel is also littered with dead trees. In the upper basin channel, there seems to be quite a lot of vegetation removal from the center of the channel and some stretches have avulsed (Figure 53a and b). Additionally, some sediment erosion took place near the headwaters of the main channel, which would contribute to debris flow.



Figure 51. Avulsion channel in lower South Puyallup channel with log and boulder jams.



Figure 52. a) Google Earth image of South Puyallup Drainage from 2006.



Figure 52. b) Google Earth image of South Puyallup Drainage from 2009.

Since I was unable to document strong evidence of levees, and I cannot rely solely on evidence collected by aerial photography, the basin was run through the regression as both a "yes" and a "no" in order to generate the most accurate model. The potential initiation site occurs at 1573.4 m, and it received 36 cm of rain during the event. I picked this location as it occurs just below the snow of the glacier, which receded quite a lot in this location between 2006 and 2009, exposing material that would easily contribute to debris flow (Figure 53a and b). Just below this area there is a portion of weathered material that was eroded, in addition to some vegetation that was removed from the sidewall and from the middle of the channel.

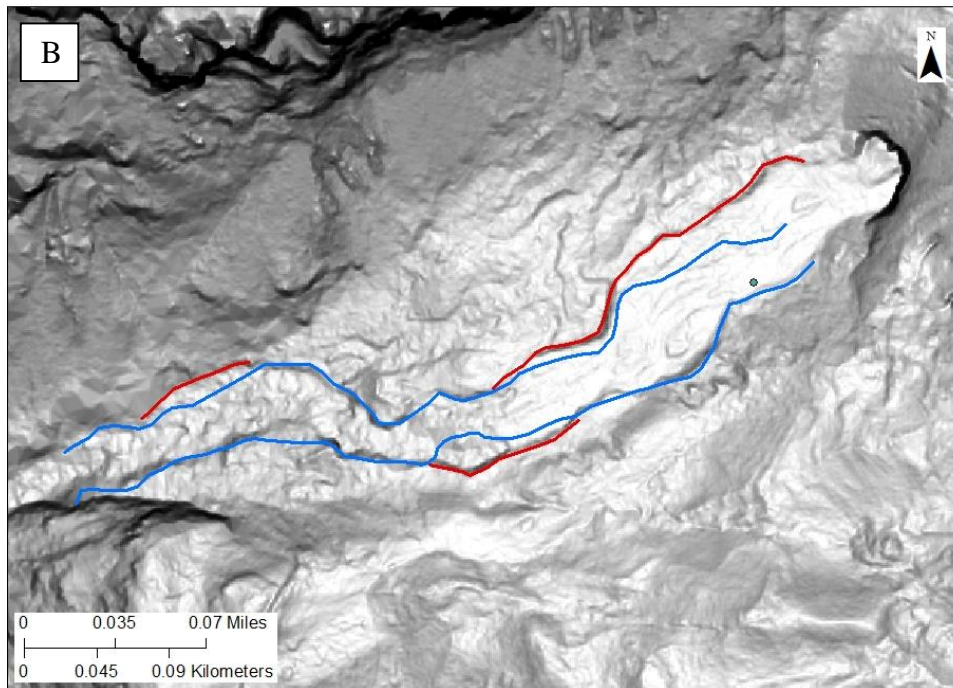
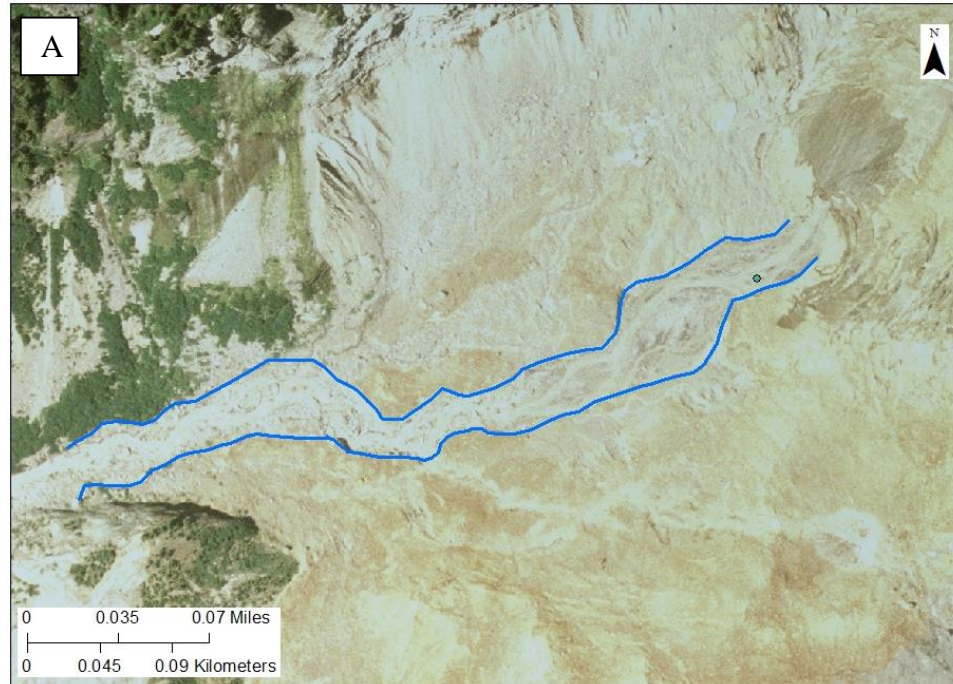


Figure 53. a) Imagery from 2006 (blue) and b) from 2008 (red) showing the major erosion from proglacial material with likely contributed to a debris flow, the initiation site for which is shown by the blue dot.

4.22.3 Basin Attributes

The total basin area for this drainage is 19.8 km², while the upper basin is 12.1 km². In the upper basin, 42% of slopes are steeper than 33°. The gradient of the upper basin is 35.4% while the gradient of the whole basin is 25%. Much of Tahoma Glacier and Liberty Cap Glacier occur in the upper basin. Parts of the South Mowich and Puyallup glaciers also occur in the upper basin. Collectively they occupy 45% of the upper basin. A quarter of the upper basin is covered with vegetation, at 26%. The geology is 28% bedrock and 25% surficial deposits. During the 2006 event, the upper basin received an average sum of 33.5 cm.

4.23 St. Andrews Drainage Basin

4.23.1 Introduction

St. Andrews Creek Basin is located on the west side of the mountain, with North Puyallup Basin to the north, and South Puyallup Basin to the south (Figure 4 and Figure 54). The drainage is fairly well-defined by ridges on most sides and is 6 km long. Its highest elevation is 2105 m while the lowest elevation is 830 m where St. Andrews Creek flows into South Puyallup River. The Wonderland Trail passes through the upper basin and the lower basin can be accessed by hiking the West Side Road.

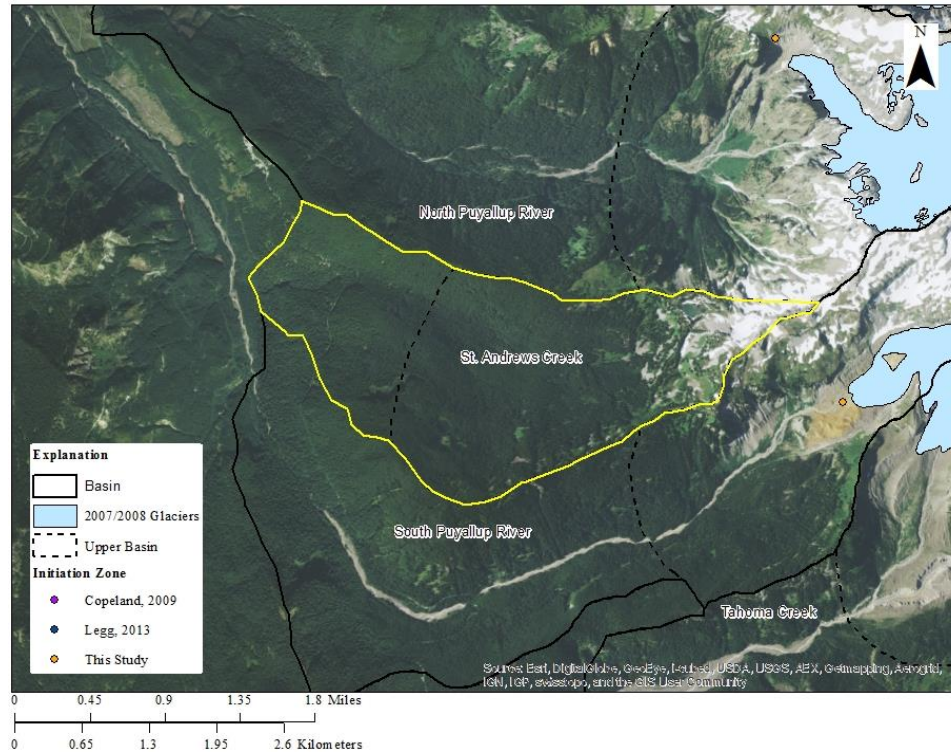


Figure 54. St. Andrews Creek basin outlined in yellow, other basins outlined in black, the upper basin outlined in dashed black, glaciers in blue, and initiation sites from Copeland (2009) in purple, Legg (2013) in blue, and this study in orange. No debris flow occurred in 2006 in this drainage.

4.23.2 2006 Event

This drainage did not have any evidence of debris flow on Google Earth (Figure 55a and b). This drainage was not investigated in the field since strong evidence against debris flow was collected using imagery.

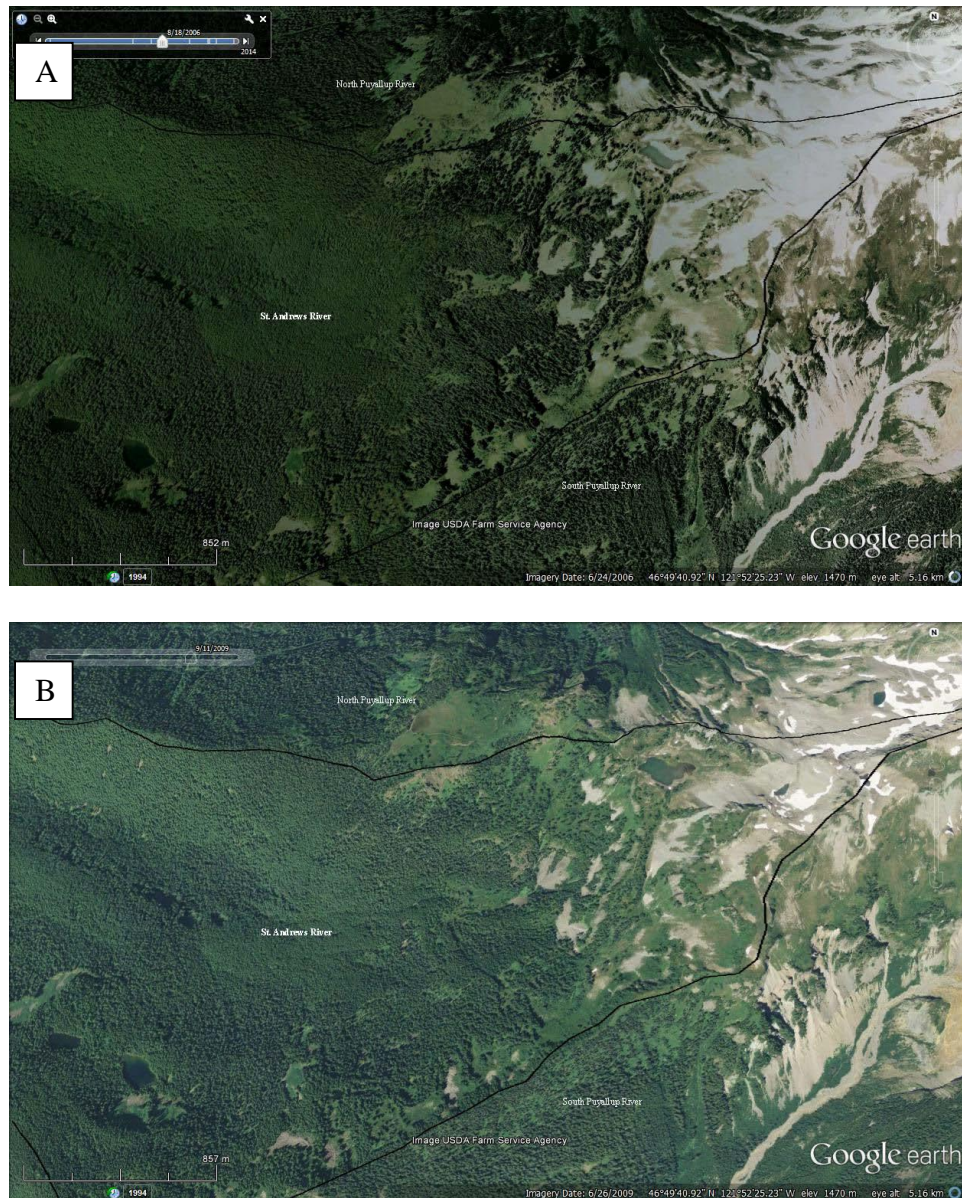


Figure 55. a) Google Earth image of St. Andrews Drainage in August 2006. b) Google Earth image of St. Andrews Drainage in September 2009.

4.23.3 Basin Attributes

The total basin area for this drainage is 7.6 km², while the upper basin is 5.2 km². In the upper basin, 51% of slopes are steeper than 33°. The gradient of the upper basin is 22% while the gradient of the whole basin is 21%. No glaciers are located in this basin. Over three fourths of the basin is covered in vegetation, at 87%. The geology is 84%

4.24.2 2006 Event

This drainage looked like there was potential for debris flow in Google Earth (Figure 57a and b). Upon further field investigation, no evidence of debris flow was found (Figure 58).

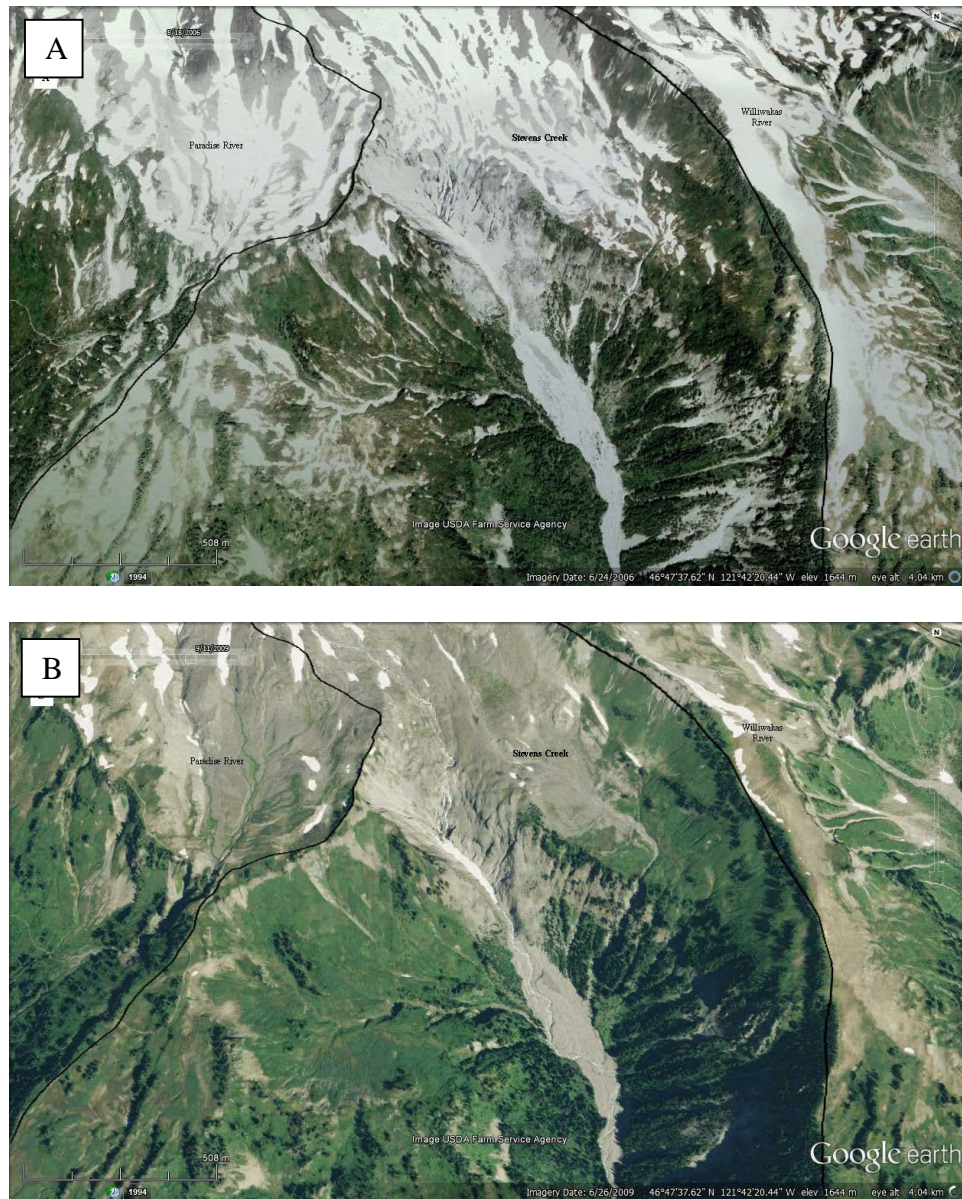


Figure 57. a) Google Earth image of the drainage in August 2006 b) Google Earth image of the drainage in September 2009.

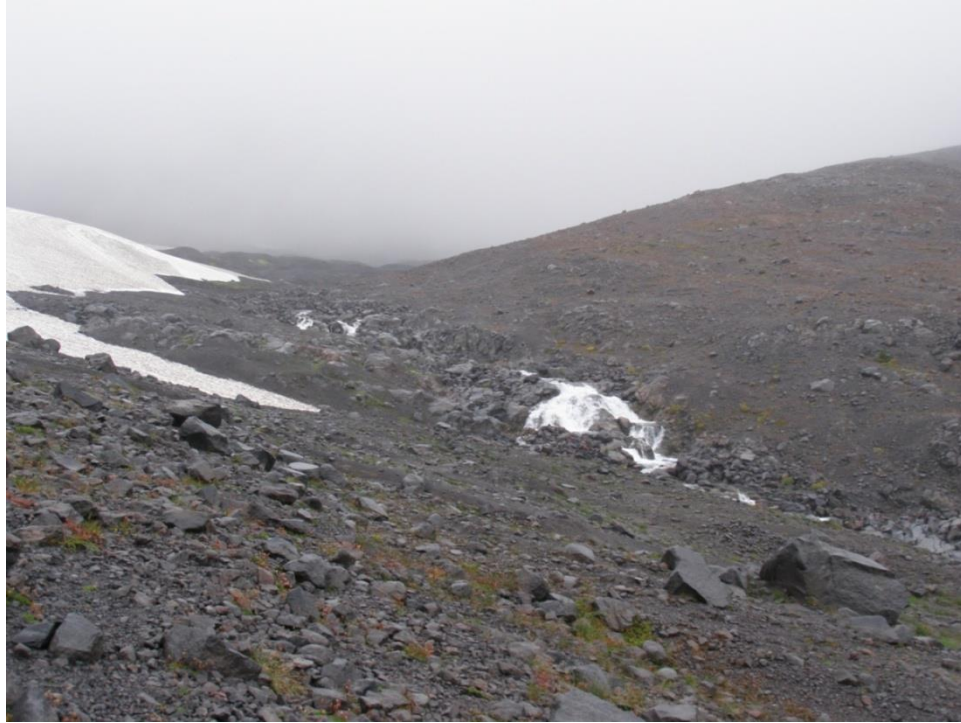


Figure 58. Photograph of the upper reaches of the Stevens Creek. No debris flow levees were noted and bedrock was prominent in the river channel.

4.24.3 Basin Attributes

The total basin area for this drainage is 6 km², while the upper basin is 2.3 km². In the upper basin, 88% of slopes are steeper than 33°. The gradient of the upper basin is 22% while the gradient of the whole basin is 20%. Part of the Williwakas and Paradise glaciers are located in the upper basin, occupying 1% of it. One third of the basin is covered in vegetation, at 33%. The geology is 49% bedrock and 49% surficial deposits. During the 2006 event, the upper basin received an average sum of 31.7cm of rain.

4.25 Sunbeam Drainage Basin

4.25.1 Introduction

Sunbeam Creek Basin is located on the south side of the mountain, with Tatoosh Basin to the west, Stevens Basin to the north, and Unicorn Basin to the east (Figure 4 and Figure 59). The drainage is somewhat well-defined by ridges on most sides and is 3.6 km long. Its highest elevation is 1908 m while the lowest elevation is 1092 m where Sunbeam Creek flows into Stevens Creek. The basin is easily accessed by hiking the Wonderland Trail.

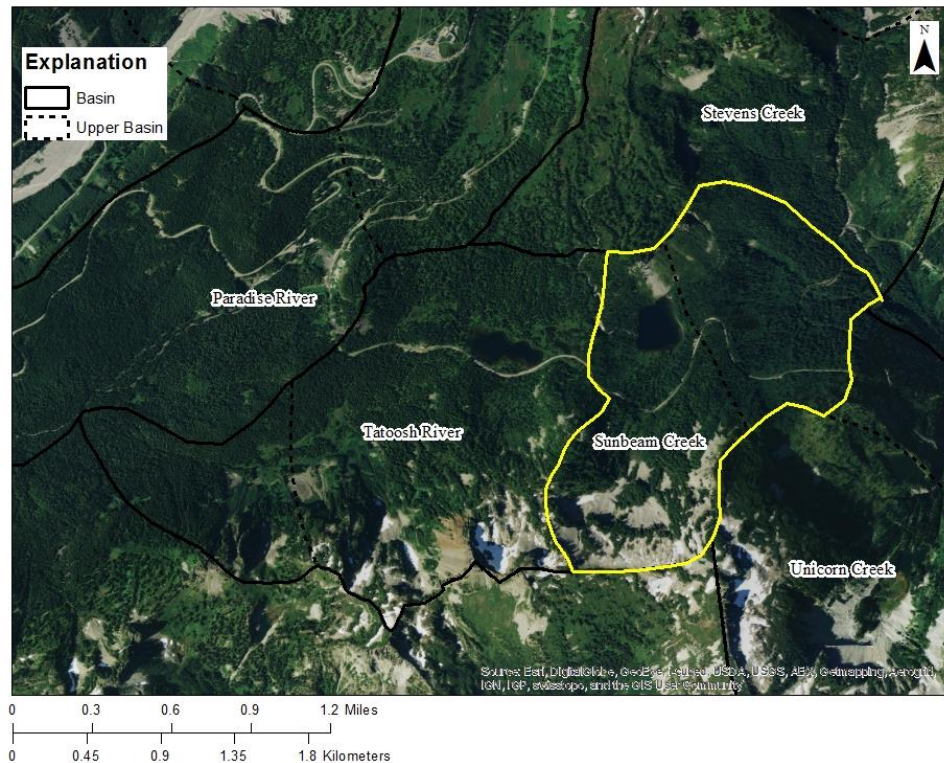


Figure 59. Sunbeam Creek basin outlined in yellow, other basins outlined in black, the upper basin outlined in dashed black, glaciers in blue, and initiation sites from Copeland (2009) in purple, Legg (2013) in blue, and this study in orange. No debris flow was recorded in 2006 in this drainage.

4.25.2 2006 Event

This drainage did not have any evidence of debris flow on Google Earth (Figure 60a and b). This drainage was not investigated in the field since strong evidence against debris flow was collected using imagery.

4.25.3 Basin Attributes

The total basin area for this drainage is 2.8 km², while the upper basin is 1.5 km². In the upper basin, 63% of slopes are steeper than 33°. The gradient of the upper basin is 25% while the gradient of the whole basin is 22%. There are no glaciers in this basin. Over half the upper basin is covered with vegetation, at 66%. The geology is 71% bedrock and 25% surficial deposits. There is a small discrepancy here because there's a small lake in the upper basin. During the 2006 event, the upper basin received an average sum of 30.9 cm.

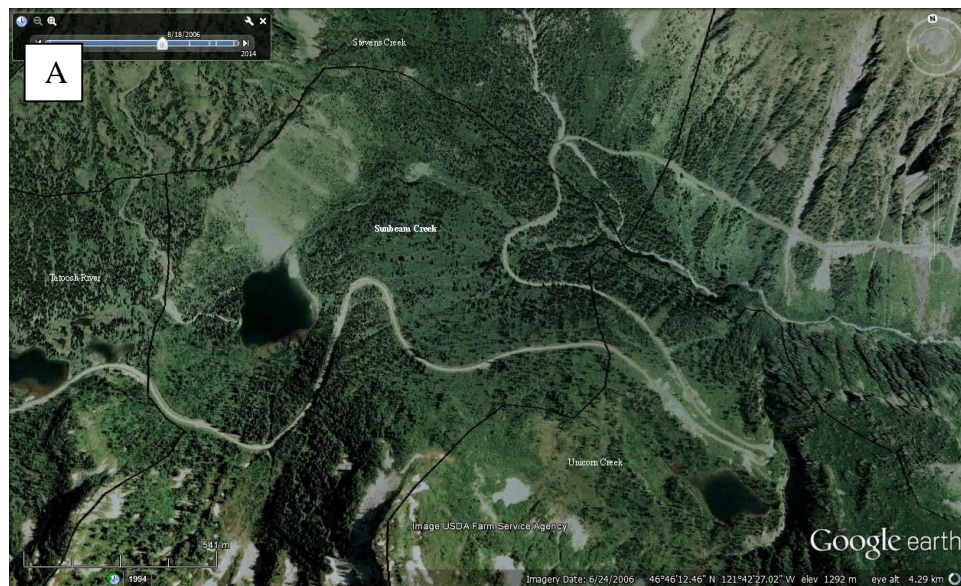


Figure 60. a) Google Earth image of Sunbeam Drainage in August 2006.

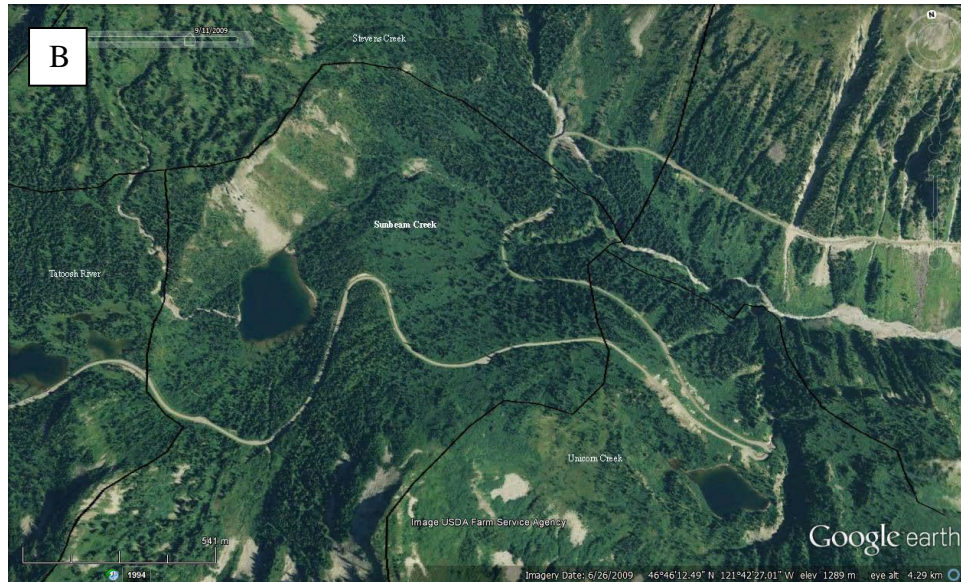


Figure 60. b) Google Earth image of Sunbeam Drainage in September 2009.

4.26 Swift Drainage Basin

4.26.1 Introduction

Swift Creek Basin is located on the west side of the mountain, with Rushing Water Basin to the north, South Mowich Basin to the east, and North Puyallup Basin to the south (Figure 4 and Figure 61). The drainage is somewhat well-defined by ridges on most sides and is 6.5 km long. Its highest elevation is 1743 m while the lowest elevation is 659 m where Swift Creek flows into Puyallup River. The Wonderland Trail passes through the upper basin.

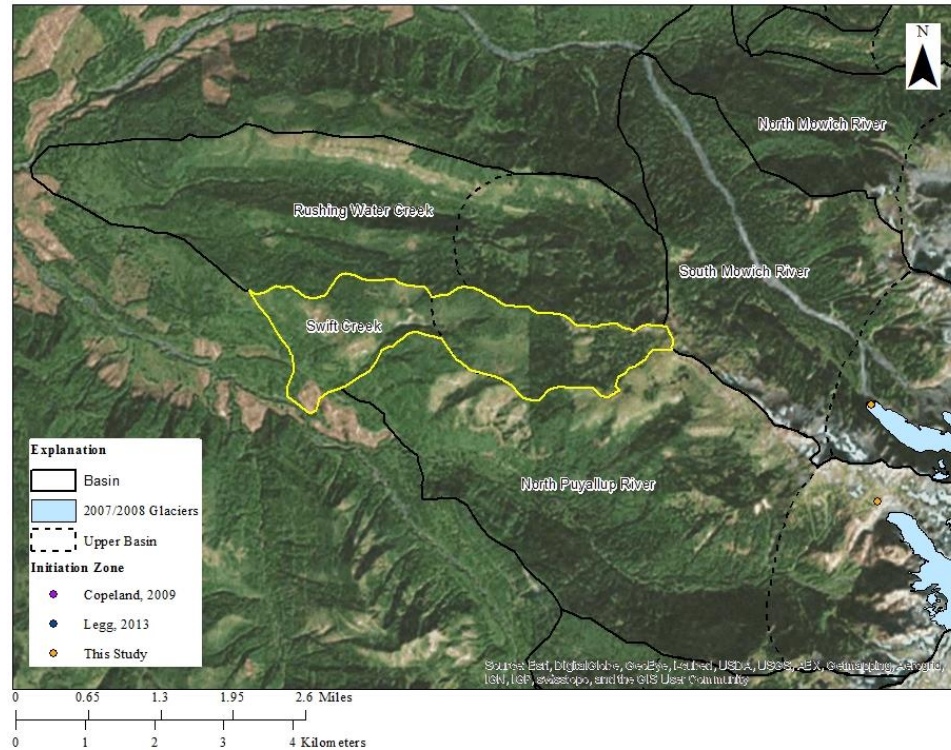


Figure 61. Swift Creek basin outlined in yellow, other basins outlined in black, the upper basin outlined in dashed black, glaciers in blue, and initiation sites from Copeland (2009) in purple, Legg (2013) in blue, and this study in orange. No 2006 debris flow was documented in this drainage.

4.26.2 2006 Event

This drainage did not have any evidence of debris flow on Google Earth (Figure 62a and b). This drainage was not investigated in the field since strong evidence against debris flow was collected using imagery.

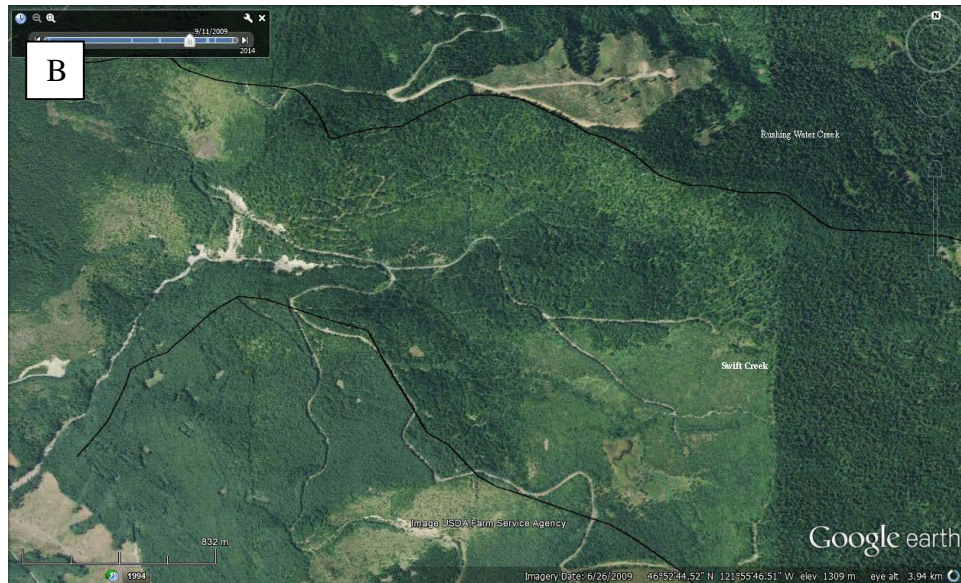
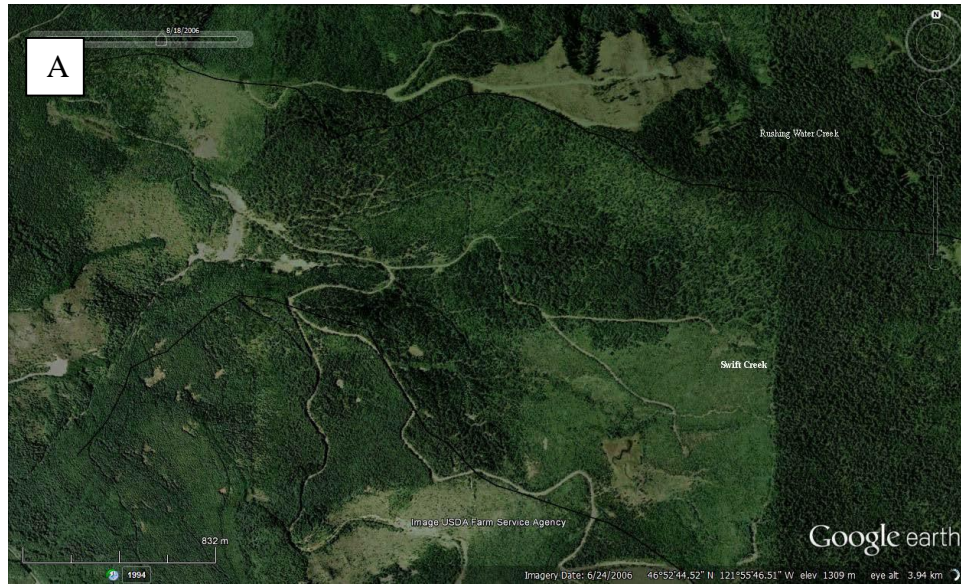


Figure 62. a) Google Earth image of Swift Drainage in August 2006. b) Google Earth image of Swift Drainage in September 2009.

4.26.3 Basin Attributes

The total basin area for this drainage is 6 km², while the upper basin is 3.2 km². In the upper basin, 54% of slopes are steeper than 33°. The gradient of the upper basin is 13% while the gradient of the whole basin is 17%. There are no glaciers in this basin. Almost the entire upper basin is covered in vegetation, at 99%. The geology is 72%

bedrock and 28% surficial deposits. During the 2006 event, the upper basin received an average sum of 23.3 cm.

4.27 Tahoma Drainage Basin

4.27.1 Introduction

Tahoma Creek Basin is located on the southwest side of the mountain, with South Puyallup and Fish basins to the north and Pyramid and Kautz basins to the south (Figure 4 and Figure 63). The drainage is well-defined by ridges on the most sides and is 18.7 km long. Its highest elevation is 4381 m while the lowest elevation of 631 m just at the confluence with Nisqually River. The lower basin is easily accessed by the West Side Road, but the Tahoma Creek Trail was destroyed. A section of the Wonderland Trail does, however, cross the lower part of the upper basin.

Tahoma is well known for generating debris flows, with at least 28 events occurring from 1967 to 2006 (Walder and Driedger, 1994a and b). Copeland (2009) documented initiation from South Tahoma Glacier in 2005. Glacier outburst floods have been a large contributor to debris flow initiation, with the majority of debris flows between 1985 and 1992 initiated this way (Walder and Driedger, 1994a and b).

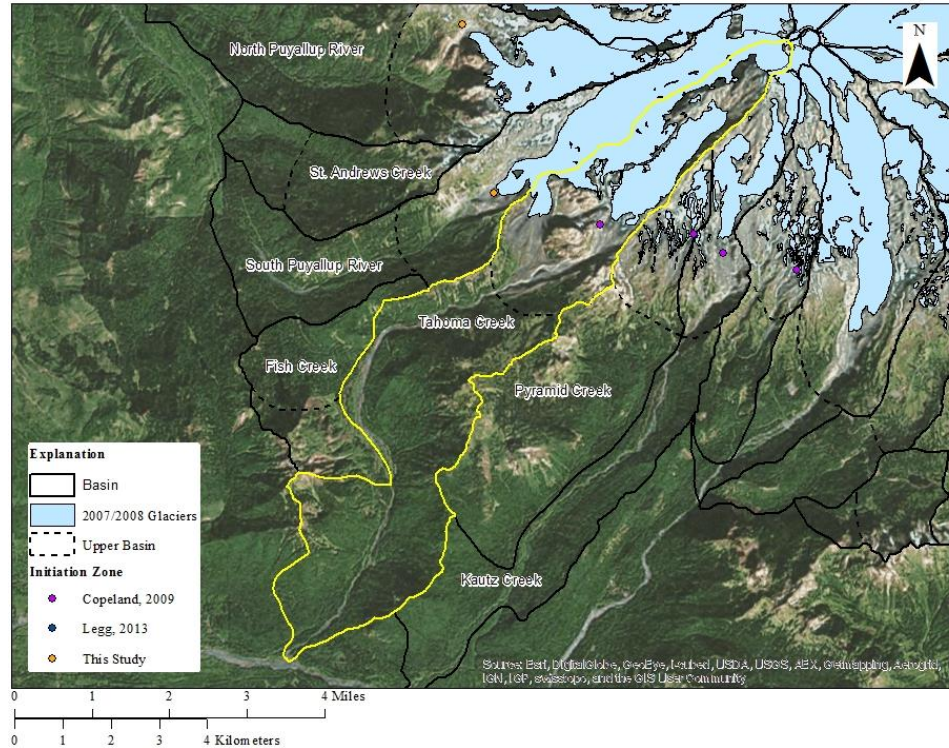


Figure 63. Tahoma Creek basin outlined in yellow, other basins outlined in black, the upper basin outlined in dashed black, glaciers in blue, and initiation sites from Copeland (2009) in purple, Legg (2013) in blue, and this study in orange.

4.27.2 2006 Event

Copeland (2009) documented a debris flow initiated by the 2006 rainstorm event. Evidence includes boulder levees. The gullies that contribute to debris flow in this drainage are located on stagnant ice over 100 m from South Tahoma Glacier (Copeland, 2009). Multiple debris flows have been initiated at locations adjacent to the glacier in the past as well (Copeland, 2009). The initiation occurred at 2046.1 m, and it received 36 cm of rain during the event (Figure 63). I did not hike into the upper basin since she had documented this event.

4.27.3 Basin Attributes

The total basin area for this drainage is 32.8 km², while the upper basin is 12.6 km². In the upper basin, 42% of slopes are steeper than 33°. The gradient of the upper basin is 41.3% while the gradient of the whole basin is 20%. Much of Tahoma Glacier and South Tahoma Glacier occur in the upper basin. Parts of Kautz-Success, Columbia, and Nisqually glaciers also occur in the upper basin. Collectively they occupy 36% of the upper basin. A small portion of the upper basin is covered with vegetation, at 12%. The geology is 31% bedrock and 33% surficial deposits. During the 2006 event, the upper basin received an average sum of 34.1 cm of rain.

4.28 Tatoosh Drainage Basin

4.28.1 Introduction

Tatoosh River Basin is located on the south side of the mountain, with Paradise and Stevens basins to the north, and Sunbeam Basin to the east (Figure 4 and Figure 64). The drainage is somewhat well-defined by ridges on most sides and is 3.2 km long. Its highest elevation is 2000 m while the lowest elevation is 1153 m where Tatoosh River flows into Paradise River. The upper basin is easily accessed by multiple trails.

4.28.2 2006 Event

This drainage did not have any evidence of debris flow on Google Earth (Figure 65a and b). This drainage was not investigated in the field since strong evidence against debris flow was collected using imagery.

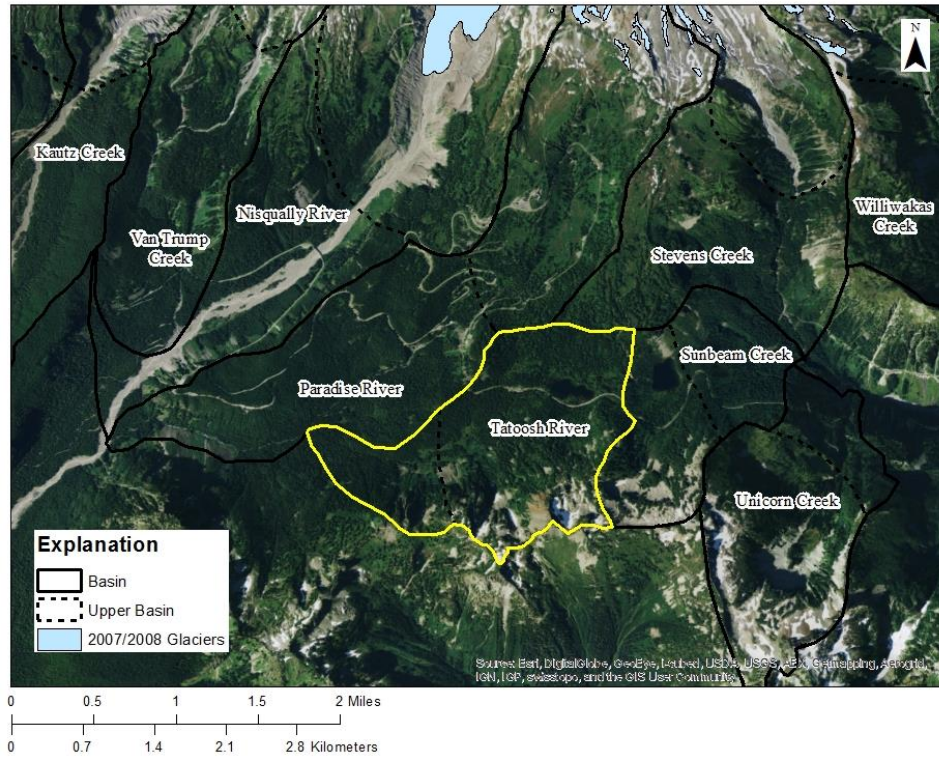


Figure 64. Tatoosh River basin outlined in yellow, other basins outlined in black, the upper basin outlined in dashed black, glaciers in blue.



Figure 65. a) Google Earth image of Tatoosh Drainage in August 2006.



Figure 65. b) Google Earth image of Tatoosh Drainage in September 2009.

4.28.3 Basin Attributes

The total basin area for this drainage is 4.2 km², while the upper basin is 3.2 km². In the upper basin, 20% of slopes are steeper than 33°. The gradient of the upper basin is 35% while the gradient of the whole basin is 26%. There are no glaciers in this basin. Three quarters of the upper basin is covered in vegetation, at 75%. The geology is 65% bedrock and 34% surficial deposits. During the 2006 event, the upper basin received an average sum of 31 cm.

4.29 Unicorn Drainage Basin

4.29.1 Introduction

Unicorn Creek Basin is located on the south side of the mountain, with Sunbeam Basin to the west (Figure 4 and Figure 66). The drainage is somewhat well-defined by ridges on most sides and is 3.6 km long. Its highest elevation is 2109 m while the lowest

elevation is 1035 m where Unicorn Creek flows into Stevens Creek. The Wonderland Trail passes through the lower basin.

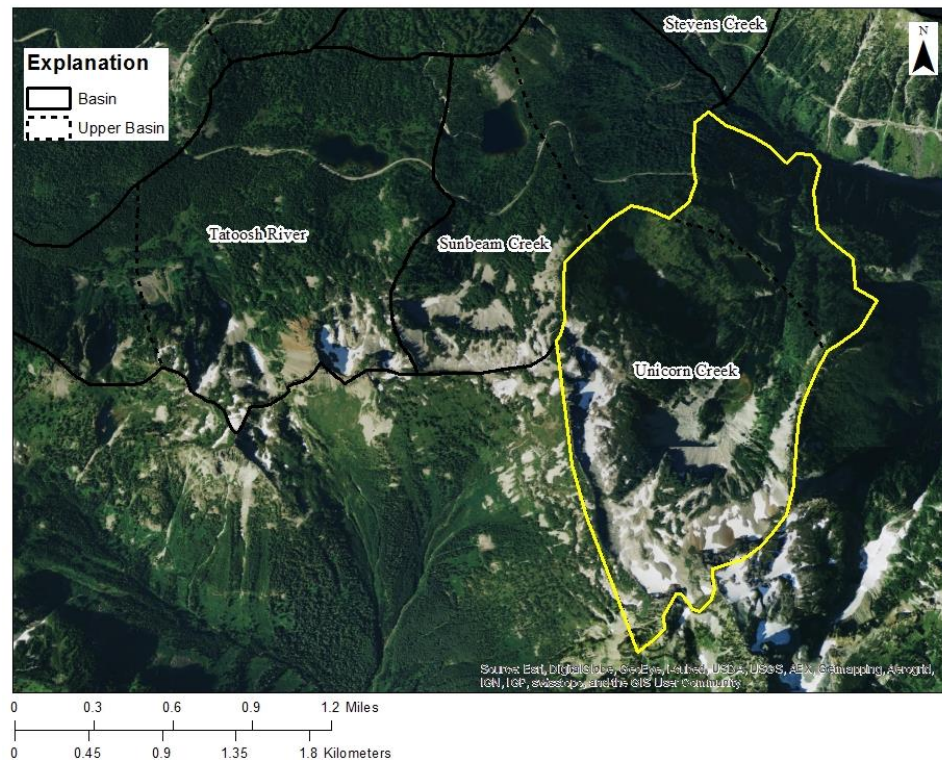


Figure 66. Unicorn Creek basin outlined in yellow, other basins outlined in black, the upper basin outlined in dashed black, glaciers in blue.

4.29.2 2006 Event

This drainage did not have any evidence of debris flow on Google Earth (Figure 67a and b). This drainage was not investigated in the field since strong evidence against debris flow was collected using imagery.

4.29.3 Basin Attributes

The total basin area for this drainage is 3.7 km², while the upper basin is 2.9 km². In the upper basin, 52.1% of slopes are steeper than 33°. The gradient of the upper basin is 29.4% while the gradient of the whole basin is 29.7%. There are no glaciers in this

basin. A little less than half the basin is covered in vegetation, at 41.6%. The geology is 58.5% bedrock and 40% surficial deposits. During the 2006 event, the upper basin received an average sum of 30.1 cm.

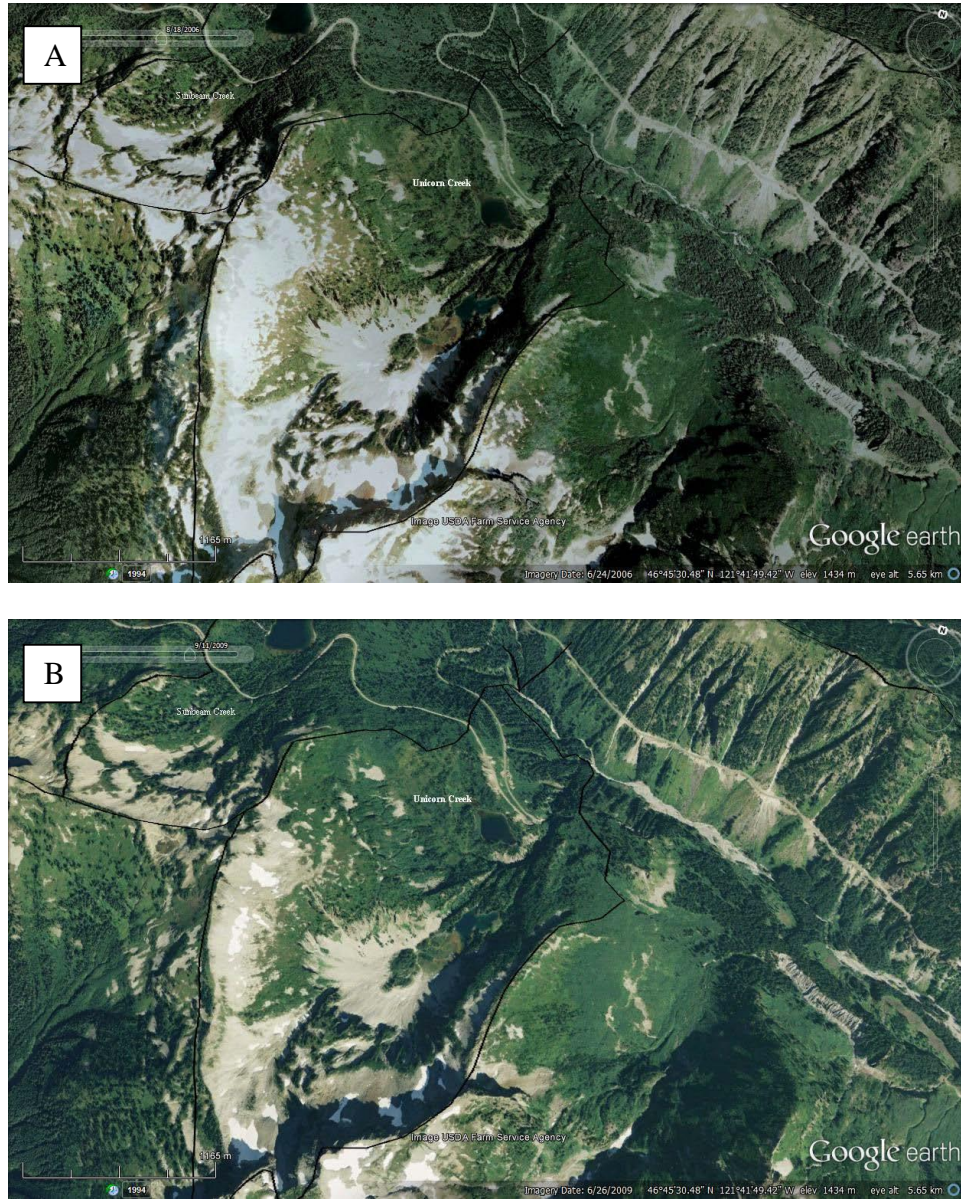


Figure 67. a) Google Earth image Unicorn Drainage in August 2006. b) Google Earth image Unicorn Drainage in September 2009.

4.30 Van Trump Drainage Basin

4.30.1 Introduction

Van Trump Creek Basin is located on the south side of the mountain, with Kautz Basin to the west and Nisqually Basin to the east (Figure 4 and Figure 68). The drainage is well-defined by ridges on the most sides and is 9.4 km long. Its highest elevation is 4228 m while the lowest elevation is 1014 m just at the confluence with Nisqually River. The lower basin is accessed by the Comet Falls-Van Trump Trail.

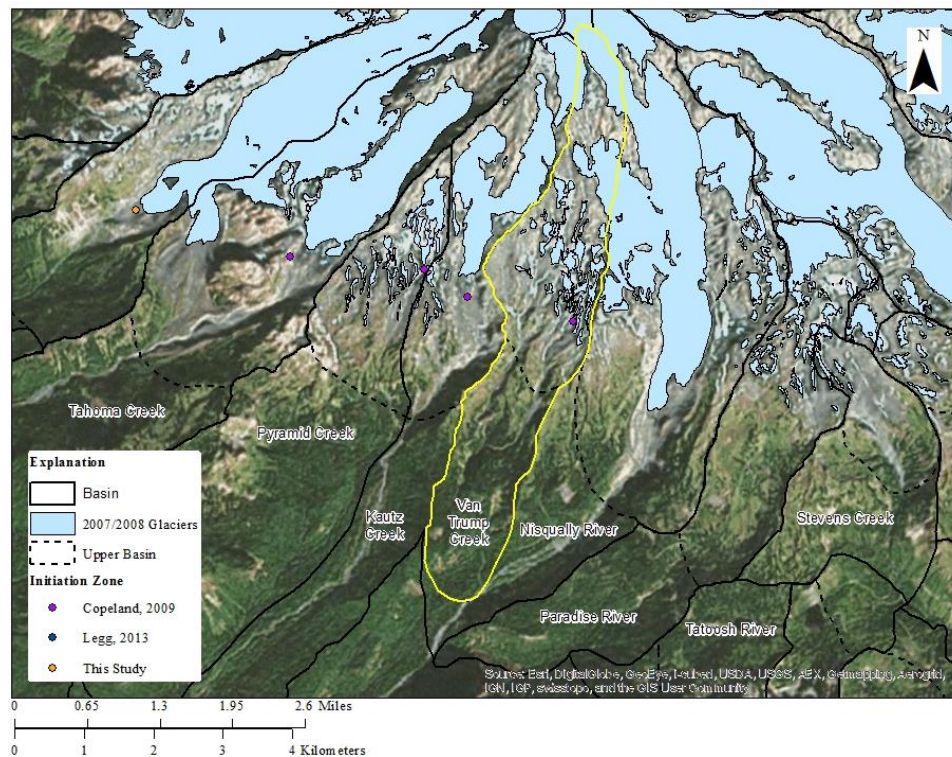


Figure 68. Van Trump Creek basin outlined in yellow, other basins outlined in black, the upper basin outlined in dashed black, glaciers in blue, and initiation sites from Copeland (2009) in purple, Legg (2013) in blue, and this study in orange.

Landslide deposits from sector collapses have been mapped and dated to 11,000-15,000 years ago in this drainage (Crandell, 1969). Debris flows are known to have occurred in very recent history. Vallance et al. (2002) documented a debris flow initiated

in Kautz that flowed into Van Trump in 2001. Legg (2013) documented a similar occurrence in 1975. It initiated from slumping caused by meltwater erosion in a gully occurring in the left lateral moraine of Kautz Glacier. Additionally, Copeland (2009) documented debris flows occurring in the 2003 and again in 2005, which were rainstorm initiated.

4.30.2 2006 Event

Copeland (2009) documented a debris flow initiated by the 2006 rainstorm event. Evidence includes boulder levees and broken trees. The initiation occurs at 2088 m and it received 33.8 cm of rain during the event (Figure 68). I did not hike into the upper basin since she had documented this event and thought it would be better to prioritize other drainages.

4.30.3 Basin Attributes

The total basin area for this drainage is 9.0 km², while the upper basin is 5.3 km². In the upper basin, 74% of slopes are steeper than 33°. The gradient of the upper basin is 46% while the gradient of the whole basin is 34%. Much of Van Trump glacier occurs in the upper basin, in addition to parts of Kautz, Nisqually, and Wilson glaciers. Collectively they occupy 27% of the upper basin. A small portion of the upper basin is covered with vegetation, at 5%. The geology is 41% bedrock and 25% surficial deposits. Discrepancies in percent glacier and geology are similar to Nisqually Drainage. During the 2006 event, the upper basin received an average sum of 33.4 cm of rain.

4.31 West Fork of the White Drainage Basin

4.31.1 Introduction

West Fork of the White River Basin is located on the north side of the mountain, with Carbon Basin to the west and White River and Inter Fork basins to the east (Figure 4 and Figure 69). The drainage is well-defined by ridges on the most sides and is 14.2 km long. Its highest elevation is 4393 m while the lowest elevation is 1041 m where Lodi Creek flows into West Fork of the White River. The upper basin is easily accessed by the Wonderland Trail, which crosses just below the Winthrop Glacier.

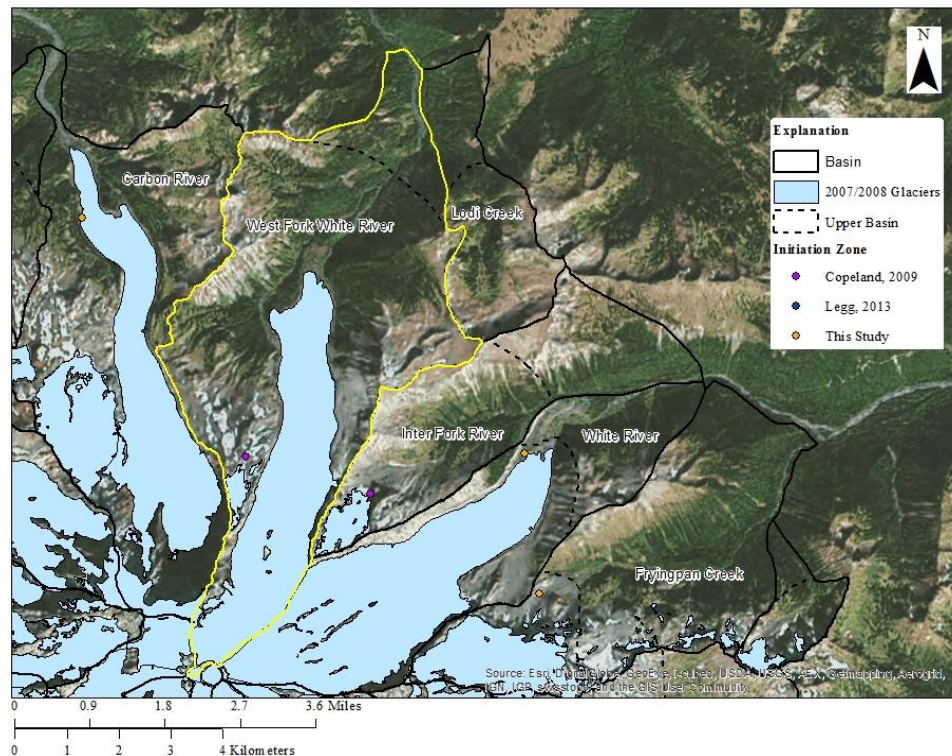


Figure 69. West Fork of the White River basin outlined in yellow, other basins outlined in black, the upper basin outlined in dashed black, glaciers in blue, and initiation sites from Copeland (2009) in purple, Legg (2013) in blue, and this study in orange.

The Osceola Mudflow impacted this drainage, in addition to the White River, 5,600 years ago (Vallance and Scott, 1997). The only debris flow documented in

recorded history in this drainage was documented by Walder and Driedger (1994b), and it occurred in 1987.

4.31.2 2006 Event

Copeland (2009) documented a debris flow initiated by the 2006 rainstorm event. Evidence includes boulder levees. Copeland (2009) states that the debris flow may have initiated by perturbation of a lake adjacent to the Winthrop Glacier. The initiation occurs at 2448 m, and it received 30.1 cm of rain during the event (Figure 69). I did not hike into the upper basin since she had documented this event and thought it would be better to prioritize other drainages.

4.31.3 Basin Attributes

The total basin area for this drainage is 35.8 km², while the upper basin is 32.7 km². In the upper basin, 14% of slopes are steeper than 33°. The gradient of the upper basin is 29% while the gradient of the whole basin is 24%. Much of the Curis Glacier and Winthrop Glacier occur in the upper basin. Parts of Liberty Cap and Columbia Crest glaciers also occur in the upper basin. Collectively they occupy 27% of the upper basin. About a third of the upper basin is covered with vegetation, at 34%. The geology is 34% bedrock and 38% surficial deposits. During the 2006 event, the upper basin received an average sum of 26.6 cm of rain.

4.32 White Drainage Basin

4.32.1 Introduction

White River Basin is located on the northeast side of the mountain, with West Fork of the White and Inter Fork basins to the northwest and Muddy Fork Cowlitz,

Basalt, and Fryingpan basins to the southeast (Figure 4 and Figure 70). The drainage is well-defined by ridges on the most sides and is 10.7 km long. Its highest elevation is 4337 m while the lowest elevation is 1269 m just below its confluence with Inter Fork River. The lower basin is easily accessed by the Wonderland Trail. From there it is easy to hike into the upper basin.

White River has been impacted by many lahars in the past, including the Osceola Mudflow (Czuba et al., 2012). Aside from prehistoric debris flows and lahars, little debris flow activity has been recorded in this drainage in recent history.

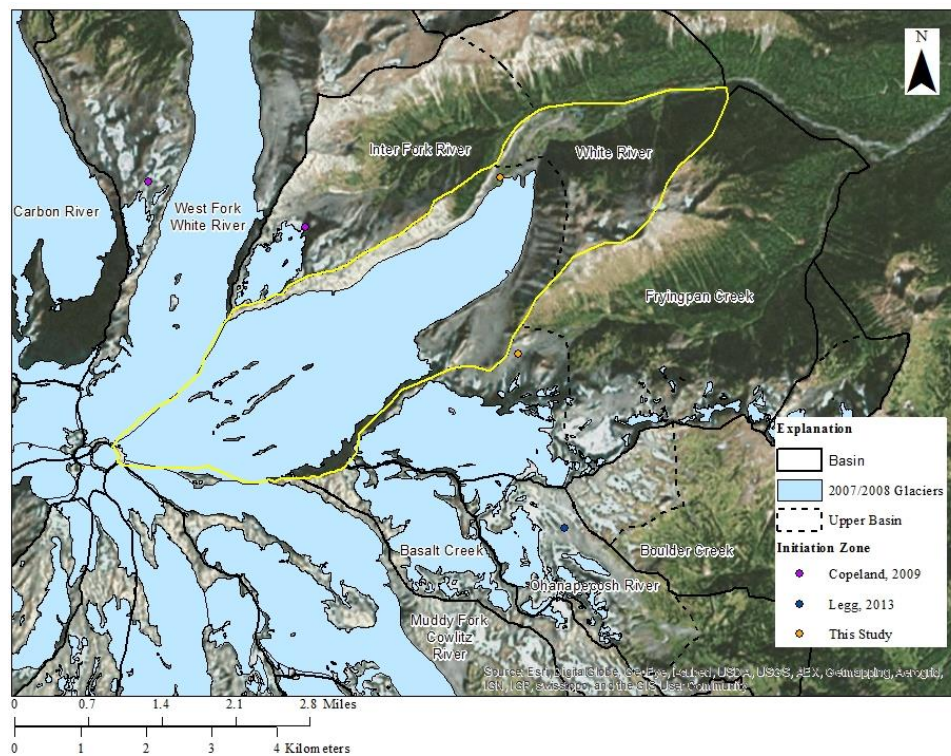


Figure 70. White River basin outlined in yellow, other basins outlined in black, the upper basin outlined in dashed black, glaciers in blue, and initiation sites from Copeland (2009) in purple, Legg (2013) in blue, and this study in orange.

4.32.2 2006 Event

The White River showed evidence of debris flow activity on aerial photographs. Field reconnaissance was conducted during the summer of 2014. I hiked into the upper drainage with park geomorphologist, Paul Kennard. We were able to locate a small levee (Figure 71). After comparing aerial photography, some vegetation and erosion occurred in the upper drainage. Further down in the drainage, above the confluence with Inter Fork, there is a lot of cutbank erosion and vegetation removal as well.

A possible initiation zone was identified using aerial photography. There was a failure along a cut bank to the north of the glacier. Across from the failure, there was some erosion (Figure 72a and b). The potential initiation occurs at 1560 m, and it received 25.3 cm of rain during the event.



Figure 71. Small levee just below the western edge of the glacier.

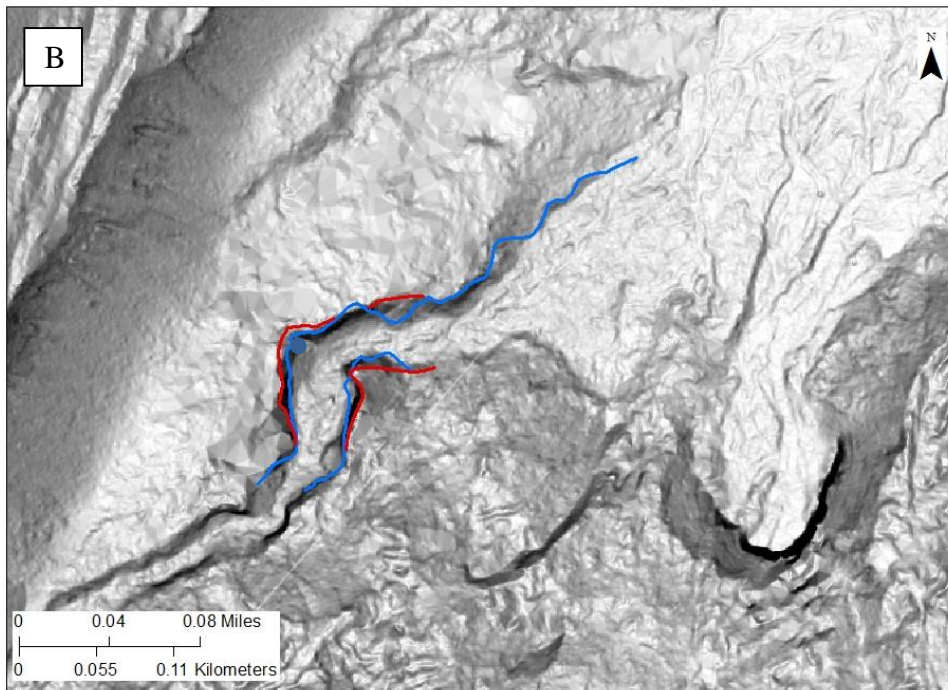
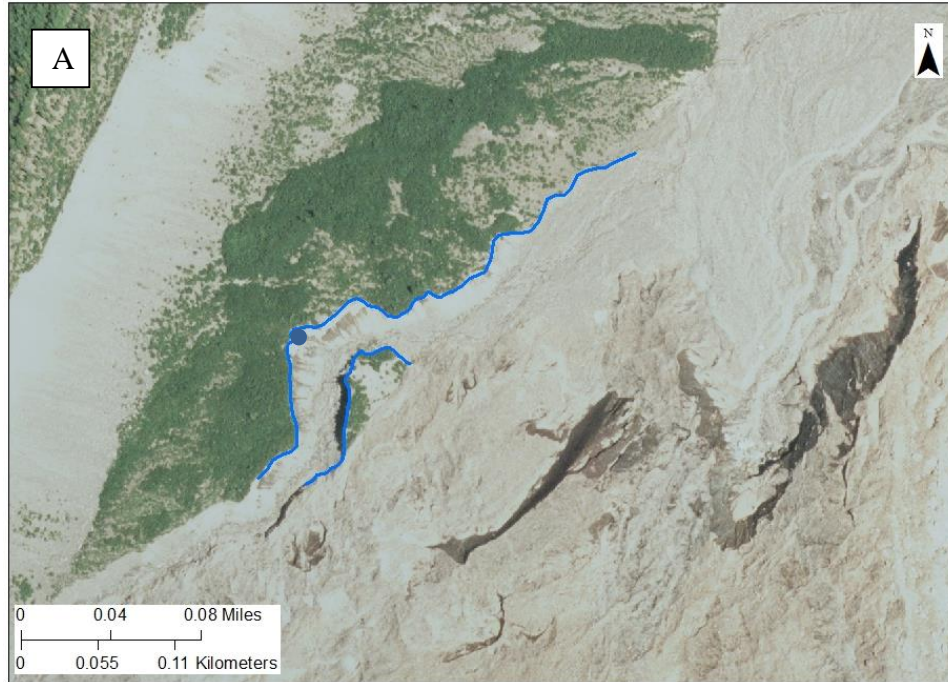


Figure 72. a) Imagery from 2006 showing outlines of channel margins in 2006 (blue). b) Imagery from 2008 (red) showing the major erosion from proglacial material with likely contributed to a debris flow, the initiation site for which is shown by the blue dot.

4.32.3 Basin Attributes

The total basin area for this drainage is 20.5 km², while the upper basin is 15.7 km². In the upper basin, 37% of slopes are steeper than 33°. The gradient of the upper basin is 34% while the gradient of the whole basin is 29%. Much of the Emmons Glacier occurs in the upper basin, with parts of the Inter, Ingraham, Fryingpan, and Winthrop glaciers. Collectively they occupy 71% of the upper basin. A small part of the upper basin is covered by vegetation at 3%. The geology is 6% bedrock and 22% surficial deposits. During the 2006 event, the upper basin received an average sum of 28.3 cm of rain.

4.33 Williwakas Drainage Basin

4.33.1 Introduction

Williwakas Creek Basin is located on the southeast side of the mountain, with Muddy Fork Cowlitz Basin to the northeast and Stevens Basin to the southwest (Figure 4 and Figure 73). The drainage is somewhat well-defined by ridges on most sides and is 5.9 km long. Its highest elevation is 2165 m while the lowest elevation is 1007 m, where Wright Creek flows into Fryingpan River. The whole basin is inaccessible by trail.

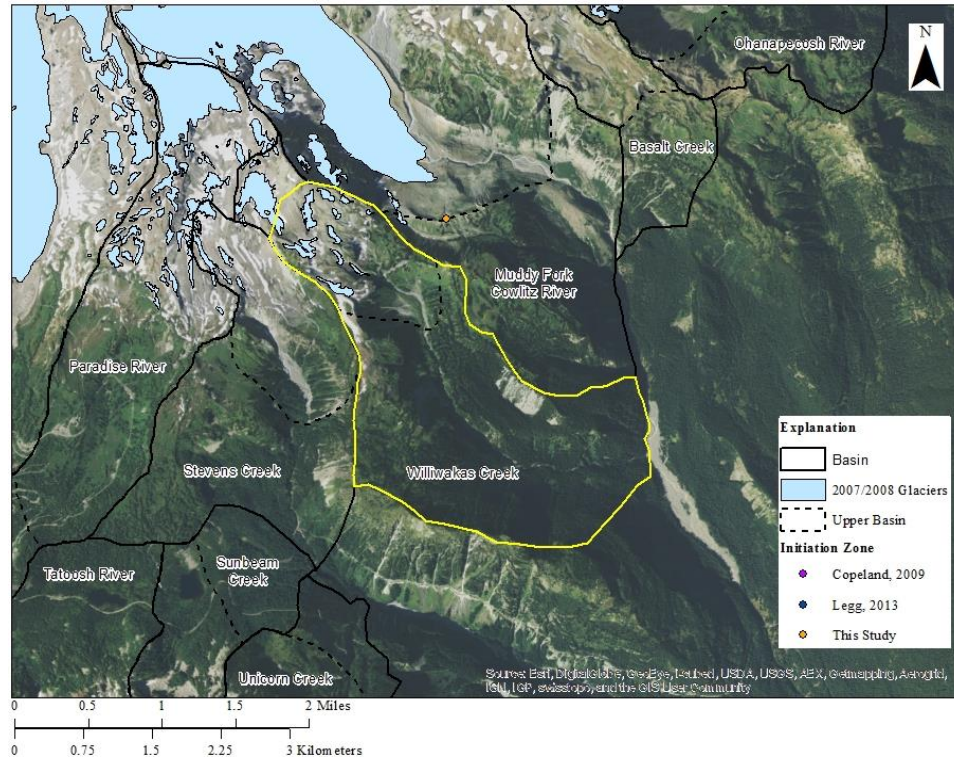


Figure 73. Williwakas Creek basin outlined in yellow, other basins outlined in black, the upper basin outlined in dashed black, glaciers in blue, and initiation sites from Copeland (2009) in purple, Legg (2013) in blue, and this study in orange. No 2006 debris flow was documented in this drainage basin.

4.33.2 2006 Event

This drainage did not have any evidence of debris flow on Google Earth (Figure 74a and b). This drainage was not investigated in the field since strong evidence against debris flow was collected using imagery.

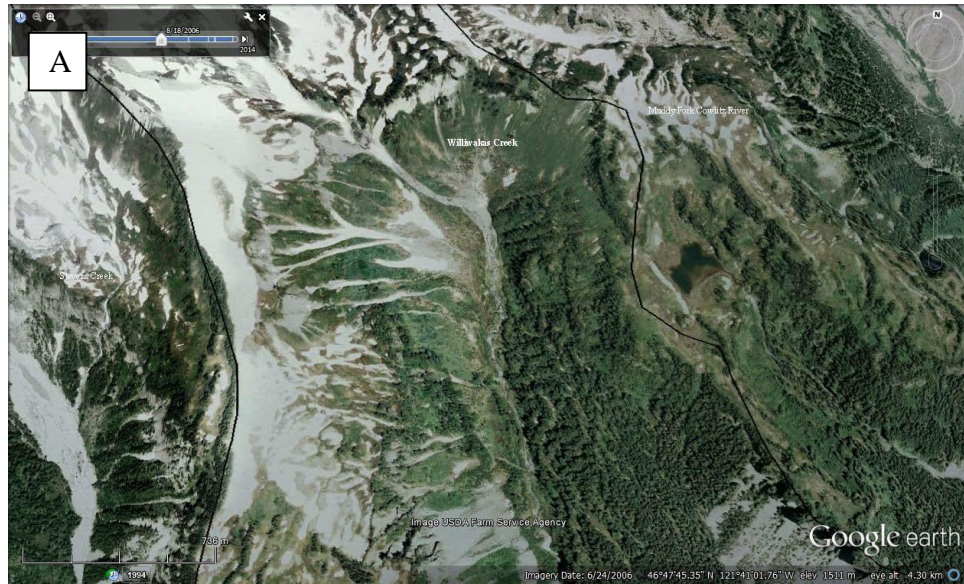


Figure 74. a) Google Earth image of Williwakas Drainage in August 2006. b) Google Earth image of Williwakas Drainage in September 2009.

4.33.3 Basin Attributes

The total basin area for this drainage is 7.8 km², while the upper basin is 1.8 km². In the upper basin, 83% of slopes are steeper than 33°. The gradient of the upper basin is 28% while the gradient of the whole basin is 20%. Part of the Williwakas Glacier occupies less than 1% of the upper basin. Very little of the upper basin is covered with

vegetation, at 6%. The geology is 63% bedrock and 36% surficial deposits. During the 2006 event, the upper basin received an average sum of 30.8 cm.

4.34 Wright Drainage Basin

4.34.1 Introduction

Wright Creek Basin is located on the east side of the mountain, with Boulder Basin to the south and Fryingpan Basin to the west. (Figure 4 and Figure 75). The drainage is somewhat well-defined by ridges on most sides and is 3.7 km long. Its highest elevation is 2266 m while the lowest elevation is 1211 m, just above where Williwakas Creek flows into Muddy Fork Cowlitz River. The Wonderland Trail passes through the upper basin.

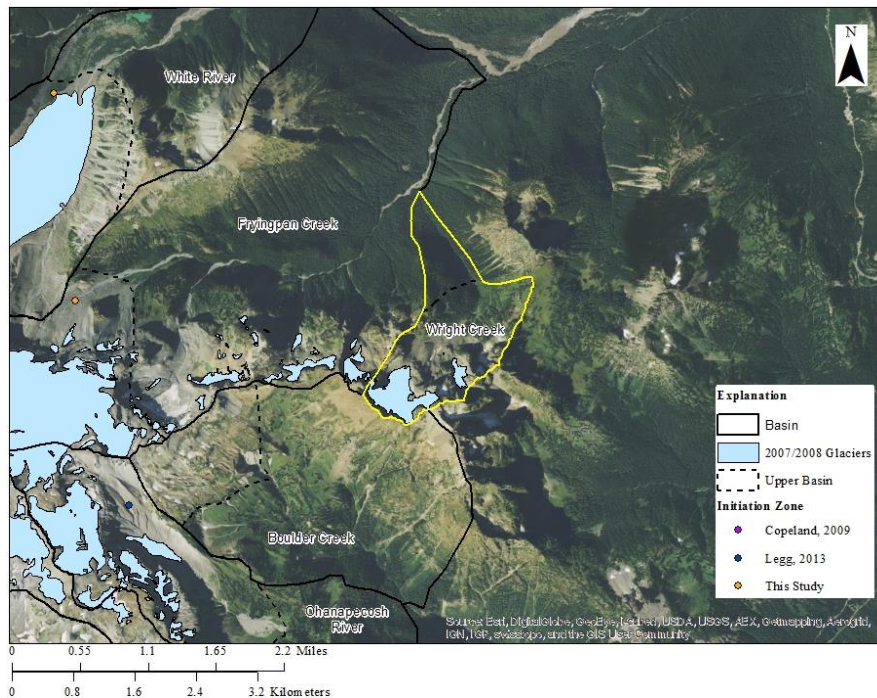


Figure 75. Wright Creek basin outlined in yellow, other basins outlined in black, the upper basin outlined in dashed black, glaciers in blue, and initiation sites from Copeland (2009) in purple, Legg (2013) in blue, and this study in orange. No 2006 debris flow was recorded in this drainage.

4.34.2 2006 Event

This drainage did not have any evidence of debris flow on Google Earth (Figure 76a and b). This drainage was not investigated in the field since strong evidence against debris flow was collected using imagery.

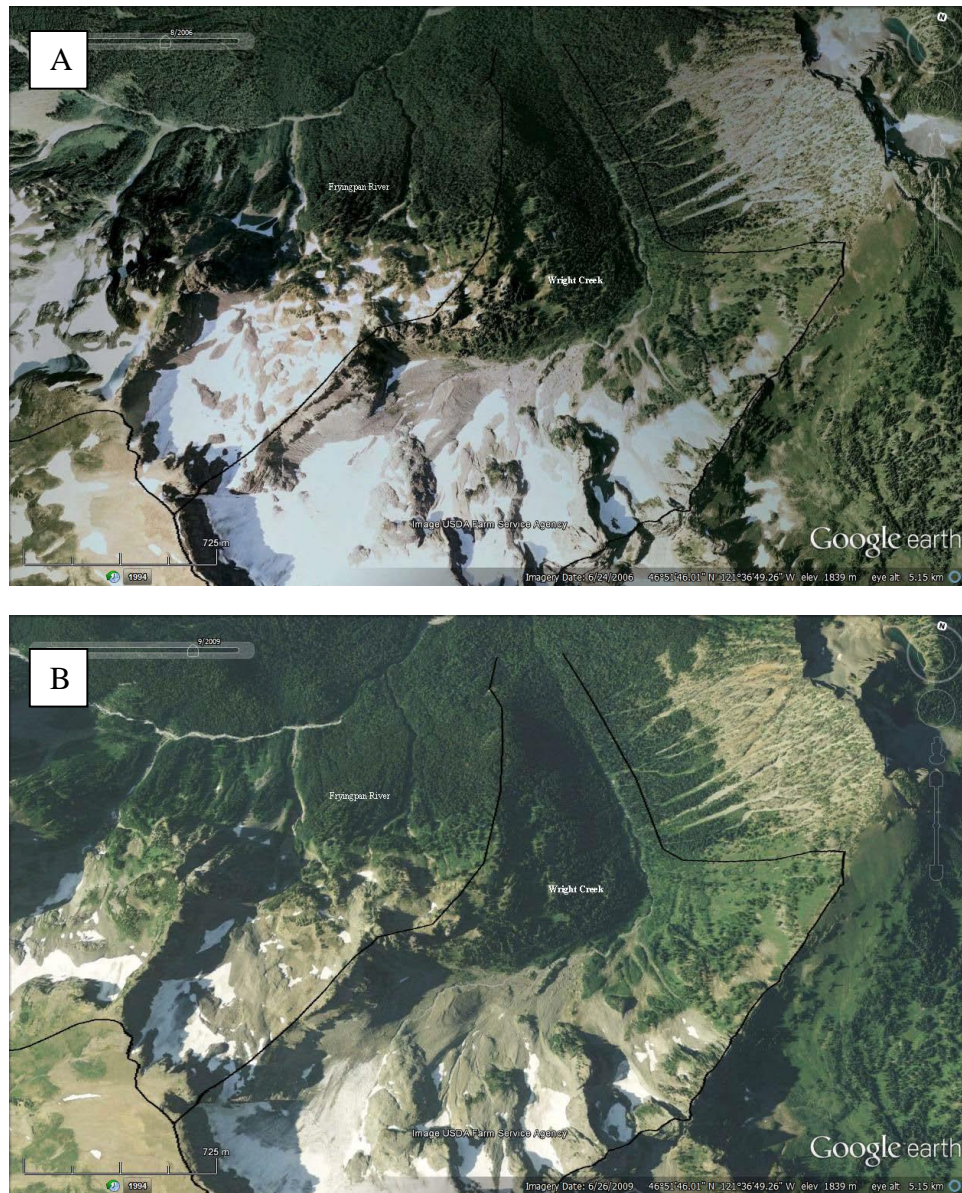


Figure 76. a) Google Earth image of Wright Drainage in August 2006. b) Google Earth image of Wright Drainage in September 2009.

4.34.3 Basin Attributes

The total basin area for this drainage is 2.9 km², while the upper basin is 2.2 km². In the upper basin, 53% of slopes are steeper than 33°. The gradient of the upper basin is 34% while the gradient of the whole basin is 29%. Sarvent Glacier occupies 13% of the upper basin. A third of the upper basin is covered in vegetation, at 34%. The geology is 52% bedrock and 34% surficial deposits. During the 2006 event, the upper basin received an average sum of 22 cm.

Summary

During the two-day Pineapple Express event in November, 2006, 10 of 34 drainages definitely experienced debris flows: Carbon, Inter Fork, Kautz, North Puyallup, Ohanapecosh, Pyramid, South Mowich, Tahoma, Van Trump, and West Fork of the White Basins. Four other drainages showed some evidence of debris flow activity during the event, but will be run as "yes" and "no" through the regression to determine the best model: Fryingpan, Muddy Fork Cowlitz, South Puyallup, and White. The remaining 20 drainages showed no evidence of debris flow. My study adds a net of three drainages with definite debris flows and four drainages with possible debris flows.

The 2006 debris flows identified by Copeland (2009) and Legg (2013) were all initiated by proglacial gully erosion and expansion (headless initiation), with exception to the West Fork of the White River, which was initiated partially by a glacial lake outburst flood. All of the debris flows identified in this study also experienced headless initiation. Carbon, Muddy Fork Cowlitz, North Puyallup, and White River also initiated partially by landslides.

Chapter 5: Statistics

5.1 ANOVA

An analysis of variance, or ANOVA, test was conducted to compare the attributes of those drainages that had a debris flow and those that did not. Drainages with a debris flow include: Carbon, Fryingpan, Inter Fork, Kautz, Muddy Fork Cowlitz, North Puyallup, Ohanapecosh, Pyramid, South Mowich, South Puyallup, Tahoma, Van Trump, West Fork of the White, and White drainages. Those without evidence include: Basalt, Boulder, Cataract and Marmot, Crater, Fish, Grand and Spray, Lee, Lodi, Nisqually, North Mowich, Paradise, Rushing Water, St. Andrews, Stevens, Sunbeam, Swift, Tatoosh, Unicorn, Williwakas, and Wright. Of the attributes measureable across all drainages, total basin area, upper basin area, percent vegetation in upper basin, highest elevation is the total basin, highest elevation is the upper drainage, height of the total basin, height of the upper basin, length of the total basin, length of the upper basin, gradient of the upper basin, MRN of the total basin, MRN of the upper basin, percent bedrock in the upper basin, percent glacier coverage in the upper basin, stream with direct connection to glacier, average annual precipitation, event precipitation, and peak precipitation have different means between the two groups. Steep slopes, lowest elevation of the total basin, lowest elevation of the upper basin, gradient of the total basin, and percent surficial deposits in the upper basin had means that were not measurably different. The results are presented in Appendix B.

5.2 Mt. Rainier Multiple Regression

There were a total of 13 variables that were measurable across all the upper drainages, and therefore used for the regression (Table 1). Only the attributes measured exclusively in the upper basin were used because initiation and most entrainment occurs in the upper basin in this environment for these smaller types of debris flows. Of the 13, a few had some overlap and could not be run in the same regression as this would create redundancies.

Table 1. The drainage basin attributes that were used for the regression analysis. Those highlighted were swapped depending on the combination since they could not be run through the regression together.

Basin Attribute	Variable
Percent Vegetation	X1
Percent Steep Slopes	X2
Gradient of Upper	X3
MRN of Upper	X4
Height of Upper	X5
Upper Basin Area	X6
Percent Bedrock	X7
Percent Surficial deposits	X8
Percent Glacier	X9
Direct Connection with Glacier	X10
Average Annual Precipitation	X11
Event Precipitation	X12
Peak Precipitation	X13

The raw and normalized data for the regression are presented in Appendix C. This yielded eight variable combinations. Additionally, four of the drainages were run as both "yes" (had a debris flow in 2006) and "no" (did not have a debris flow in 2006) in order to generate the most accurate model. That yielded 16 basin combinations with four drainages varying between having an occurrence or not having an occurrence. There were two resulting regression models with the same accuracy and slightly different outcomes.

The two best models supported the debris flow evidence found in the field and on imagery and identified that the four "questionable" (yes/no) drainages did had debris flows in 2006. Both models correctly identified 31 of the 34 drainages (91% accuracy).

5.3 Model 1

The regression analysis removed X5 first, then X1, X2, X7, X12, X11, and X9, respectively. Model 1 was found by then adding each previously removed variable back into the model individually to determine if they had significance. Variable X7 was added back in, which lowered the significance of X10, and it was consequently removed. These iterations are presented in Appendix C. X3, X6, and X7 are gradient of the upper basin, area of the upper basin, and percent bedrock, respectively. Y values of 0.5 or greater indicate a debris flow initiation. It incorrectly predicted Nisqually and North Mowich as false positives and Inter Fork as a false negative (Table 2). The model has an accuracy of 91%. The following equation is the equation for Model 1:

$$Y = \frac{e^{(0.31X_3+0.25X_6-0.39X_7)}}{1 + e^{(0.31X_3+0.25X_6-0.39X_7)}}$$

Table 2. Results of Model 1. The bolded drainages and Y values are drainages that experienced a debris flow. Inter Fork, Nisqually, and North Mowich are highlighted because they were run as "no" but were predicted to have a debris flow.

Drainage	Y
Carbon River	0.78
White River	0.75
West Fork of the White River	0.74
South Mowich River	0.72
Nisqually River	0.71
Kautz Creek	0.70
North Mowich River	0.70
Tahoma Creek	0.70
Fryingpan River	0.68
South Puyallup River	0.66

Muddy Fork Cowlitz River	0.64
Van Trump Fall Creek	0.64
Pyramid Creek	0.60
North Puyallup River	0.59
Ohanapecosh River	0.53
Grant and Spray Creek	0.48
Inter Fork	0.48
Cataract and Marmot Creek	0.46
Wright Creek	0.45
Lodi Creek	0.43
Tatoosh River	0.42
Basalt Creek	0.40
Unicorn Creek	0.40
Crater Creek	0.37
Stevens Creek	0.36
Williwakas Creek	0.35
Fish Creek	0.34
Lee Creek	0.34
Paradise River	0.33
Sunbeam Creek	0.30
St Andrews Creek	0.26
Boulder Creek	0.24
Swift Creek	0.23
Rushing Water Creek	0.21

5.4 Model 2

The regression removed X2 first, then X1, X3, X10, X12, X11, and X9, respectively. The most significant variables in this model are MRN (X4) and Bedrock (X7). It predicted Basalt, Nisqually, and North Mowich as false positives (Table 3). The model has an accuracy of 91%. The iterations of this regression are presented in Appendix C. The following equation is the equation for Model 2:

$$Y = \frac{e^{(0.41X_4 - 0.42X_7)}}{1 + e^{(0.41X_4 - 0.42X_7)}}$$

Table 3. Results of Model 2. The bold are the drainages that experienced a debris flow. Basalt, Nisqually, and North Mowich are highlighted because they were run as "no" but were predicted to have a debris flow.

Drainage	Y
Kautz Creek	0.79
Van Trump Fall Creek	0.74
White River	0.73
South Puyallup River	0.72
Tahoma Creek	0.70
North Mowich River	0.69
Nisqually River	0.68
Pyramid Creek	0.67
Fryingpan River	0.66
South Mowich River	0.66
Carbon River	0.64
Muddy Fork Cowlitz River	0.64
Ohanapecosh River	0.58
West Fork of the White River	0.55
North Puyallup River	0.54
Basalt Creek	0.53
Inter Fork	0.50
Grant and Spray Creek	0.49
Wright Creek	0.45
Lodi Creek	0.44
Stevens Creek	0.43
Cataract and Marmot Creek	0.41
Paradise River	0.40
Unicorn Creek	0.40
Williwakas Creek	0.39
Crater Creek	0.35
Sunbeam Creek	0.33
Tatoosh River	0.33
Lee Creek	0.31
St Andrews Creek	0.28
Swift Creek	0.27
Boulder Creek	0.24
Fish Creek	0.24
Rushing Water Creek	0.21

5.5 Mt. Hood Comparison

The results from Model 1 and Model 2 were applied to the data from Mt. Hood. The raw and normalized data from Mt. Hood used to test the predictive model are presented in Appendix C. The Mt. Hood equation for Model 1 is:

$$Y = \frac{e^{(-0.52X_3 - 0.60X_6 - 0.01X_7)}}{1 + e^{(-0.52X_3 - 0.60X_6 - 0.01X_7)}}$$

Model 1 had an accuracy of 82%, predicting 2 false negatives of 11 drainages (Table 4).

Table 4. Drainages that experienced debris flows on Mt. Hood are bolded. A Y above 0.50 indicates a debris flow occurred. Yellow are incorrectly identified drainages.

Drainage	Y
Ladd	0.69
Clark	0.68
Salmon	0.64
Newton	0.62
Elliot	0.51
Coe	0.48
Zigzag	0.46
White	0.45
Sandy	0.40
Polallie	0.40
Muddy	0.20

The Mt. Hood equation for Model 2 is:

$$Y = \frac{e^{(0.28X_4 - 0.35X_7)}}{1 + e^{(0.28X_4 - 0.35X_7)}}$$

Model 2 has an accuracy of 73% with 2 false negatives and 1 false positive (Table 5).

Table 5. Drainages that experienced debris flows on Mt. Hood are bolded. A Y above 0.50 indicates a debris flow occurred. Yellow are incorrectly identified drainages.

Drainage	Y
Elliot	0.66
White	0.62
Newton	0.56
Clark	0.53
Polallie	0.53
Salmon	0.52
Zigzag	0.48
Sandy	0.47
Coe	0.46
Ladd	0.35
Muddy	0.33

5.6 Combined Multiple Regression

A regression analysis was conducted on the Mt. Adams, Mt. Hood, Mt. St. Helens, and Mt. Rainier datasets combined into one data set to determine susceptibility and accuracy for all four volcanoes. Six variables were measured for all the drainages for all volcanoes (Table 6). The raw and normalized data for those used in the combined regression are presented in Appendix D. The iterations are also presented in Appendix D. The regression shows that percent vegetation and percent ice/glaciers are the most significant variables.

Table 6. Basin attributes that were used in the combined multiple regression analysis of Mt. Hood, Mt. Adams, Mt. St. Helens, and Mt. Rainier.

Basin Attributes	Variable
Gradient	X1
Percent Steep Slopes	X2
Percent Vegetation	X3
MRN for Upper Basin	X4
Connection with Glacier	X5
Percent Ice/Glacier in Upper	X6

The resulting model has an accuracy of 77%, with 22 of 95 drainages predicted incorrectly; 4 false positives and 6 false negatives on Mt. St. Helens, 3 false positives and 1 false negative on Mt. Adams, 3 false positives on Mt. Hood, and 3 false positives and 2 false negatives on Mt. Rainier (Appendix D). A comparison of the variables, drainage prediction, and accuracy of combined models from Pirot (2010), Williams (2011), and St. Helens (2012) are presented in Table 7.

Table 7. Combined regression results from each previous study and this one. The accuracy of each model was reduced from each previous study until this study, where the results increased the accuracy from 69% to 77%.

Mountains	Significant Attributes	False Positive	False Negative	Accuracy
Hood (Pirot, 2010)	Percent Vegetation, Gradient, River Connection to Glacier	0	1	91%
Hood, Adams (Williams, 2011)	River Connection to Glacier, Percent Glacier Coverage	5	0	83%
Hood, Adams, St. Helens (Olson, 2012)	River Connection to Glacier, Percent Vegetation	6	8	69%
Hood, Adams, St. Helens, Rainier (this study)	Percent Vegetation, Percent Glacier Coverage	13	9	77%

The two most significant variables in this analysis match the next most recent study done by Olson (2012) with combined data from Mt. St. Helens, Mt. Hood, and Mt. Adams. The accuracy of the combined model in that study was 69%. This study has increased the accuracy of the combined model to 77%. Two variables, percent vegetation and river connection to glacier, were found to be significant by 3 of 4 regression

analyses. Percent glacier coverage was found significant by 2 of 4 regression analyses. Gradient was found significant in only 1 regression analysis.

5.6 Limitations, Assumptions, and Sources of Error

There were numerous assumptions and limitations that could contribute to errors in this analysis of debris flow initiation on Mt. Rainier. One large source of potential error comes from how the upper basin is defined. Another comes from digitization of the vegetation shapefile. There were some areas that I wouldn't consider vegetation, but other researchers might have. There was also no differentiation between dense vegetation and sparse vegetation. The combined geology shapefile is another source. The original shapefile was drawn at a larger scale, which contributes to inaccuracy. In an effort to minimize that, I hand digitized what geology was visible. Many of the variables rely on accuracy from other datasets, like the basin outlines, glacier outlines, and rainfall data.

The ANOVA test in this study uses a significance level of 0.05 which means there is a 5% chance the null hypothesis is incorrectly rejected (Davis, 2002). An assumption of the ANOVA test is that replicates in a sample group represent a random sample from a different population, each group is part of a normally distributed population, and each group has the same variance (Davis, 2002).

Most of the source of error with the statistical analysis lie with the Wald Test. The likelihood-ratio test is a preferred test to this, as the sample sizing is much smaller (Agresti, 1996). It has preferred use in this study and the three previous studies due to limitations conducting alternative likelihood ratio test. The Wald Test may yield inconsistent results. Limitations of the regression include variable and sample sizes

(Olson, 2012; Lewicki and Hill, 2007). Others would suggest keeping the number of variables to a minimum (Olson, 2012; Hosmer and Lemshow, 1989).

Lastly, this collection of attributes and specific methods should only be used in this type of environment. The major sources for methodology come from studies conducted in maritime climate and mountainous environments similar to the Cascade Range.

5.7 Summary

Of the 23 basin attributes that were able to have an ANOVA test done, 18 had measurably different means and 5 did not, with an error potential of 5%. The regression analysis found two models to have the same accuracy of 91%. Model 1 found gradient, upper basin area, and percent bedrock (low percentage) to be the most significant variables. It incorrectly predicted that Inter Fork did not have a debris flow and Nisqually and North Mowich did. Model 2 found MRN and percent bedrock (low percentage) to be the most significant. It incorrectly predicted that Basalt, Nisqually, and North Mowich had debris flows.

These models are also extremely similar in terms of variables as well. Basin area, from Model 1, is used to calculate MRN, Model 2. Gradient seems to have taken the place of what would be basin height in the MRN calculation. Basin height (highest basin elevation minus lowest basin elevation) is used to calculate gradient, Model 1.

Six variables were used for the combined regression of Mt. Hood, Mt. Adams, and Mt. St. Helens; gradient, percent steep slopes, percent vegetation, MRN, connection with glacier, and percent ice/glacier. The regression found percent ice/glacier and percent

vegetation to be the most significant variables, which are consistent with what Olson (2012) found. The resulting model had a 77% accuracy, increasing from the 69% accuracy from the combined regression done by Olson (2012). Comparatively, Williams (2010) had a combined model of 83% accuracy, and percent glacial coverage and average annual precipitation were the most significant variables.

Chapter 6: Discussion

6.1 Attributes

This study provides a dataset of 29 attributes for Mt. Rainier drainages. These attributes are related to topography, rainfall, glacier data, vegetation, and geology. The vegetation shapefile was digitized by hand using 2006 imagery as forest shapefiles could not be found. Additionally, the geology shapefile used in this study was updated somewhat from the DNR geology shapefile for the mountain using 2006 imagery.

6.2 Storm Event

The 2006 rainstorm event occurred over two days, November 6th and 7th, in 2006. The system brought over 22-50 cm of rainfall to Mt. Rainier. During the event, there was insignificant snow on the mountain, which acts as a buffer for precipitation. In cases like this, where a warm rainstorm passes over a region with thin snowpack, it is more likely that the snow will melt and increase runoff. This increased runoff may subsequently increase the likelihood for mass wasting events. This Pineapple Express system triggered numerous debris flows by generating landslide and causing increased stream flow and erosion.

Debris flows were initiated on all sides of the mountain (Figure 77). The heaviest precipitation occurred on the west and northwest sides of the mountain, which are the most remote areas of the mountain. Many debris flows were initiated in the western drainages, in addition to drainages located on the southern, eastern, and northern side of the mountain.

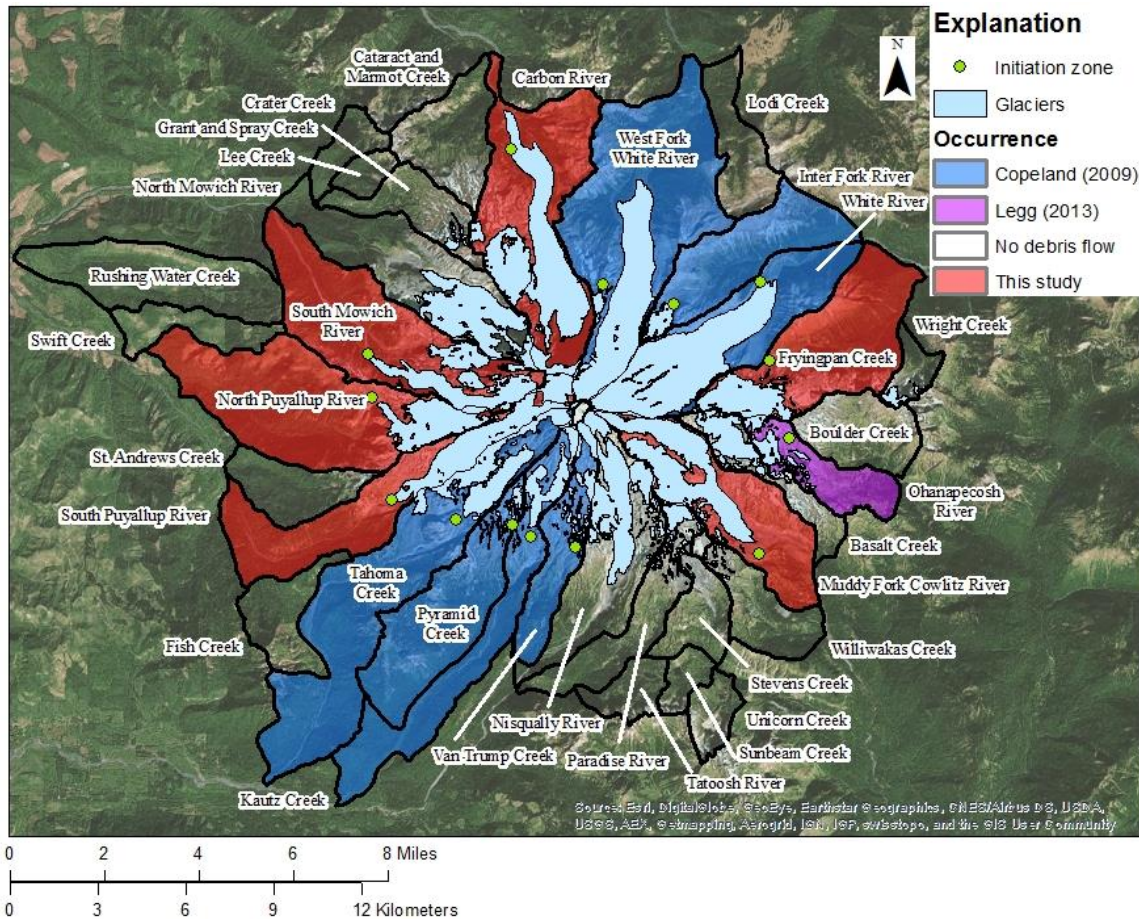


Figure 77. Colored drainages are drainages that experienced debris flows in 2006. Seven were added by this study and are shown in red. Initiation zones are shown in green.

A likely contribution comes from recent glacial recession. Steep, unstable moraines are exposed during glacial retreat. The material then becomes readily available for events like this and can contribute significant amounts of debris. I determined that there has been an average recession of 82.3 m from 1994 to 2007/2008, with a maximum of 262.9 m of parts of the South Mowich and Edmunds glaciers and 212.8 m from the Cowlitz-Ingraham Glacier.

Another factor contributing to initiation of debris flows on the east side of the mountain may stem from lower precipitation on a yearly basis. Normal, regular

precipitation can transport sediment in less catastrophic events. Smaller rainfall amounts may mean lower volumes of sediment transported regularly, which allows more sediment to remain in unstable moraine environments to be mobilized during larger rainfall events. The mountain received a yearly average of 21.9 cm of precipitation between 1995 and 2005, while the 2006 event delivered over twice that much in two days as determined from the PRISM data (PRISM Climate Group, 2007).

6.3 MRN

The Melton's Ruggedness Number is defined as an index for a basins ruggedness or average slope (Melton, 1965). All upper basins in this study have a MRN greater than 0.3, an average of 0.6 ± 0.2 , except for Swift Creek at 0.28, which indicates that they may all be capable of debris flows in the future if all other factors are appropriate for initiation (Jackson et al., 1987).

6.4 Initiation Sites

Copeland (2009) and Legg (2013) identified seven drainages with debris flows initiated in 2006: Inter Fork, Kautz, Ohanapecosh, Pyramid, Tahoma, Van Trump, and West Fork of the White River. All were initiated by proglacial gully expansion and bulking up (headless). West Fork of the White River was also initiated at least partially by a glacial lake outburst flood (Copeland, 2009). This study adds seven more debris flow initiations in 2006 to the dataset. A similar bulking up process occurred in Fryingpan, South Mowich, and South Puyallup. Carbon, Muddy Fork Cowlitz, North Puyallup, and White River drainages were partially initiated by landslides in regions close to the glacier. All of the landslides occurred in the upper regions of the sidewall of

the drainage, save for White River, which occurred in the cutbank of a small channel adjacent to Emmons Glacier.

Initiation site elevations range from 1442 m to 2448 m. Six of the thirteen sites are above 2000 m. Proglacial gully erosion initiated debris flows seem to occur at all elevations. Those debris flows initiated partially by landslides occurred between 1400 and about 1800 m, which are at lower elevations than the headless debris flows.

6.5 Statistical Analysis

There were two models that were generated that have the same accuracy, and the highest of all the models. Model 1 found that gradient, upper basin area and percent bedrock are most significant variables to initiation. Gradient seems counterintuitive at first glance, as drainages with higher gradients typically have higher erosion rates. The drainages that experienced debris flows have an average gradient of $37\% \pm 0.1\%$ while the non-debris flow producing drainages have a gradient of $28\% \pm 0.1\%$. A likely influence is recent glacial recession. Unstable material has only recently been exposed, and therefore erosion processes have not had enough time to entirely remove the material at typical erosion rates. There may be an excess of material ready for mobilizing in events like this. A possible explanation for the significance of basin area could be that, generally, in mountainous environments like the Cascade Range, basins with larger areas may have a large contribution of sediment and rainfall occurs over a larger area, which may mean a higher probability of sediment being mobilized. The average upper basin area for those basins with debris flows is $12.4 \text{ km}^2 \pm 8.5$, and those drainages without debris flows is $4.8 \text{ km}^2 \pm 3.5$. Percent bedrock is also not surprising, as the absence or

presence of bedrock plays a major control on debris flow initiation. More bedrock in a drainage basin would indicate a lower likelihood of initiation. The average for those drainages with initiation is $31\% \pm 10\%$ and for those without debris flow is $62\% \pm 21\%$. The ANOVA test determined that all three attributes are statistically different between non-producing debris flow basins and debris flow producing basins.

Model 2 found that MRN and percent bedrock are the most significant attributes to initiation. These variables are expected, as MRN is thought to be a good indicator of a drainages potential to produce debris flows (Melton, 1965). The average for those drainages with initiation is 0.77 ± 0.2 and for those without debris flows is 0.47 ± 0.14 . Percent bedrock was also found to be significant in Model 1 and is not surprising as described above. The ANOVA test determined that both attributes are statistically different between non-producing debris flow basins and debris flow producing basins. A map of the drainages that experienced debris flows in 2006 is shown in Figure 78.

Attributes that were expected to play a large role but did not include percent steep slopes, average vegetation, and percent glacier. Olson (2013) found that steep slopes were significant, Williams (2011) found that percent glacier was significant, and Pirot (2010) found that vegetation was significant. Additionally, steep slopes seem intuitive as material residing on steep slopes is more likely to mobilize. In the case of Mt. Rainier, glacial recession has exposed high amounts of material on steep slopes. In the case of glacier coverage, there were no basins with recorded debris flows that did not also have a large glacier occupying much of the area in the upper basin. If glacial recession and surface area reduction had been measureable across all drainages, I believe the model

could have found it to be a significant factor in debris flow initiation. Lastly, vegetation seems intuitive as vegetation has a tendency to hold material together. Most debris flow generating drainages have a lower percentage of vegetation growth in the upper basin. The ANOVA test determined that percent steep slopes was not statistically different between groups, while the other two are statistically different.

Both models had a slightly lower accuracy for Mt. Hood than what Pirot (2010) reported for the mountain. Pirot found that percent vegetation, gradient, and river connection with a glacier were the most significant attributes to debris flow initiation. This model had an accuracy of 91%. Model 1 (82%) for Mt. Rainier has a slightly better accuracy for Mt. Hood than Model 2 (73%). This is probably accounted for because gradient is included in Model 1 for Rainier and was a significant attribute for Mt. Hood. This application was not done by Pirot (2010), Williams (2011), or Olson (2012).

6.6 Glaciers

If percent surface area change had been measureable across all drainages, it may have been a large contributor to debris flow initiation. Glacial change varies around the mountain. Mt Rainier has seen a decrease of 14% in glacier area between 1987 and 2005 (Ellinger, 2010). Prior to this, Nylén (2004) documented a loss of 18.5% of glacial area between 1913 and 1972, which averages about 3% per year.

Three of the debris flow producing drainages documented by Copeland (2009), Inter Fork, Pyramid Creek, and Van Trump, experienced debris flows for the first time in 2006. All three of the glaciers in these drainages lost 28.6%, 60.5%, and 51.8% of their

debris-free ice, respectively, and all the initiation zones occur within the glacial recession boundaries of 1987 to 2005 (Ellinger, 2010).

Fryingpan is another drainage with little known recent debris flow history that is documented as having a debris flow in 2006 in this study. It experienced a 20% reduction in glacier surface area between 1994 and 2008. The initiation zone for this debris flow is documented at 1898 m. The initiation zone here is plotted somewhat lower in the drainage than other proglacial initiation zones because there was significant snow cover in the imagery used to collect evidence of erosion and debris flows. It is possible, however, that the initiation occurs further up in the drainage, closer to the current glacier terminus, which would put it within the glacier recession boundaries of 1994 to 2007.

Furthermore, only drainage basins that are directly connected to glaciers produced debris flows in 2006, indicating a strong connection between glaciers occupation in the upper basin and debris flow initiation.

6.7 Susceptibility Map

Since there were two models with the same accuracy and slightly different results, two susceptibility maps were generated for this study (Figure 78 and Figure 79). The drainages are color coded by converting the Y value generated by each model to a percentage of failure likelihood. The values were separated in four groups delineated by Williams (2011) and Olson (2012): 35% or less is very low and shown as green. 35-50% is low and shown as yellow. 51-65% is moderate and shown as orange, and greater than 65% is high and shown as red.

According to this distribution, Model 1 shows that nine drainages are characterized as very low susceptibility: Lee, Rushing Water, Swift Creek, St. Andrews, Fish, Paradise, Sunbeam, Williwakas, and Boulder Basins. Ten are characterized as low: Cataract and Marmont, Grant and Spray, Crater, Tatoosh, Unicorn, Stevens, Basalt, Wright, Inter Fork, and Lodi Basins. Five are characterized as moderate: North Puyallup, Pyramid, Van Trump, Muddy Fork Cowlitz, and Ohanapecosh Basins. Ten are characterized as high: Carbon, North Mowich, South Mowich, South Puyallup, Tahoma, Kautz, Nisqually, Fryingpan, White, and West Fork of the White Basins.

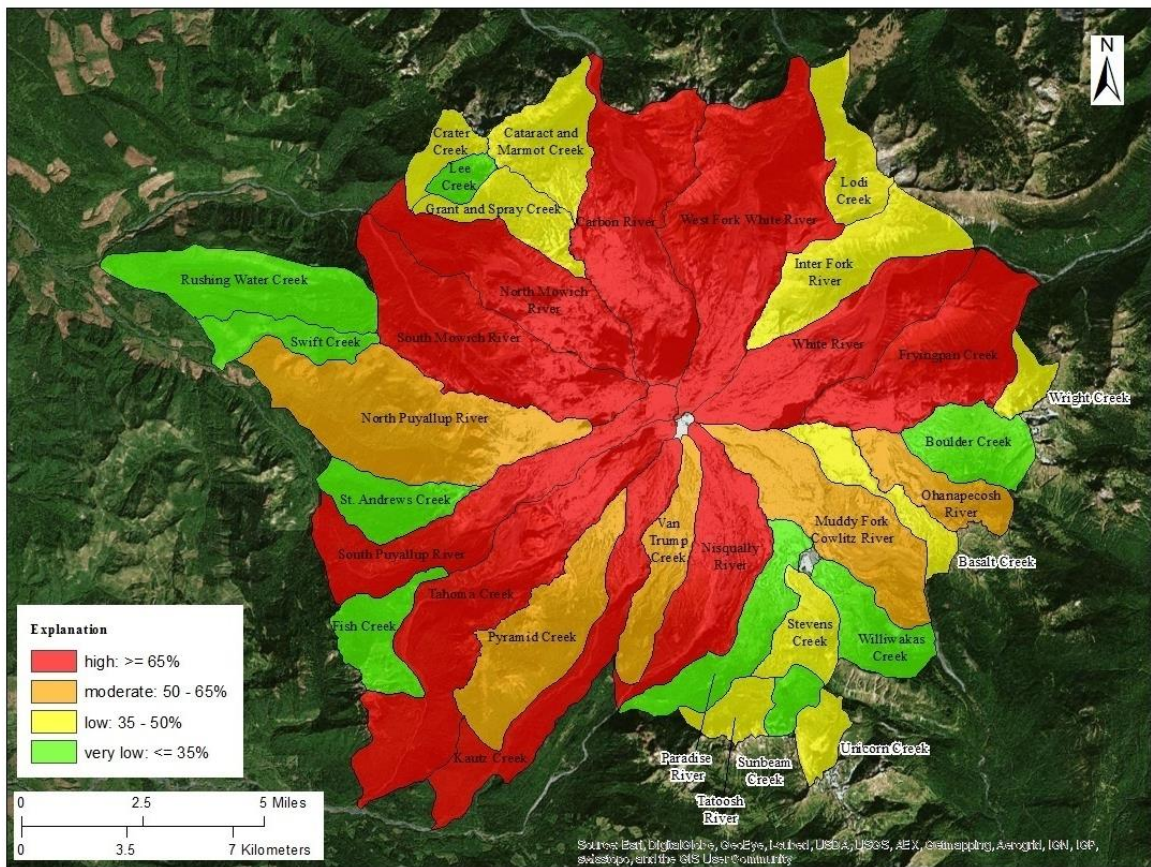


Figure 78. Susceptibility map for drainages on Mt. Rainier based on Model 1 results.

Model 2 shows that nine drainages are characterized as very low susceptibility: Crater, Lee, Rushing Water, Swift, St. Andrews, Fish, Tatoosh Sunbeam, and Boulder Basins. Nine are characterized as low: Cataract and Marmot, Grant and Spray, Paradise, Stevens, Unicorn, Williwakas, Wright, Inter Fork, and Lodi Basins. Six are characterized as moderate: Carbon, North Puyallup, Muddy Fork Cowlitz, Basalt, Ohanapecosh, and West Fork of the White Basins. Ten are characterized as high: North Mowich, South Mowich, White River, Frypan, North Puyallup, Van Trump, Nisqually, Muddy Fork Cowlitz, South Puyallup, and White River Basins.

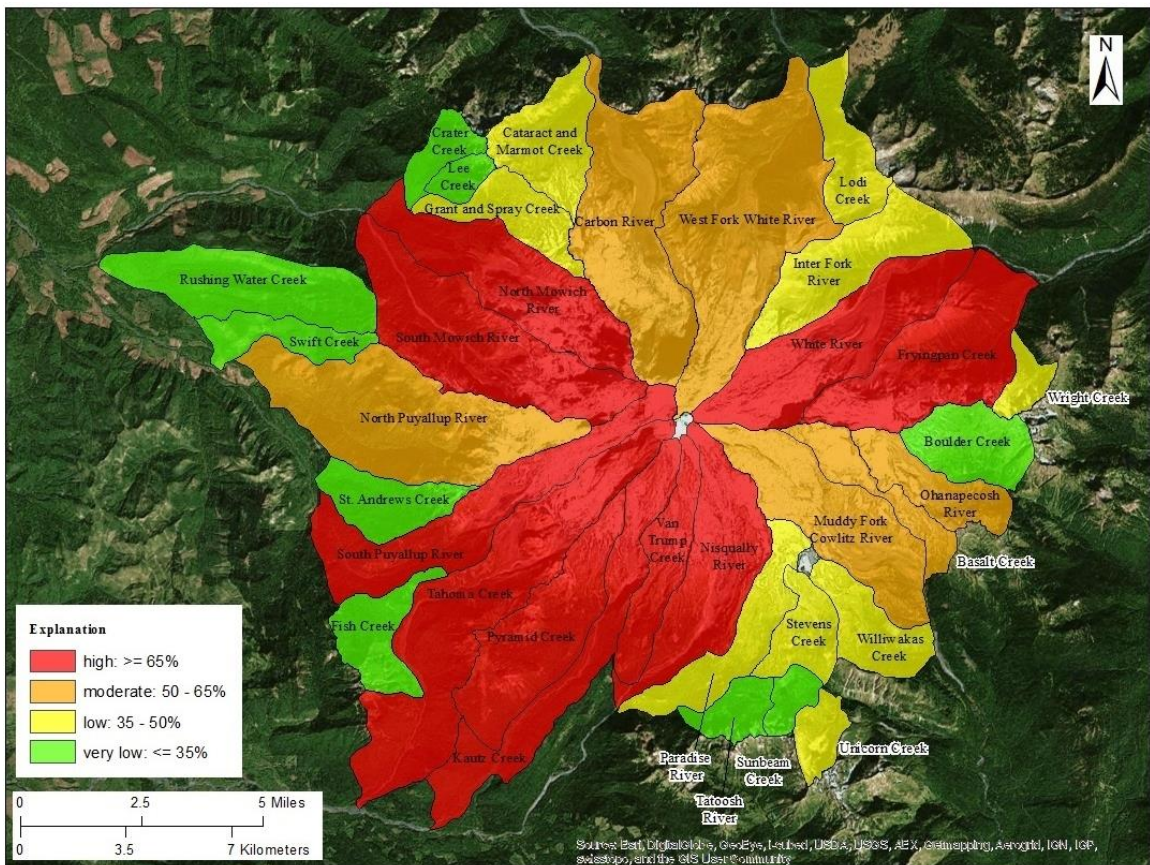


Figure 79. Susceptibility map for drainages on Mt. Rainier based on Model 2 results.

Nine drainages changed by one magnitude up or down between the models. They are listed in Table 8.

Table 8. Difference between models.

Drainage	Model 1	Model 2
Basalt	Low	Moderate
Carbon	High	Moderate
Crater	Low	Very Low
Paradise	Very Low	Low
Pyramid	Moderate	High
Tatoosh	Low	Very Low
Van Trump	Moderate	High
West Fork of the White	High	Moderate
Williwakas	Very Low	Low

Chapter 7: Conclusions

- Four drainages were run as both yes and no in the multiple regression and were determined all yes by the two most accurate regressions.
- Copeland (2009) and Legg (2013) identified seven drainages that had debris flow initiation in 2006: Inter Fork, Kautz, Ohanapecosh, Pyramid, Tahoma, Van Trump, and West Fork of the White Basins.
- This study identifies seven additional drainages that had debris flow initiation in 2006: Carbon, Fryingpan, Middy Fork Cowlitz, North Puyallup, South Mowich, South Puyallup, and White Basins.
- Of the 14 flows, 9 were initiated partially or entirely by proglacial gully erosion and expansion or headless: Fryingpan, South Mowich, South Puyallup, Inter Fork, Kautz, Ohanapecosh, Pyramid, Tahoma, Van Trump, and West Fork of the White.
- Carbon, Muddy Fork of the Cowlitz, North Puyallup, and White River were initiated partially by landslide failure in regions near the glacier.
- As determined in this study, and in previous studies, there is no single factor, like unstable moraine material acting as sediment supply and heavy rainfall, associated with debris flow initiation on Mt. Rainier.
- Mt. Rainier received 22-50 cm of rainfall during this event, the heaviest of which occurred on the west and northwest side of the mountain.
- All upper basins in this study have a MRN greater than 0.3, except for Swift Creek at 0.28, which indicates that they may all be capable of debris flow activity

in the future if all other factors are appropriate for initiation. The average for the mountain is 0.6 ± 0.2 .

- Of the 23 basin attributes that were able to have an ANOVA test done, 18 had measurably different means and five did not, measured at the 0.05 confidence level.
- Initiation site elevations range from 1442 m to 2448 m. Six of the thirteen sites are above 2000 m.
- Proglacial gully erosion initiated debris flows seem to occur at a wide range of elevations. Those debris flows initiated partially by landslides occurred between 1400 and about 1800 m.
- Only drainage basins that are directly connected to glaciers produced debris flows in 2006.
- Glacial retreat distance ranges from 85.8 m to 212.8 m. Additionally, surface area decrease ranges from 1.2 to 20.4% between 1996 and 2008.
- Two models, both with an accuracy of 91%, were generated for the mountain. The two models are very similar in terms of significant attributes contributing to debris flow initiation.
- Model 1 found gradient of the upper basin, upper basin area, and percent bedrock to be the most significant. It incorrectly predicted that Inter Fork did not have a debris flow and Nisqually and North Mowich did. The model predicted ten potential high drainages: Carbon, North Mowich, South Mowich, South Puyallup,

Tahoma, Kautz, Nisqually, Fryingpan, White, and West Fork of the White Basins. Of the remaining drainages five are moderate, ten are low, and nine are very low.

- Model 2 found MRN and percent bedrock to be the most significant variables. It incorrectly predicted that Basalt, Nisqually, and North Mowich had debris flows. The model predicted ten potential high drainages: North Mowich, South Mowich, South Puyallup, Tahoma, Pyramid, Kautz, Van Trump, Nisqually, Fryingpan, and White River Basins. Of the remaining drainages six are moderate, nine are low, and nine are very low.
- When comparing the models with Mt. Hood data, Model 1 had a predictive accuracy of 82% while Model 2 had an accuracy of 73%. Model 1 is likely more accurate because gradient is a variable used in that equation and was found significant by Pirot (2010), while Model 2 does not include significant variables from Pirot (2010).
- Both models had ten drainages predicted as high, eight of which were predicted by both models: White, Fryingpan, Nisqually, Kautz, Tahoma, South Puyallup, South Mowich, and North Mowich. Four are high in either Model 1 or Model 2: Carbon, West Fork of the White, Van Trump, and Pyramid.
- Six variables were used for the Mt. Hood, Mt. Adams, Mt. St. Helens, and Mt. Rainier combined regression; gradient, percent steep slopes, percent vegetation, MRN, connection with glacier, and percent ice/glacier. The regression found percent ice/glacier and percent vegetation to be the most significant variables, which are consistent with what Olson (2012) found.

- The resulting combined model had a 77% accuracy for the four volcanoes, increasing from the 69% accuracy from the combined regression done by Olson (2012).

Chapter 8: Future Work

The west side of the mountain is very remote, therefore more work should be done in those regions, like in North Mowich drainage, to identify prehistoric and historic debris flows to better improve the understanding of initiation on the mountain. This type of regression analysis can be useful for predicting other debris flows in similar settings. As technology advances, basin attribute collection will become more accurate and, therefore, more accurate models can be produced.

Debris flows play a major role in sediment transport on the mountain and as glacier retreat continues, more and more unstable material will be exposed as fuel to initiation of these events. Continued monitoring and evaluation is necessary to predicting events and building better infrastructure.

These methods can also be applied to models for the rest of Cascade volcanoes to make debris flow susceptibility maps for Glacier Peak, Mt. Baker, Mt. Jefferson, Three Sisters, and others. The Mt. Rainier model has an accuracy of 91% while the combined model for Mt. Hood, Mt. Adams, Mt. St. Helens, and Mt. Rainier is 72%.

References

- Agresti, A., 1996, An introduction to categorical data analysis: New York, John Wiley and Sons, Inc., p. 290.
- Brantley and Powers, 1985, Reports from the U.S. Geological Survey's Cascades Volcano Observatory at Vancouver, Washington: Earthquake Information Bulletin, v.17, n.1, January-February 1985, p.20.
- Cascade Volcano Observatory, 2014, Debris flows at Mount Rainier, Washington: USGS Cascade Volcano Observatory. (Accessed at http://volcanoes.usgs.gov/volcanoes/mount_rainier/geo_hist_debris_flows.html).
- Copeland, E., 2009, Recent periglacial debris flows from Mount Rainier, Washington: Master's Thesis, Oregon State University.
- Crandell, D. R., 1969, Surficial deposits geology of Mount Rainier National Park, Washington: US Geological Survey Bulletin 1288. (Accessed at http://www.cr.nps.gov/history/online_books/geology/publications/bul/1238/sec2.htm).
- Crandell, D. R., 1971, Postglacial lahars from Mount Rainier Volcano, Washington: US Geological Survey Professional Paper 667, 75 p (Also available at <http://pubs.usgs.gov/pp/0677/report.pdf>).
- Crandell, D. R., and Mullineaux, D. R., 1967, Volcanic hazards at Mount Rainier, Washington: Geological Society of America Bulletin 1238.
- Czuba, J. A., Magirl, C. S., Czuba, C. R., Curran, C. A., Johnson, K. H., Olson, T. D., Kimball, H. K., and Gish, C. C., 2012, Geomorphic analysis of the river response

- to sedimentation downstream of Mount Rainier, Washington: US Geological Survey, Open File Report 2012-1242.
- Davis, J. C., 2002, *Statistics and Data Analysis in Geology*, 3rd edition: New York, NY, pp. 638.
- Ellinger, J.R., 2010, *The changing glaciers of Mt. Hood, Oregon and Mt. Rainier, Washington—Implications of periglacial debris flows: Master’s Thesis*, Oregon State University.
- Fiske, R.S., Hopson, C.A., and Waters, A.C., 1963, *Geology of Mount Rainier National Park*, Washington: U.S. Geological Survey Professional Paper 444, 93 p.
- Godt, J. W., and Coe, J. A., 2007, Alpine debris flows triggered by a 28 July 1999 thunderstorm in the Central Front Range, Colorado: *Geomorphology* v. 84, pp 80-97.
- Gottschalk, J., Kousky, V., Higgins, W., and L’Heureux, M., 2005, Madden Julian Oscillation (MJO) summary: National Weather Service Climate Prediction Center. (Website accessed on February 21, 2013 at www.cpc.ncep.noaa.gov/products/precip/CWlink/MJO/MJO_summary.pdf)
- Grater, R.K., 1947, *Report on Kautz Creek Flood: National Park Service Memorandum*, pp. 1–3.
- Hosmer, D. W., and Lemshaw, S., 1989, *Applied Logistical Regression*: John Wiley & Sons Inc., New York, NY, pp 307.
- Iverson, R., 1997, The physics of debris flows: *Reviews of Geophysics*, v. 35, no. 3, p. 245-296.

- Jackson Jr., L. E., Kostaschuk, R. A., and MacDonald, G. M., 1987, Identification of debris flow hazard on alluvial fans in the Canadian Rocky Mountains: Reviews in Engineering Geology, v. VII, pp. 115-124.
- Kachigan, S.K., 1991, Multivariate Statistical Analysis—A Conceptual Introduction: Radius Press, New York, NY, 303 p.
- Legg, N., 2013, Debris flows in glaciated catchments—A case study on Mount Rainier, Washington: Master's Thesis, Oregon State University.
- Lewicki, P., and Hill, T., 2007, Statistics—Methods and Applications: Statsoft, Inc., 719 p.
- Melton, M. A., 1965, The geomorphic and paleoclimatic significance of alluvial deposits in Southern Arizona: Journal of Geology, v. 73, pp. 1-38.
- Matthes, F.E., 1928, Mount Rainier and its glaciers: United States Government Printing Office (accessed at http://www.nps.gov/history/history/online_books/mora/matthes/).
- Myers, B., and Brantley, S.R., 1995, Volcanic hazards fact sheet—Hazardous phenomena at volcanoes: USGS Open-File Report 95-231.
- NASA Earth Observatory, 2006, Record rain in the pacific northwest: NASA (accessed at <http://earthobservatory.nasa.gov/IOTD/view.php?id=7101>).
- National Oceanic and Atmospheric Administration (NOAA), 2005, NOAA catches a culprit behind western storms: accessed at <http://www.noaanews.noaa.gov/stories2005/s2367.htm>.

- Nylen, T. H., 2004, Spatial and temporal variations of glaciers (1913-1994) on Mt. Rainier and the relation with climate: Master's Thesis, Portland State University.
- Olson, K., 2012, Inventory and initiation zone characteristics of debris flows on Mount St. Helens, Washington initiated during a major storm event in November, 2006: Master's Thesis, Portland State University.
- Paterson, W. S. B., 1994, The Physics of Glaciers, 3rd Edition: Oxford, New York, 480 p.
- Pierson, T., 2005, Distinguishing between debris flows and floods from field evidence in small watersheds: US Geological Survey, Fact Sheet 2004-3142.
- Pirot, R., 2010, Initiation zone characterization of debris flows in November, 2006, Mount Hood, Oregon: Master's Thesis, Portland State University.
- PRISM Climate Group, Oregon State University (OSU), 2007, Average annual precipitate gridded data for the Continental United State from 1995 to 2006: Oregon State University. (Accessed at <http://www.prism.oregonstate.edu/>)
- Scott, K.M., and Vallance, J.W., 1995, Debris flow, debris avalanche, and flood hazards at and downstream from Mount, Rainier, Washington: Hydrologic Atlas 729, 9 p.
- Sisson, T., and Vallance, J., 2011, Living with a Volcano in Your Backyard—An Educators Guide, Appendix II—A Short History of Mount Rainier: U.S. Geological Survey GIP 19.
- Sobieszczyk, S., Uhrich, M.A., David, R., and Bragg, H.A., 2009, Analysis of geomorphic and hydrologic characteristics of Mount Jefferson debris flow, Oregon, November 6, 2006: Abstracts with Programs, October 2009, Geological Society of America, v. 41, no. 7, 499 p.

- Tilling, R.I, Topinka, L., and Swanson, D.A., 1990, Eruptions of Mount St. Helens—
Past, present, and future: U.S. Geological Survey Special Interested Publication,
56 p.
- Topinka, L., 1997, Major Cascade Range Volcanoes of Washington, Oregon, and
Northern California: USGS/CVO. (Also accessed at
http://vulcan.wr.usgs.gov/Volcanoes/Cascades/Maps/map_cascades_locationmap.html)
- US Geological Survey, 2008, Light detection and ranging (lidar) of Mount Rainier
National Park: US Geological Survey. (Accessed at <http://pubs.usgs.gov/ds/549/>.)
- US Geological Survey, Glaciers help to Shape Mount Rainier: US Geological Survey.
(Accessed at
http://volcanoes.usgs.gov/volcanoes/mount_rainier/mount_rainier_geo_hist_77.html).
- Vallance, J. W., and Scott, K. M., 1997, The Osceola Mudflow from Mount Rainier--
Sedimentology and hazard implications of a huge clay-rich debris flow:
Geological Society of America Bulletin, v. 109, no. 2, pp 143-163.
- Vallance, J.W., Cunico, M. L., and Schilling, S. P., 2003, Debris flow hazards caused by
hydrologic events at Mount Rainier, Washington: US Geological Survey, Open-
File Report 03-368.
- Vallance, J. W., Driedger, C. L., and Scott, W. E., 2002, Division meltwater from Kautz
Glacier initiates small debris flow near Van Trump Park, Mount Rainier,
Washington: Washington Geology, v. 30, no. 1/2, pp. 17-19.

- Walder, R. J., and Driedger, C. L., 1994a, Rapid geomorphic change caused by glacial outburst floods and debris flows along Tahoma Creek, Mount Rainier, Washington, U.S.A.: Arctic and Alpine Research, v. 26, no. 4, p 319-327.
- Walder, R.J., and Driedger, C.L., 1994b, Geomorphic change caused by outburst floods and debris flows at Mount Rainier, Washington, with emphasis on Tahoma Creek Valley: US Geological Survey, Water-Resources Investigations Report 93-4093.
- Washington Department of Natural Resources (DNR), Division of Geology and Earth Resources, 2010, Digital geology of Washington State at 1:100,000, version 3.0: WA DNR, Division of Geology and Earth Resources, Olympia, WA.
- Western Regional Climate Center, 2013, Climate of Washington: website accessed at <http://www.wrcc.dri.edu/narratives/WASHINGTON.htm>.
- Wilford, D.J, Sakals, M.E., Innes, J.L., Sidle, R.C., and Bergerud, W.A., 2004, Recognition of debris flows, debris floods, and flood hazard through watershed morphometrics: Landslides 1, p 61-66.
- Williams, K., 2011, Analysis and characterization of debris flows in November, 2006, Mount Adams, Washington: Master's Thesis, Portland State University.

Appendix A: Drainage Basin Data

Table A1. Station vs. PRISM data for each drainage for the two-day event.

Drainage	Station	Station (in)	PRISM (in)
Basalt Creek	COOP Paradise	17.9	11.7
Boulder Creek	NPS Sunrise	7.4	10.2
Carbon River	NPS Sunrise	7.4	11.9
Cataract and Marmot Creek	SNOTEL Mowich	0.6	11.7
Crater Creek	SNOTEL Mowich	0.6	10.4
Fish Creek	SNOTEL Paradise	2.6	10.6
Fryingpan	COOP Paradise	17.9	10.9
Grant and Spray Creek	SNOTEL Mowich	0.6	12.6
Inter Fork River	NPS Sunrise	7.4	10.2
Kautz Creek	COOP Paradise	17.9	13.0
Lee Creek	SNOTEL Mowich	0.6	11.5
Lodi Creek	NPS Sunrise	7.4	8.5
Muddy Fork Cowlitz River	COOP Paradise	17.9	12.3
Nisqually River	COOP Paradise	17.9	13.0
North Mowich River	SNOTEL Mowich	0.6	13.3
North Puyallup River	SNOTEL Mowich	0.6	13.1
Ohanapecosh River	COOP Paradise	17.9	10.9
Paradise River	COOP Paradise	17.9	12.8
Pyramid Creek	COOP Paradise	17.9	19.8
Rushing Water Creek	SNOTEL Mowich	0.6	9.1
South Mowich River	SNOTEL Mowich	0.6	13.5
South Puyallup River	COOP Paradise	17.9	13.2
St Andrews Creek	COOP Paradise	17.9	11.5
Stevens Creek	COOP Paradise	17.9	12.5
Sunbeam Creek	SNOTEL Paradise	2.6	12.2
Swift Creek	SNOTEL Mowich	0.6	9.2
Tahoma Creek	COOP Paradise	17.9	13.4
Tatoosh River	SNOTEL Paradise	2.6	12.2
Unicorn Creek	SNOTEL Paradise	2.6	11.9
Van Trump Fall Creek	COOP Paradise	17.9	13.1
West Fork White River	NPS Sunrise	7.4	10.5
White River	NPS Sunrise	7.4	11.1
Williwakas Creek	COOP Paradise	17.9	12.1
Wright Creek	NPS Sunrise	7.4	8.7

Table A2. Raw drainage basin data for the 34 drainages examined in this study (IZ = initiation zone).

Drainage	Had a debris flow	Total Basin Area (km²)	Upper Basin area (km²)	Percent Vegetation Coverage	Elevation of IZ (m)
Basalt Creek	no	6.5	5.1	1.0	N/A
Boulder Creek	no	8.9	1.8	5.3	N/A
Carbon River	yes	27.9	27.3	19.2	1484
Cataract and Marmot Creek	no	10.3	8.1	46.2	N/A
Crater Creek	no	3.8	2.4	65.2	N/A
Fish Creek	no	7.4	4.6	96.3	N/A
Fryingpan River	maybe	21.3	5.3	1.1	1898.1
Grant and Spray Creek	no	7.4	6.3	35.3	N/A
Inter Fork	yes	14.1	8.8	42.0	2209.7
Kautz Creek	yes	17.2	6.1	8.4	1959.8
Lee Creek	no	2.3	1.9	81.4	N/A
Lodi Creek	no	7.9	5.4	47.8	N/A
Muddy Fork Cowlitz River	maybe	19.0	14.6	3.6	1697.5
Nisqually River	no	17.7	14.0	16.2	N/A
North Mowich River	no	19.3	12.6	5.7	N/A
North Puyallup River	yes	29.5	10.8	10.7	1812.6
Ohanapecosh River	yes	8.0	5.1	11.5	2058.2
Paradise River	no	10.4	6.3	36.7	N/A
Pyramid Creek	yes	17.5	3.8	14.8	2243.6
Rushing Water Creek	no	16.3	5.5	91.6	N/A
South Mowich River	yes	25.3	13.5	12.4	1442.2
South Puyallup River	maybe	19.8	12.1	25.5	1573.4
St Andrews Creek	no	7.6	5.2	87.3	N/A
Stevens Creek	no	6.0	2.3	33.1	N/A
Sunbeam Creek	no	2.8	1.5	65.5	N/A
Swift Creek	no	6.0	3.2	99.4	N/A
Tahoma Creek	yes	32.8	12.6	12.2	2046.1
Tatoosh River	no	4.2	3.2	74.8	N/A
Unicorn Creek	no	3.7	2.9	41.6	N/A
Van Trump Creek	yes	9.0	5.3	4.7	2088
West Fork of the White River	yes	35.8	32.7	33.5	2448
White River	yes	20.5	15.7	3.1	1560
Williwakas Creek	no	7.8	1.8	6.4	N/A
Wright Creek	no	2.9	2.2	33.9	N/A

Drainage	Distance of IZ from glacier (m)	Highest elevation is Total Basin (m)	Lowest Elevation of Total Basin (m)	Highest elevation is Upper Basin (m)	Lowest Elevation of Upper Basin (m)
Basalt Creek	N/A	3394.5	1176.0	3394.5	1850.4
Boulder Creek	N/A	2335.3	1166.6	2335.3	1702.9
Carbon River	0	4304.1	873.1	4304.1	1021.5
Cataract and Marmot Creek	N/A	2205.2	885.3	2205.5	1123.9
Crater Creek	N/A	1993.3	862.3	1993.3	1391.6
Fish Creek	N/A	1842.6	790.3	1673.2	900.1
Fryingpan River	716	3215.5	1139.3	3215.5	1736.5
Grant and Spray Creek	N/A	2626.0	879.1	2626.0	1204.4
Inter Fork	45	2960.5	1252.9	2960.5	1501.5
Kautz Creek	301	4310.9	672.8	4310.9	1393.7
Lee Creek	N/A	1985.1	1181.4	1985.1	1362.1
Lodi Creek	N/A	2249.4	1060.8	2249.4	1546.3
Muddy Fork Cowlitz River	437	4280.0	1105.1	4267.2	1398.2
Nisqually River	N/A	4330.7	959.2	4330.7	1236.1
North Mowich River	N/A	4222.6	789.5	4222.6	1460.8
North Puyallup River	235	3167.3	709.2	3167.3	1052.1
Ohanapecosh River	363	2836.2	1140.3	2836.2	1549.7
Paradise River	N/A	2582.9	952.9	2582.9	1427.9
Pyramid Creek	58	3139.9	857.6	3139.9	1439.3
Rushing Water Creek	N/A	1713.0	545.5	1713.0	939.1
South Mowich River	41	4303.8	790.1	4303.8	1272.5
South Puyallup River	355	4384.8	843.1	4384.8	1214.9
St Andrews Creek	N/A	2104.9	830.0	2104.9	1165.8
Stevens Creek	N/A	2060.3	1093.0	2060.3	1407.9
Sunbeam Creek	N/A	1908.0	1092.3	1908.0	1401.4
Swift Creek	N/A	1742.7	658.8	1742.7	1237.6
Tahoma Creek	283	4380.9	631.0	4380.9	1294.6
Tatoosh River	N/A	2000.1	1153.1	2000.1	1361.2
Unicorn Creek	N/A	2109.0	1034.5	2109.0	1311.5
Van Trump Creek	20	4227.7	1013.8	4227.7	1684.2
West Fork of the White River	171	4392.6	1041.1	4392.5	1203.7
White River	31	4337.2	1269.2	4337.2	1468.1
Williwakas Creek	N/A	2165.0	1006.8	2165.0	1497.5
Wright Creek	N/A	2265.9	1211.4	2265.9	1487.9

Drainage	Height of Total Basin (m)	Height of Upper Basin (m)	Length of Total Basin (km)	Length of Upper Basin (km)	Gradient of Total Basin	Gradient of Upper Basin
Basalt Creek	2218.5	1544.1	8.7	6.4	25.5	24.1
Boulder Creek	1168.7	632.4	5.1	2.1	23.0	30.3
Carbon River	3431.0	3282.5	11.5	9.7	29.7	33.9
Cataract and Marmot Creek	1320.0	1081.6	5.2	4.1	25.5	26.6
Crater Creek	1131.0	601.7	4.1	2.0	27.8	29.5
Fish Creek	1052.3	773.0	4.3	2.1	24.4	36.1
Fryingpan River	2076.2	1479.0	10.5	3.8	19.8	38.9
Grant and Spray Creek	1746.9	1421.6	6.7	4.7	26.2	30.1
Inter Fork	1707.6	1459.1	8.5	6.1	20.1	23.8
Kautz Creek	3638.1	2917.2	16.6	6.0	21.9	48.9
Lee Creek	803.7	623.1	2.6	1.8	30.5	34.5
Lodi Creek	1188.6	703.1	6.2	3.8	19.2	18.6
Muddy Fork Cowlitz River	3174.9	2869.0	9.7	8.5	32.8	33.6
Nisqually River	3371.5	3094.6	10.9	7.3	30.9	42.4
North Mowich River	3433.1	2761.8	10.5	7.5	32.8	36.9
North Puyallup River	2458.0	2115.2	11.9	5.7	20.6	36.8
Ohanapecosh River	1696.0	1286.6	6.7	4.6	25.5	28.2
Paradise River	1630.1	1155.1	10.7	6.3	15.2	18.4
Pyramid Creek	2282.3	1700.6	11.5	4.1	19.9	41.7
Rushing Water Creek	1167.5	774.0	10.9	3.9	10.7	20.1
South Mowich River	3513.7	3031.3	12.5	6.7	28.0	45.0
South Puyallup River	3541.7	3169.9	14.4	8.9	24.6	35.4
St Andrews Creek	1274.9	939.1	6.0	4.2	21.1	22.3
Stevens Creek	967.2	652.3	4.8	3.0	20.3	21.5
Sunbeam Creek	815.7	506.6	3.6	2.0	22.4	25.1
Swift Creek	1084.0	505.1	6.5	3.8	16.7	13.4
Tahoma Creek	3750.0	3086.4	18.7	7.5	20.1	41.3
Tatoosh River	847.0	638.8	3.2	1.8	26.3	35.0
Unicorn Creek	1074.4	797.5	3.6	2.7	29.7	29.4
Van Trump Creek	3213.9	2543.5	9.4	5.5	34.3	46.1
West Fork of the White River	3351.5	3188.8	14.2	11.2	23.7	28.5
White River	3068.0	2869.2	10.7	8.3	28.6	34.5
Williwakas Creek	1158.2	667.5	5.9	2.4	19.7	28.0
Wright Creek	1054.6	778.0	3.7	2.3	28.7	33.6

Drainage	MRN for Total Basin	MRN for Upper Basin	Percent Bedrock in Upper	Percent Surficial deposits in Upper	Percent Glacier in Upper
Basalt Creek	0.87	0.68	50.7	0.0	43.6
Boulder Creek	0.39	0.47	100.0	0.0	0.0
Carbon River	0.65	0.63	21.9	36.2	41.4
Cataract and Marmot Creek	0.41	0.38	47.8	52.2	0.0
Crater Creek	0.58	0.39	63.7	18.0	0.0
Fish Creek	0.39	0.36	90.4	6.9	0.0
Fryingpan River	0.45	0.64	16.2	23.8	60.4
Grant and Spray Creek	0.64	0.57	48.3	47.2	4.5
Inter Fork	0.45	0.49	39.2	52.3	7.9
Kautz Creek	0.88	1.18	34.1	32.8	33.1
Lee Creek	0.53	0.45	78.1	23.4	0.0
Lodi Creek	0.42	0.30	33.1	66.9	0.0
Muddy Fork Cowlitz River	0.73	0.75	33.4	12.4	50.9
Nisqually River	0.80	0.83	31.6	23.3	34.7
North Mowich River	0.78	0.78	20.0	40.0	43.1
North Puyallup River	0.45	0.64	43.0	24.0	33.7
Ohanapecosh River	0.60	0.57	27.9	39.6	26.6
Paradise River	0.50	0.46	58.7	23.1	11.6
Pyramid Creek	0.54	0.87	37.5	40.7	13.3
Rushing Water Creek	0.29	0.33	95.4	2.9	0.0
South Mowich River	0.70	0.83	34.3	31.3	38.4
South Puyallup River	0.80	0.91	27.8	24.9	44.8
St Andrews Creek	0.46	0.41	84.1	15.4	0.0
Stevens Creek	0.39	0.43	49.2	49.1	1.3
Sunbeam Creek	0.49	0.41	70.8	24.7	0.0
Swift Creek	0.44	0.28	72.0	28.0	0.0
Tahoma Creek	0.65	0.87	30.7	33.3	36.0
Tatoosh River	0.42	0.36	64.5	33.5	0.0
Unicorn Creek	0.56	0.46	58.5	40.0	0.0
Van Trump Creek	1.07	1.10	40.9	25.4	26.5
West Fork of the White River	0.56	0.56	34.3	38.3	27.2
White River	0.68	0.72	6.1	21.6	71.3
Williwakas Creek	0.41	0.50	63.4	36.1	0.7
Wright Creek	0.62	0.52	52.2	34.1	13.3

Drainage	Connecti on to Glacier	Distance Stream to Glacier (m)	Percent Glacier Surface Area Change	Retreat Distance of Glacier (m)
Basalt Creek	TRUE	2312.8	-6.6	-67.9
Boulder Creek	FALSE	N/A	-100.0	-3.3
Carbon River	TRUE	0	-8.6	-92.3
Cataract and Marmot Creek	FALSE	N/A	-100.0	-565.1
Crater Creek	FALSE	N/A	N/A	N/A
Fish Creek	FALSE	N/A	N/A	N/A
Fryingpan River	TRUE	585.1	-20.4	-79.1
Grant and Spray Creek	TRUE	1154.4	-34.1	-35.0
Inter Fork	TRUE	0	-16.0	-108.3
Kautz Creek	TRUE	0	-3.3	-62.8
Lee Creek	FALSE	N/A	N/A	N/A
Lodi Creek	FALSE	N/A	N/A	N/A
Muddy Fork Cowlitz River	TRUE	0	-4.4	-212.8
Nisqually River	TRUE	0	-19.8	-168.5
North Mowich River	TRUE	0	-11.1	-262.9
North Puyallup River	TRUE	0	-11.1	-135.1
Ohanapecosh River	TRUE	0	-11.1	-35.7
Paradise River	TRUE	0	-32.0	-67.0
Pyramid Creek	TRUE	0	-15.8	-53.1
Rushing Water Creek	FALSE	N/A	N/A	N/A
South Mowich River	TRUE	0	-10.7	-98.1
South Puyallup River	TRUE	0	-4.2	-56.9
St Andrews Creek	FALSE	N/A	N/A	N/A
Stevens Creek	TRUE	0	8.0	48.9
Sunbeam Creek	FALSE	N/A	N/A	N/A
Swift Creek	FALSE	N/A	N/A	N/A
Tahoma Creek	TRUE	0	-10.4	-112.6
Tatoosh River	FALSE	N/A	N/A	N/A
Unicorn Creek	FALSE	N/A	N/A	N/A
Van Trump Creek	TRUE	0	-13.8	-57.5
West Fork of the White River	TRUE	0	-10.7	-53.9
White River	TRUE	0	-1.2	-85.8
Williwakas Creek	TRUE	533.7	13543.0	97.2
Wright Creek	TRUE	0	297667.0	291.3

Drainage	Average Annual Precipitation (cm)	Event Precipitation Sum (cm)	Total Precipitation at IZ (cm)	Peak Precipitation (cm)
Basalt Creek	25.3	29.6	N/A	20.9
Boulder Creek	20.9	26.0	N/A	18.5
Carbon River	21.4	30.2	32.7	20.5
Cataract and Marmot Creek	21.4	29.8	N/A	21.9
Crater Creek	18.0	26.5	N/A	19.8
Fish Creek	18.4	27.0	N/A	20
Fryingpan River	23.4	27.8	25.3	20.6
Grant and Spray Creek	24.2	32.1	N/A	22.3
Inter Fork	20.4	25.9	28.9	20.1
Kautz Creek	23.9	33.1	32.5	23.6
Lee Creek	19.8	28.3	N/A	20.5
Lodi Creek	15.4	21.7	N/A	16.5
Muddy Fork Cowlitz River	25.6	31.2	28.7	22
Nisqually River	23.7	33.0	N/A	22.4
North Mowich River	25.4	33.7	N/A	22.9
North Puyallup River	25.6	33.3	36.0	23.4
Ohanapecosh River	22.9	27.7	29.1	19.8
Paradise River	24.6	32.5	N/A	22.2
Pyramid Creek	24.2	50.4	36.1	23.6
Rushing Water Creek	13.8	23.0	N/A	15.6
South Mowich River	25.7	34.3	28.4	23.3
South Puyallup River	24.2	33.5	36.0	23.6
St Andrews Creek	19.9	29.1	N/A	22
Stevens Creek	24.1	31.7	N/A	21.9
Sunbeam Creek	22.8	30.9	N/A	21.4
Swift Creek	14.3	23.3	N/A	18.1
Tahoma Creek	25.0	34.1	36.0	23.8
Tatoosh River	22.8	31.0	N/A	21.5
Unicorn Creek	21.9	30.1	N/A	21.1
Van Trump Creek	23.3	33.4	33.8	22.9
West Fork of the White River	18.6	26.6	30.1	22.2
White River	22.7	28.3	25.3	22
Williwakas Creek	23.6	30.8	28.7	21.7
Wright Creek	16.0	22.0	N/A	16.3

Table A3. Average, standard deviation, maximum, and minimum for numerical attributes (IZ = initiation zone).

	Total Basin Area (km²)	Upper Basin area (km²)	Percent Vegetation Coverage	Elevation of IZ (m)	Distance of IZ from glacier (m)
average	13.4	7.9	34.5	1894.4	218.3
standard deviation	9.2	7.0	30.9	310.4	207.2
maximum	35.8	32.7	99.4	2448.0	716.0
minimum	2.3	1.5	1.0	1442.2	0.0

	Percent Steep Slopes in Upper	Highest elevation is Total Basin (m)	Lowest Elevation of Total Basin (m)	Highest elevation is Upper Basin (m)	Lowest Elevation of Upper Basin (m)
average	51.7	3002.3	960.8	2996.9	1360.2
standard deviation	19.5	1012.6	194.0	1018.4	218.6
maximum	87.6	4392.6	1269.2	4392.5	1850.4
minimum	13.7	1713.0	545.5	1673.2	900.1

	Height of Total Basin (m)	Height of Upper Basin (m)	Length of Total Basin (km)	Length of Upper Basin (km)	Gradient of Total Basin
average	2041.5	1636.7	8.5	5.0	24.3
standard deviation	1045.8	1019.1	4.1	2.5	5.4
maximum	3750.0	3282.5	18.7	11.2	34.3
minimum	803.7	505.1	2.6	1.8	10.7

	Gradient of Upper Basin	MRN for Total Basin	MRN for Upper Basin	Percent Bedrock in Upper	Percent Surficial deposits in Upper	Percent Glacier
average	31.5	0.6	0.6	48.9	29.56	19.5
standard deviation	8.5	0.2	0.2	23.3	15.3	21.1
maximum	48.9	1.1	1.2	100.0	66.9	71.3
minimum	13.4	0.3	0.3	6.1	0.0	0.0

	Distance Stream to Glacier (m)	Percent Change in Surface Area of Glacier	Retreat Distance of Glacier (m)	Average Annual Precipitation (cm)	Event Precipitation Sum (cm)
average	208.5	12948.9	-82.3	21.9	30.1
standard deviation	550.0	60707.8	147.2	3.4	5.1
maximum	2312.8	297667.0	291.3	25.7	50.4
minimum	0.0	-100.0	-565.1	13.8	21.7

	Total Precipitation at IZ (cm)	Peak Precipitation (cm)
average	31.2	21.1
standard deviation	3.8	2.1
maximum	36.1	23.8
minimum	25.3	15.6

Appendix B: ANOVA Results

Table B1. ANOVA analysis for all drainage basin attributes measurable across all drainages.

Total Basin Area						
<i>Groups</i>	<i>Count</i>	<i>Sum</i>	<i>Average</i>	<i>Variance</i>		
Debris flow	14	2.98 E+08	2.13 E+07	6.82E+13		
Non debris flow	20	1.59 E+08	7.95 E+06	2.36E+13		
ANOVA						
<i>Source of Variation</i>	<i>SS</i>	<i>df</i>	<i>MS</i>	<i>F</i>	<i>P-value</i>	<i>F crit</i>
Between Groups	1.45E+15	1	1.45E+15	34.9	1.41E-06	4.15
Within Groups	1.33E+15	32	4.17E+13			
Total	2.79E+15	33				
Upper Basin Area						
<i>Groups</i>	<i>Count</i>	<i>Sum</i>	<i>Average</i>	<i>Variance</i>		
Debris flow	14	1.74E+08	1.24E+07	7.18E+13		
Non debris flow	20	9.65 E+07	4.82 E+06	1.19E+13		
ANOVA						
<i>Source of Variation</i>	<i>SS</i>	<i>df</i>	<i>MS</i>	<i>F</i>	<i>P-value</i>	<i>F crit</i>
Between Groups	4.73E+14	1	4.73E+14	13.1	1.02E-3	4.15
Within Groups	1.16E+15	32	3.62E+13			
Total	1.63E+15	33				
Percent Vegetation						
<i>Groups</i>	<i>Count</i>	<i>Sum</i>	<i>Average</i>	<i>Variance</i>		
Debris flow	14	202	14.5	143		
Non debris flow	20	1.02 E+03	51.0	1.45 E+03		
ANOVA						
<i>Source of Variation</i>	<i>SS</i>	<i>df</i>	<i>MS</i>	<i>F</i>	<i>P-value</i>	<i>F crit</i>
Between Groups	1.10 E+04	1	1.10 E+04	12.0	1.56 E-03	4.15
Within Groups	2.94 E+04	32	919			
Total	4.04E+04	33				
Percent Steep Slopes						
<i>Groups</i>	<i>Count</i>	<i>Sum</i>	<i>Average</i>	<i>Variance</i>		
Debris flow	14	712	50.8	311		
Non debris flow	20	1.05 E+03	52.3	449		
ANOVA						
<i>Source of Variation</i>	<i>SS</i>	<i>df</i>	<i>MS</i>	<i>F</i>	<i>P-value</i>	<i>F crit</i>
Between Groups	18.8	1	18.4	0.0470	0.820	4.15

Within Groups	1.26 E+04	32	393
Total	1.26 E+04	33	

Highest elevation is Total Basin

<i>Groups</i>	<i>Count</i>	<i>Sum</i>	<i>Average</i>	<i>Variance</i>
Debris flow	14	5.42 E+04	3.87 E+03	4.03 E+05
Non debris flow	20	4.78 E+04	2.39 E+03	5.53 E+05

ANOVA

<i>Source of Variation</i>	<i>SS</i>	<i>df</i>	<i>MS</i>	<i>F</i>	<i>P-value</i>	<i>F crit</i>
Between Groups	1.81 E+07	1	1.81 E+07	36.8	8.94E-07	4.15
Within Groups	1.57E+07	32	4.92 E+05			
Total	3.38 E+07	33				

Lowest Elevation of Total Basin

<i>Groups</i>	<i>Count</i>	<i>Sum</i>	<i>Average</i>	<i>Variance</i>
Debris flow	14	1.33 E+04	953	4.54 E+04
Non debris flow	20	1.93 E+04	9.67 E+03	3.42 E+04

ANOVA

<i>Source of Variation</i>	<i>SS</i>	<i>df</i>	<i>MS</i>	<i>F</i>	<i>P-value</i>	<i>F crit</i>
Between Groups	1.54 E+03	1	1.54 E+03	0.040	0.843	4.15
Within Groups	1.24 E+06	32	3.88 E+04			
Total	1.24E+06	33				

Highest elevation is Upper Basin

<i>Groups</i>	<i>Count</i>	<i>Sum</i>	<i>Average</i>	<i>Variance</i>
Debris flow	14	5.42 E+04	3.87 E+03	4.02 E+05
Non debris flow	20	4.77 E+04	2.38 E+03	5.64 E+05

ANOVA

<i>Source of Variation</i>	<i>SS</i>	<i>df</i>	<i>MS</i>	<i>F</i>	<i>P-value</i>	<i>F crit</i>
Between Groups	1.83 E+07	1	1.83 E+07	36.7	9.15E-07	4.15
Within Groups	1.59 E+07	32	4.98 E+05			
Total	3.42 E+07	33				

Lowest Elevation of Upper Basin

<i>Groups</i>	<i>Count</i>	<i>Sum</i>	<i>Average</i>	<i>Variance</i>
Debris flow	14	1.92 E+04	1.37 E+03	4.52 E+04
Non debris flow	20	2.70 E+04	1.35 E+03	5.19 E+04

ANOVA

<i>Source of Variation</i>	<i>SS</i>	<i>df</i>	<i>MS</i>	<i>F</i>	<i>P-value</i>	<i>F crit</i>
Between Groups	4.27 E+03	1	4.27 E+03	0.087	0.77	4.15
Within Groups	1.57 E+06	32	4.92 E+04			

Total	1.58 E+06	33
-------	-----------	----

Height of Total Basin

<i>Groups</i>	<i>Count</i>	<i>Sum</i>	<i>Average</i>	<i>Variance</i>
Debris flow	14	4.09 E+04	2.92 E+03	5.28 E+05
Non debris flow	20	2.85 E+04	1.43 E+03	5.68 E+05

ANOVA

<i>Source of Variation</i>	<i>SS</i>	<i>df</i>	<i>MS</i>	<i>F</i>	<i>P-value</i>	<i>F crit</i>
Between Groups	1.84 E+07	1	1.84 E+07	33.4	2.05E-06	4.15
Within Groups	1.77 E+07	32	5.52 E+05			
Total	3.61 E+07	33				

Height of Upper Basin

<i>Groups</i>	<i>Count</i>	<i>Sum</i>	<i>Average</i>	<i>Variance</i>
Debris flow	14	3.50 E+04	2.50 E+03	5.38 E+05
Non debris flow	20	2.07 E+04	1.03 E+03	5.02 E+05

ANOVA

<i>Source of Variation</i>	<i>SS</i>	<i>df</i>	<i>MS</i>	<i>F</i>	<i>P-value</i>	<i>F crit</i>
Between Groups	1.77 E+07	1	1.77 E+07	34.3	1.64E-06	4.15
Within Groups	1.65 E+07	32	5.17 E+05			
Total	3.43 E+07	33				

Length of Total Basin

<i>Groups</i>	<i>Count</i>	<i>Sum</i>	<i>Average</i>	<i>Variance</i>
Debris flow	14	1.67 E+05	1.19 E+04	1.03 E+07
Non debris flow	20	1.23 E+05	6.16 E+03	7.56 E+06

ANOVA

<i>Source of Variation</i>	<i>SS</i>	<i>df</i>	<i>MS</i>	<i>F</i>	<i>P-value</i>	<i>F crit</i>
Between Groups	2.72 E+08	1	2.72E+08	31.4	3.39E-06	4.15
Within Groups	2.77 E+08	32	8.66 E+06			
Total	5.50 E+08	33				

Length of Upper Basin

<i>Groups</i>	<i>Count</i>	<i>Sum</i>	<i>Average</i>	<i>Variance</i>
Debris flow	14	9.67 E+04	6.90 E+03	4.86 E+06
Non debris flow	20	7.42 E+04	3.71 E+03	3.45 E+08

ANOVA

<i>Source of Variation</i>	<i>SS</i>	<i>df</i>	<i>MS</i>	<i>F</i>	<i>P-value</i>	<i>F crit</i>
Between Groups	8.40 E+07	1	8.40 E+07	20.9	6.87E-05	4.15
Within Groups	1.29E+08	32	4.02 E+06			
Total	2.13E+08	33				

Gradient of Total Basin						
<i>Groups</i>	<i>Count</i>	<i>Sum</i>	<i>Average</i>	<i>Variance</i>		
Debris flow	14	3.50	0.250	2.48E-3		
Non debris flow	20	4.77	0.238	3.28 E-3		
ANOVA						
<i>Source of Variation</i>	<i>SS</i>	<i>df</i>	<i>MS</i>	<i>F</i>	<i>P-value</i>	<i>F crit</i>
Between Groups	1.06 E-3	1	1.06 E-3	0.358	0.554	4.15
Within Groups	9.48 E-2	32	02.96 E-3			
Total	9.58 E-2	33				
Gradient of Upper Basin						
<i>Groups</i>	<i>Count</i>	<i>Sum</i>	<i>Average</i>	<i>Variance</i>		
Debris flow	14	5.17	0.369	5.28 E-3		
Non debris flow	20	5.56	0.278	5.48 E-3		
ANOVA						
<i>Source of Variation</i>	<i>SS</i>	<i>df</i>	<i>MS</i>	<i>F</i>	<i>P-value</i>	<i>F crit</i>
Between Groups	6.84 E-2	1	6.84 E-2	12.7	1.19 E-3	4.15
Within Groups	0.173	32	5.40 E-3			
Total	0.241	33				
MRN of Total Basin						
<i>Groups</i>	<i>Count</i>	<i>Sum</i>	<i>Average</i>	<i>Variance</i>		
Debris flow	14	9.22	0.658	3.06 E-2		
Non debris flow	20	10.4	0.521	2.42 E-2		
ANOVA						
<i>Source of Variation</i>	<i>SS</i>	<i>df</i>	<i>MS</i>	<i>F</i>	<i>P-value</i>	<i>F crit</i>
Between Groups	0.156	1	0.156	5.82	2.17 E-2	4.15
Within Groups	0.858	32	2.68 E-2			
Total	1.01	33				
MRN of Upper Basin						
<i>Groups</i>	<i>Count</i>	<i>Sum</i>	<i>Average</i>	<i>Variance</i>		
Debris flow	14	10.8	0.769	4.15 E-2		
Non debris flow	20	9.37	0.468	2.16E-2		
ANOVA						
<i>Source of Variation</i>	<i>SS</i>	<i>df</i>	<i>MS</i>	<i>F</i>	<i>P-value</i>	<i>F crit</i>
Between Groups	0.746	1	0.746	25.1	1.92E-05	4.15
Within Groups	0.950	32	2.97 E-2			
Total	1.70	33				

Percent Bedrock in Upper						
<i>Groups</i>	<i>Count</i>	<i>Sum</i>	<i>Average</i>	<i>Variance</i>		
Debris flow	14	430	30.7	106		
Non debris flow	20	1.24 E+3	61.8	449		
ANOVA						
<i>Source of Variation</i>	<i>SS</i>	<i>df</i>	<i>MS</i>	<i>F</i>	<i>P-value</i>	<i>F crit</i>
Between Groups	7.97 E+3	1	7.97 E+3	25.7	1.62E-05	4.15
Within Groups	9.92 E+4	32	310			
Total	1.79 E+4	33				

Percent Surficial deposits in Upper						
<i>Groups</i>	<i>Count</i>	<i>Sum</i>	<i>Average</i>	<i>Variance</i>		
Debris flow	14	440	31.4	99.3		
Non debris flow	20	566	28.3	439		
ANOVA						
<i>Source of Variation</i>	<i>SS</i>	<i>df</i>	<i>MS</i>	<i>F</i>	<i>P-value</i>	<i>F crit</i>
Between Groups	80.0	1	80.0	0.266	0.610	4.15
Within Groups	9.63 E+3	32	301			
Total	9.71 E+3	33				

Percent Glacier in Upper						
<i>Groups</i>	<i>Count</i>	<i>Sum</i>	<i>Average</i>	<i>Variance</i>		
Debris flow	14	512	36.5	288		
Non debris flow	20	155	7.74	225		
ANOVA						
<i>Source of Variation</i>	<i>SS</i>	<i>df</i>	<i>MS</i>	<i>F</i>	<i>P-value</i>	<i>F crit</i>
Between Groups	6.83 E+3	1	6.83 E+3	27.3	1.04E-05	4.15
Within Groups	8.02 E+3	32	251			
Total	1.49 E+4	33				

Average Annual Precipitation						
<i>Groups</i>	<i>Count</i>	<i>Sum</i>	<i>Average</i>	<i>Variance</i>		
Debris flow	14	327	23.3	4.30		
Non debris flow	20	416	20.8	13.8		
ANOVA						
<i>Source of Variation</i>	<i>SS</i>	<i>df</i>	<i>MS</i>	<i>F</i>	<i>P-value</i>	<i>F crit</i>
Between Groups	52.5	1	52.5	5.27	2.83 E-2	4.15
Within Groups	319	32	9.96			
Total	371	33				

Event Precipitation Sum						
<i>Groups</i>	<i>Count</i>	<i>Sum</i>	<i>Average</i>	<i>Variance</i>		
Debris flow	14	450	32.1	36.6		
Non debris flow	20	572	28.6	14.1		
ANOVA						
<i>Source of Variation</i>	<i>SS</i>	<i>df</i>	<i>MS</i>	<i>F</i>	<i>P-value</i>	<i>F crit</i>
Between Groups	102	1	102	4.38	4.43E-2	4.15
Within Groups	743	32	23.2			
Total	845	33				

Peak Precipitation						
<i>Groups</i>	<i>Count</i>	<i>Sum</i>	<i>Average</i>	<i>Variance</i>		
Debris flow	14	311	22.2	2.10		
Non debris flow	20	408	20.4	4.91		
ANOVA						
<i>Source of Variation</i>	<i>SS</i>	<i>df</i>	<i>MS</i>	<i>F</i>	<i>P-value</i>	<i>F crit</i>
Between Groups	28.7	1	28.7	7.63	9.44 E-3	4.15
Within Groups	121	32	3.77			
Total	149	33				

Appendix C: Regression Data

Table C 1. Raw data used for the regression analysis. Bolded drainages are those that were run as both "yes" and "no".

Drainage	Y	X1	X2	X3	X4	X5
Basalt Creek	0	0.97	74.0	0.24	0.68	1544.09
Boulder Creek	0	5.29	78.1	0.30	0.47	632.4
Carbon River	1	19.20	42.4	0.34	0.63	3282.53
Cataract and Marmot Creek	0	46.18	50.6	0.27	0.38	1081.63
Crater Creek	0	65.22	14.3	0.29	0.39	601.7
Fish Creek	0	96.31	48.7	0.36	0.36	773.02
Fryingpan River	1	1.08	78.9	0.39	0.64	1478.99
Grant and Spray Creek	0	35.28	34.4	0.30	0.57	1421.6
Inter Fork	1	41.96	55.0	0.24	0.49	1459.07
Kautz Creek	1	8.45	30.3	0.49	1.18	2917.22
Lee Creek	0	81.43	31.1	0.35	0.45	623.06
Lodi Creek	0	47.76	48.7	0.19	0.30	703.08
Muddy Fork Cowlitz River	1	3.55	57.7	0.34	0.75	2868.98
Nisqually River	0	16.16	40.9	0.42	0.83	3094.58
North Mowich River	0	5.68	63.9	0.37	0.78	2761.78
North Puyallup River	1	10.66	66.3	0.37	0.64	2115.16
Ohanapecosh River	1	11.48	64.7	0.28	0.57	1286.57
Paradise River	0	36.65	22.7	0.18	0.46	1155.08
Pyramid Creek	1	14.79	53.2	0.42	0.87	1700.64
Rushing Water Creek	0	91.59	77.3	0.20	0.33	773.99
South Mowich River	1	12.38	54.6	0.45	0.83	3031.31
South Puyallup River	1	25.49	41.7	0.35	0.91	3169.88
St Andrews Creek	0	87.32	51.2	0.22	0.41	939.1
Stevens Creek	0	33.14	87.6	0.21	0.43	652.33
Sunbeam Creek	0	65.50	62.6	0.25	0.41	506.6
Swift Creek	0	148.88	53.8	0.13	0.28	505.1
Tahoma Creek	1	12.19	42.3	0.41	0.87	3086.38
Tatoosh River	0	74.84	19.5	0.35	0.36	638.83
Unicorn Creek	0	41.63	52.1	0.29	0.46	797.45
Van Trump Fall Creek	1	4.65	73.8	0.46	1.10	2543.5
West Fork of the White River	1	33.54	13.7	0.28	0.56	3188.79
White River	1	3.07	37.3	0.35	0.72	2869.15
Williwakas Creek	0	6.36	83.0	0.28	0.50	667.49
Wright Creek	0	33.85	52.6	0.34	0.52	778

Drainage	X6	X7	X8	X9	X10	X11	X12	X13
Basalt Creek	5.1	50.7	0	43.6	100	25.3	29.6	20.9
Boulder Creek	1.8	100.00	0	0.0	0	20.9	25.6	18.5
Carbon River	27.3	21.9	36.2	41.4	100	21.4	30.3	20.5
Cataract and Marmot Creek	8.1	47.8	52.2	0.0	0	21.4	29.9	21.9
Crater Creek	2.4	63.7	18.0	0.0	0	18.0	26.5	19.8
Fish Creek	4.6	90.4	6.9	0.0	0	18.4	27.0	20
Fryingpan River	5.3	16.2	23.8	60.4	100	23.4	27.8	20.6
Grant and Spray Creek	6.3	48.3	47.2	4.5	100	24.2	32.1	22.3
Inter Fork	8.8	39.2	52.3	7.9	100	20.4	25.9	20.1
Kautz Creek	6.1	34.1	32.8	33.1	100	23.9	33.1	23.6
Lee Creek	1.9	78.1	23.4	0.0	0	19.8	28.3	20.5
Lodi Creek	5.4	33.1	66.9	0.0	0	15.4	21.7	16.5
Muddy Fork Cowlitz River	14.6	33.4	12.4	50.9	100	25.6	31.2	22
Nisqually River	14.0	31.6	23.3	34.7	100	23.7	33.0	22.4
North Mowich River	12.6	22.0	40.0	43.1	100	25.4	33.7	22.9
North Puyallup River	10.8	44.7	25.8	33.7	100	25.6	33.3	23.4
Ohanapecosh River	5.1	28.0	39.6	26.6	100	22.9	27.7	19.8
Paradise River	6.3	58.7	23.1	11.6	100	24.6	32.5	22.2
Pyramid Creek	3.8	37.5	40.7	13.3	100	24.2	50.4	23.6
Rushing Water Creek	5.5	95.4	2.9	0.0	0	13.8	23.0	15.6
South Mowich River	13.5	34.4	31.3	38.4	100	25.7	34.3	23.3
South Puyallup River	12.1	27.9	24.9	44.8	100	24.2	33.5	23.6
St Andrews Creek	5.2	84.1	15.4	0.0	0	19.9	29.1	22
Stevens Creek	2.3	49.2	49.1	1.3	100	24.1	31.7	21.9
Sunbeam Creek	1.5	70.8	24.7	0.0	0	22.8	30.9	21.4
Swift Creek	3.2	72.0	28.0	0.0	0	14.3	23.3	18.1
Tahoma Creek	12.6	30.7	33.4	36.0	100	25.0	34.1	23.8
Tatoosh River	3.2	64.5	33.5	0.0	0	22.8	31.0	21.5
Unicorn Creek	2.9	58.5	40.0	0.0	0	21.9	30.1	21.1
Van Trump Fall Creek	5.3	40.9	25.4	26.5	100	23.3	33.4	22.9
West Fork of the White River	32.7	34.3	38.3	27.2	100	18.57	26.6	22.2
White River	15.7	6.1	21.6	71.3	100	22.69	28.3	22
Williwakas Creek	1.8	63.5	36.1	0.7	100	23.63	30.8	21.7
Wright Creek	2.2	52.2	34.1	13.3	100	15.97	22.0	16.3

Table C 2. Normalized data used for the regression analysis.

Drainage	Y	X1	X2	X3	X4	X5	X6	X7
Basalt Creek	-0.82	-1.00	1.14	-0.87	0.40	-0.09	-0.40	0.08
Boulder Creek	-0.82	-0.88	1.35	-0.15	-0.56	-0.99	-0.87	2.20
Carbon River	1.18	-0.48	-0.48	0.28	0.16	1.61	2.75	-1.16
Cataract and Marmot Creek	-0.82	0.29	-0.06	-0.58	-0.94	-0.54	0.03	-0.05
Crater Creek	-0.82	0.84	-1.92	-0.24	-0.89	-1.02	-0.79	0.64
Fish Creek	-0.82	1.72	-0.15	0.54	-1.02	-0.85	-0.48	1.79
Fryingpan River	1.18	-1.00	1.39	0.86	0.22	-0.15	-0.37	-1.41
Grant and Spray Creek	-0.82	-0.02	-0.89	-0.16	-0.11	-0.21	-0.23	-0.03
Inter Fork	1.18	0.17	0.17	-0.91	-0.44	-0.17	0.12	-0.42
Kautz Creek	1.18	-0.79	-1.10	2.04	2.60	1.26	-0.26	-0.64
Lee Creek	-0.82	1.30	-1.06	0.35	-0.61	-0.99	-0.86	1.26
Lodi Creek	-0.82	0.34	-0.16	-1.51	-1.28	-0.92	-0.36	-0.68
Muddy Fork Cowlitz River	1.18	-0.93	0.30	0.24	0.70	1.21	0.94	-0.67
Nisqually River	-0.82	-0.57	-0.56	1.26	1.04	1.43	0.86	-0.75
North Mowich River	-0.82	-0.87	0.62	0.62	0.81	1.10	0.67	-1.16
North Puyallup River	1.18	-0.72	0.75	0.62	0.22	0.47	0.41	-0.18
Ohanapecosh River	1.18	-0.70	0.66	-0.39	-0.09	-0.34	-0.41	-0.90
Paradise River	-0.82	0.02	-1.49	-1.53	-0.58	-0.47	-0.24	0.42
Pyramid Creek	1.18	-0.60	0.08	1.18	1.24	0.06	-0.59	-0.49
Rushing Water Creek	-0.82	1.59	1.31	-1.34	-1.15	-0.85	-0.35	2.00
South Mowich River	1.18	-0.67	0.15	1.58	1.03	1.37	0.78	-0.63
South Puyallup River	1.18	-0.30	-0.51	0.45	1.41	1.50	0.59	-0.91
St Andrews Creek	-0.82	1.47	-0.03	-1.08	-0.80	-0.68	-0.39	1.51
Stevens Creek	-0.82	-0.08	1.84	-1.18	-0.70	-0.97	-0.81	0.01
Sunbeam Creek	-0.82	0.84	0.55	-0.75	-0.81	-1.11	-0.91	0.94
Swift Creek	-0.82	3.23	0.10	-2.12	-1.36	-1.11	-0.68	0.99
Tahoma Creek	1.18	-0.68	-0.48	1.14	1.22	1.42	0.67	-0.79
Tatoosh River	-0.82	1.11	-1.65	0.40	-1.04	-0.98	-0.67	0.67
Unicorn Creek	-0.82	0.16	0.02	-0.25	-0.56	-0.82	-0.71	0.41
Van Trump Fall Creek	1.18	-0.89	1.13	1.70	2.24	0.89	-0.37	-0.35
West Fork of the White River	1.18	-0.07	-1.95	-0.36	-0.15	1.52	3.51	-0.63
White River	1.18	-0.94	-0.74	0.35	0.58	1.21	1.11	-1.84
Williwakas Creek	-0.82	-0.85	1.60	-0.42	-0.43	-0.95	-0.87	0.63
Wright Creek	-0.82	-0.06	0.04	0.24	-0.32	-0.84	-0.81	0.14

Drainage	X8	X9	X10	X11	X12	X13
Basalt Creek	-1.93	1.14	0.73	1.02	-0.10	-0.11
Boulder Creek	-1.93	-0.92	-1.33	-0.30	-0.81	-1.24
Carbon River	0.44	1.03	0.73	-0.12	0.04	-0.30
Cataract and Marmot Creek	1.49	-0.92	-1.33	-0.13	-0.04	0.36
Crater Creek	-0.75	-0.92	-1.33	-1.15	-0.70	-0.63
Fish Creek	-1.48	-0.92	-1.33	-1.03	-0.60	-0.54
Fryingpan River	-0.37	1.93	0.73	0.45	-0.44	-0.26
Grant and Spray Creek	1.16	-0.71	0.73	0.69	0.40	0.54
Inter Fork	1.49	-0.55	0.73	-0.44	-0.83	-0.49
Kautz Creek	0.21	0.64	0.73	0.61	0.60	1.15
Lee Creek	-0.40	-0.92	-1.33	-0.61	-0.35	-0.30
Lodi Creek	2.45	-0.92	-1.33	-1.92	-1.65	-2.18
Muddy Fork Cowlitz River	-1.12	1.48	0.73	1.10	0.23	0.40
Nisqually River	-0.41	0.72	0.73	0.56	0.57	0.59
North Mowich River	0.69	1.11	0.73	1.06	0.72	0.83
North Puyallup River	-0.24	0.67	0.73	1.12	0.63	1.06
Ohanapecosh River	0.66	0.33	0.73	0.31	-0.47	-0.63
Paradise River	-0.42	-0.37	0.73	0.82	0.48	0.50
Pyramid Creek	0.73	-0.30	0.73	0.70	4.03	1.15
Rushing Water Creek	-1.74	-0.92	-1.33	-2.40	-1.40	-2.61
South Mowich River	0.12	0.89	0.73	1.13	0.83	1.01
South Puyallup River	-0.30	1.20	0.73	0.70	0.68	1.15
St Andrews Creek	-0.92	-0.92	-1.33	-0.58	-0.19	0.40
Stevens Creek	1.28	-0.86	0.73	0.67	0.32	0.36
Sunbeam Creek	-0.31	-0.92	-1.33	0.28	0.17	0.12
Swift Creek	-0.10	-0.92	-1.33	-2.25	-1.33	-1.43
Tahoma Creek	0.25	0.78	0.73	0.94	0.79	1.25
Tatoosh River	0.26	-0.92	-1.33	0.27	0.19	0.17
Unicorn Creek	0.68	-0.92	-1.33	0.03	0.01	-0.02
Van Trump Fall Creek	-0.27	0.33	0.73	0.42	0.66	0.83
West Fork of the White River	0.58	0.36	0.73	-0.98	-0.69	0.50
White River	-0.52	2.45	0.73	0.25	-0.34	0.40
Williwakas Creek	0.43	-0.89	0.73	0.53	0.15	0.26
Wright Creek	0.30	-0.30	0.73	-1.76	-1.59	-2.28

Table C 3. Iterations for Model 1. Bolded Coefficients and WALD values were removed as they possessed the lowest Wald value.

Regression 0		Regression 1		Regression 2		Regression 3	
Coef.	Wald	Coef.	Wald	Coef.	Wald	Coef.	Wald
β_1	0.066	β_1	0.085	β_2	0.457	β_3	1.727
β_2	0.507	β_2	0.526	β_3	2.006	β_6	1.199
β_3	1.078	β_3	1.959	β_6	1.611	β_7	0.671
β_5	0.043	β_6	1.613	β_7	0.898	β_9	1.191
β_6	0.380	β_7	0.950	β_9	0.740	β_{10}	0.949
β_7	0.897	β_9	0.651	β_{10}	0.576	β_{11}	1.235
β_9	0.402	β_{10}	0.634	β_{11}	1.260	β_{12}	0.908
β_{10}	0.514	β_{11}	0.683	β_{12}	0.925		
β_{11}	0677	β_{12}	0.680				
β_{12}	0574						
R²	0.620	R²	0.620	R²	0.618	R²	0.611
Regression 4		Regression 5		Regression 6		Regression 7	
Coef.	Wald	Coef.	Wald	Coef.	Wald	Coef.	Wald
β_3	1.647	β_3	3.549	β_3	3.178	β_3	5.649
β_6	1.593	β_6	1.914	β_6	2.617	β_6	5.517
β_9	2.770	β_9	1.826	β_9	1.621	β_{10}	5.498
β_{10}	1.906	β_{10}	2.302	β_{10}	1.891		
β_{11}	1.419	β_{11}	0.447				
β_{12}	1.152						
R²	0.601	R²	0.584	R²	0.578	R²	0.554
Regression 8		Regression 9					
Coef.	Wald	Coef.	Wald				
β_3	4.533	β_3	5.610				
β_6	2.816	β_6	3.078				
β_{10}	1.110	β_7	6.665				
β_7	2.100						
R²	0.584	R²	0.568				

Table C 4. Iterations for Model 2. Bolded Coefficients and WALD values were removed as they possessed the lowest Wald value.

Regression 0		Regression 1		Regression 2		Regression 3	
Coef.	Wald	Coef.	Wald	Coef.	Wald	Coef.	Wald
β_1	0.041	β_1	0.024	β_3	0.292	β_4	1.606
β_2	0.028	β_3	0.301	β_4	0.364	β_7	1.113
β_3	0.316	β_4	0.366	β_7	1.089	β_9	1.669
β_4	0.346	β_7	1.072	β_9	1.511	β_{10}	0.381
β_7	1.017	β_9	1.430	β_{10}	0.549	β_{11}	1.731
β_9	1.305	β_{10}	0.546	β_{11}	1.749	β_{12}	0.729
β_{10}	0.515	β_{11}	1.111	β_{12}	0.624		
β_{11}	1.046	β_{12}	0.483				
β_{12}	0.457						
R²	0.600	R²	0.599	R²	0.599	R²	0.595
Regression 4		Regression 5		Regression 6		Regression 7	
Coef.	Wald	Coef.	Wald	Coef.	Wald	Coef.	Wald
β_4	2.294	β_4	4.857	β_4	4.073	β_4	7.415
β_7	2.079	β_7	2.474	β_7	2.306	β_7	7.804
β_9	1.773	β_9	1.185	β_9	1.035		
β_{11}	1.452	β_{11}	0.810				
β_{12}	0.655						
R²	0.589	R²	0.579	R²	0.567	R²	0.553

Table C 5. Raw data from Mt. Hood applied to the models from Mt. Rainier to test predictive accuracy. Area, gradient, and percent bedrock were applied to Model 1 and percent bedrock and MRN were applied to Model 2.

Drainage	DF	Area	Gradient	Percent Bedrock	MRN
Elliot	1	3.3	0.23	3	0.85
Sandy	1	3.1	0.27	5	0.44
White	1	6.5	0.18	3	0.75
Newton	1	5.3	0.15	7	0.72
Clark	1	3.9	0.16	8	0.68
Salmon	1	1.4	0.23	0	0.43
Ladd	1	2.3	0.19	12	0.33
Zigzag	0	3.1	0.25	3	0.4
Polallie	0	7.9	0.17	1	0.46
Coe	0	2.9	0.25	9	0.53
Muddy	0	5.4	0.3	27	0.7

Table C 6. Normalized data from Mt. Hood applied to the models from Mt. Rainier to test predictive accuracy. Area, gradient, and percent bedrock were applied to Model 1 and percent bedrock and MRN were applied to Model 2.

Drainage	DF	Area	Gradient	Percent Bedrock	BR
Elliot	0.72	-0.41	0.28	-0.54	-0.54
Sandy	0.72	-0.51	1.09	-0.28	-0.28
White	0.72	1.23	-0.74	-0.54	-0.54
Newton	0.72	0.62	-1.35	-0.01	-0.01
Clark	0.72	-0.10	-1.14	0.12	0.12
Salmon	0.72	-1.39	0.28	-0.94	-0.94
Ladd	0.72	-0.92	-0.54	0.65	0.65
Zigzag	-1.26	-0.51	0.68	-0.54	-0.54
Polallie	-1.26	1.95	-0.94	-0.81	-0.81
Coe	-1.26	-0.62	0.68	0.25	0.25
Muddy	-1.26	0.67	1.70	2.64	2.64

Appendix D: Combined Regression Data

Table D 1. Raw data for all volcanoes. Y: debris flow (1 yes, 0 no) X1: Gradient. X2: Percent steep slopes in upper. X3: Percent vegetation in upper. X4: MRN for upper. X5: Stream has direct connection with glacier (1 for yes, 0 for no). X6: Percent ice/glacier in upper.

Volcano	Drainage	Y	X1	X2	X3	X4	X5	X6
St. Helens	Nelson Glacier	0	0.52	31.84	0	0.95	0	15.25
	Ape Canyon	0	0.5	38.67	0	1.24	0	38.73
	Muddy River	1	0.42	43.93	0.65	0.92	0	0
	Shoestring Glacier	1	0.37	51.39	0.7	1.16	0	18.57
	Pine Creek	1	0.4	33.55	1.2	0.87	0	0.1
	Worm Flows	0	0.34	33.13	0.44	1.09	0	1.28
	June Lake	1	0.38	43.38	0	1.52	1	24.97
	Swift Creek	0	0.42	36.16	3.2	0.83	0	13.59
	Snowfield	0	0.38	26.61	7.35	1.23	0	17.35
	Dryer Glacier	0	0.38	16.07	6.51	0.99	0	7.74
	Little Kalama	0	0.43	23.44	0	1.51	0	0
	Kalama	0	0.44	15.03	0	1.61	0	0
	Butte Camp Dome	1	0.47	35.53	0	0.83	0	0
	Blue Lake	1	0.43	33.53	2.18	1.13	0	0
	Sheep Creek	1	0.42	36.45	0.57	1.55	0	0
South Toutle	1	0.39	50.36	9.28	0.7	0	12.17	
Adams	Adams Creek	1	0.3	11	6	0.67	1	52
	Big Muddy	1	0.36	31	2	0.6	1	44
	Bird Creek	0	0.19	1	38	0.31	0	0
	Cascade Creek	0	0.37	11	6	0.78	1	19
	Crofton Creek	0	0.4	24	14	0.72	1	10
	East Fork	0	0.47	30	6	0.86	0	29
	Gotchen Creek	0	0.25	7	9	0.35	0	8
	Hellroaring Creek	0	0.29	16	29	0.49	1	22
	Horseshoe	0	0.36	8	0	0.8	0	6
	Killen Creek	0	0.23	3	18	0.43	0	11
	Lewis Creek	1	0.29	8	9	0.61	1	31
	Little Muddy	1	0.3	8	44	0.47	1	18
	Morrison Creek	0	0.36	9	6	0.7	0	11
	Muddy Fork	1	0.62	20	0	0.42	1	49
	Riley Creek	0	0.34	10	28	0.63	1	17
Rush Creek	1	0.4	25	9	0.75	1	26	
Salt Creek	1	0.38	22	0	0.79	1	39	
Trappers Creek	0	0.18	0	44	0.34	0	0	
Hood	Clark	1	0.16	27	27	0.68	1	27
	Coe	0	0.25	10	25	0.53	1	40
	Eliot	1	0.23	18	4	0.85	1	38
	Ladd	1	0.19	11	14	0.33	1	30

Hood	Muddy	0	0.3	12	32	0.7	1	34
	Newton	1	0.15	23	24	0.72	1	37
	Polallie	0	0.17	6	66	0.46	0	13
	Salmon	1	0.23	9	4	0.43	1	33
	Sandy	1	0.27	30	8	0.44	1	38
	White	1	0.18	42	0	0.75	1	24
	Zigzag	0	0.25	46	16	0.4	0	25
Rainier	Basalt Creek	0	0.24	74.0	0.97	0.68	100	43.6
	Boulder Creek	0	0.30	78.1	5.29	0.47	0	0.0
	Carbon River	1	0.34	42.4	19.20	0.63	100	41.4
	Cataract and Marmot Creek	0	0.27	50.6	46.18	0.38	0	0.0
	Crater Creek	0	0.29	14.3	65.22	0.39	0	0.0
	Fish Creek	0	0.36	48.7	96.31	0.36	0	0.0
	Fryingpan River	1	0.39	78.9	1.08	0.64	100	60.4
	Grant and Spray Creek	0	0.30	34.4	35.28	0.57	100	4.5
	Inter Fork	1	0.24	55.0	41.96	0.49	100	7.9
	Kautz Creek	1	0.49	30.3	8.45	1.18	100	33.1
	Lee Creek	0	0.35	31.1	81.43	0.45	0	0.0
	Lodi Creek	0	0.19	48.7	47.76	0.30	0	0.0
	Muddy Fork Cowlitz River	1	0.34	57.7	3.55	0.75	100	50.9
	Nisqually River	0	0.42	40.9	16.16	0.83	100	34.7
	North Mowich River	0	0.37	63.9	5.68	0.78	100	45.1
	North Puyallup River	1	0.37	66.3	10.66	0.64	100	33.7
	Ohanapecosh River	1	0.28	64.7	11.48	0.57	100	26.6
	Paradise River	0	0.18	22.7	36.65	0.46	100	11.6
	Pyramid Creek	1	0.42	53.2	14.79	0.87	100	13.3
	Rushing Water Creek	0	0.20	77.3	91.59	0.33	0	0.0
	South Mowich River	1	0.45	54.6	12.38	0.83	100	38.6
	South Puyallup River	1	0.35	41.7	25.49	0.91	100	44.8
	St Andrews Creek	0	0.22	51.2	87.32	0.41	0	0.0
	Stevens Creek	0	0.21	87.6	33.14	0.43	100	1.3
	Sunbeam Creek	0	0.25	62.6	65.50	0.41	0	0.0
	Swift Creek	0	0.13	53.8	148.88	0.28	0	0.0
	Tahoma Creek	1	0.41	42.3	12.19	0.87	100	36.0
Tatoosh River	0	0.35	19.5	74.84	0.36	0	0.0	
Unicorn Creek	0	0.29	52.1	41.63	0.46	0	0.0	

	Van Trump Fall Creek	1	0.46	73.8	4.65	1.10	100	26.5
Rainier	West Fork of the White River	1	0.28	13.7	33.54	0.56	100	27.2
	White River	0	0.35	37.3	3.07	0.72	100	71.3
	Williwakas Creek	0	0.28	83.0	6.36	0.50	100	0.7
	Wright Creek	0	0.34	52.6	33.85	0.52	100	13.3

Table D 2. Normalized data for all volcanoes. Y: debris flow. X1: Gradient. X2: Percent steep slopes in upper. X3: Percent vegetation in upper.X4: MRN for upper. X5: Stream has direct connection with glacier. X6: Percent ice/glacier in upper.

Volcano	Drainage	Y	X1	X2	X3	X4	X5	X6
St. Helens	Nelson Glacier	-0.89	1.95	-0.16	-0.78	0.80	-0.63	-0.24
	Ape Canyon	-0.89	1.75	0.16	-0.78	1.74	-0.63	1.07
	Muddy River	1.11	0.94	0.39	-0.76	0.71	-0.63	-1.09
	Shoestring Glacier	1.11	0.43	0.74	-0.76	1.48	-0.63	-0.06
	Pine Creek	1.11	0.73	-0.08	-0.74	0.55	-0.63	-1.09
	Worm Flows	-0.89	0.13	-0.10	-0.77	1.25	-0.63	-1.02
	June Lake	1.11	0.53	0.37	-0.78	2.64	-0.60	0.30
	Swift Creek	-0.89	0.94	0.04	-0.67	0.42	-0.63	-0.33
	Snowfield	-0.89	0.53	-0.39	-0.52	1.70	-0.63	-0.12
	Dryer Glacier	-0.89	0.53	-0.88	-0.55	0.93	-0.63	-0.66
	Little Kalama	-0.89	1.04	-0.54	-0.78	2.60	-0.63	-1.09
	Kalama	-0.89	1.14	-0.92	-0.78	2.92	-0.63	-1.09
	Butte Camp Dome	1.11	1.44	0.01	-0.78	0.42	-0.63	-1.09
	Blue Lake	1.11	1.04	-0.08	-0.71	1.38	-0.63	-1.09
	Sheep Creek	1.11	0.94	0.05	-0.76	2.73	-0.63	-1.09
South Toutle	1.11	0.63	0.69	-0.45	0.00	-0.63	-0.41	
Adams	Adams Creek	1.11	-0.28	-1.11	-0.57	-0.10	-0.60	1.81
	Big Muddy	1.11	0.33	-0.19	-0.71	-0.32	-0.60	1.36
	Bird Creek	-0.89	-1.40	-1.56	0.57	-1.25	-0.63	-1.09
	Cascade Creek	-0.89	0.43	-1.11	-0.57	0.26	-0.60	-0.03
	Crofton Creek	-0.89	0.73	-0.51	-0.29	0.07	-0.60	-0.53
	East Fork	-0.89	1.44	-0.24	-0.57	0.51	-0.63	0.53
	Gotchen Creek	-0.89	-0.79	-1.29	-0.46	-1.12	-0.63	-0.65
	Hellroaring Creek	-0.89	-0.38	-0.88	0.25	-0.67	-0.60	0.13
	Horseshoe	-0.89	0.33	-1.24	-0.78	0.32	-0.63	-0.76
	Killen Creek	-0.89	-0.99	-1.47	-0.14	-0.87	-0.63	-0.48
	Lewis Creek	1.11	-0.38	-1.24	-0.46	-0.29	-0.60	0.64
	Little Muddy	1.11	-0.28	-1.24	0.78	-0.74	-0.60	-0.09
	Morrison Creek	-0.89	0.33	-1.20	-0.57	0.00	-0.63	-0.48
	Muddy Fork	1.11	2.97	-0.70	-0.78	-0.90	-0.60	1.64
	Riley Creek	-0.89	0.13	-1.15	0.21	-0.22	-0.60	-0.14
Rush Creek	1.11	0.73	-0.47	-0.46	0.16	-0.60	0.36	
Salt Creek	1.11	0.53	-0.60	-0.78	0.29	-0.60	1.08	
Trappers Creek	-0.89	-1.50	-1.61	0.78	-1.16	-0.63	-1.09	
Hood	Clark	1.11	-1.70	-0.38	0.18	-0.06	-0.60	0.41
	Coe	-0.89	-0.79	-1.15	0.10	-0.55	-0.60	1.14
	Eliot	1.11	-0.99	-0.79	-0.64	0.48	-0.60	1.03
	Ladd	1.11	-1.40	-1.11	-0.29	-1.19	-0.60	0.58

Hood	Muddy	-0.89	-0.28	-1.06	0.35	0.00	-0.60	0.80
	Newton	1.11	-1.80	-0.56	0.07	0.07	-0.60	0.97
	Polallie	-0.89	-1.60	-1.33	1.56	-0.77	-0.63	-0.37
	Salmon	1.11	-0.99	-1.20	-0.64	-0.87	-0.60	0.75
	Sandy	1.11	-0.59	-0.24	-0.50	-0.83	-0.60	1.03
	White	1.11	-1.50	0.31	-0.78	0.16	-0.60	0.25
	Zigzag	-0.89	-0.79	0.49	-0.22	-0.96	-0.63	0.30
Rainier	Basalt Creek	-0.89	-0.88	1.77	-0.75	-0.05	1.60	1.34
	Boulder Creek	-0.89	-0.25	1.95	-0.60	-0.75	-0.63	-1.09
	Carbon River	1.11	0.12	0.32	-0.10	-0.23	1.60	1.22
	Cataract and Marmot Creek	-0.89	-0.63	0.70	0.86	-1.03	-0.63	-1.09
	Crater Creek	-0.89	-0.33	-0.96	1.53	-1.00	-0.63	-1.09
	Fish Creek	-0.89	0.34	0.61	2.64	-1.09	-0.63	-1.09
	Fryingpan River	1.11	0.63	1.99	-0.75	-0.19	1.60	2.28
	Grant and Spray Creek	-0.89	-0.27	-0.04	0.47	-0.43	1.60	-0.84
	Inter Fork	1.11	-0.91	0.90	0.71	-0.67	1.60	-0.65
	Kautz Creek	1.11	1.64	-0.22	-0.48	1.55	1.60	0.75
	Lee Creek	-0.89	0.18	-0.19	2.11	-0.79	-0.63	-1.09
	Lodi Creek	-0.89	-1.44	0.61	0.91	-1.28	-0.63	-1.09
	Muddy Fork Cowlitz Ri.	1.11	0.08	1.02	-0.66	0.17	1.60	1.74
	Nisqually River	-0.89	0.97	0.26	-0.21	0.41	1.60	0.84
	North Mowich River	-0.89	0.42	1.31	-0.58	0.25	1.60	1.42
	North Puyallup River	1.11	0.41	1.42	-0.40	-0.18	1.60	0.79
	Ohanapecosh River	1.11	-0.46	1.34	-0.38	-0.41	1.60	0.39
	Paradise River	-0.89	-1.45	-0.57	0.52	-0.77	1.60	-0.44
	Pyramid Creek	1.11	0.90	0.82	-0.26	0.56	1.60	-0.35
	Rushing Water Creek	-0.89	-1.29	1.92	2.47	-1.18	-0.63	-1.09
	South Mowich River	1.11	1.25	0.88	-0.34	0.41	1.60	1.06
	South Puyallup River	1.11	0.27	0.29	0.12	0.68	1.60	1.41
	St Andrews Creek	-0.89	-1.06	0.73	2.32	-0.93	-0.63	-1.09
	Stevens Creek	-0.89	-1.15	2.39	0.39	-0.86	1.60	-1.02
	Sunbeam Creek	-0.89	-0.78	1.24	1.54	-0.94	-0.63	-1.09
	Swift Creek	-0.89	-1.97	0.84	4.50	-1.34	-0.63	-1.09
	Tahoma Creek	1.11	0.86	0.32	-0.35	0.54	1.60	0.92
	Tatoosh River	-0.89	0.23	-0.72	1.87	-1.10	-0.63	-1.09
	Unicorn Creek	-0.89	-0.34	0.77	0.70	-0.76	-0.63	-1.09
	Van Trump Fall Creek	1.11	1.35	1.76	-0.62	1.29	1.60	0.39

West Fork of the White River	1.11	-0.44	-0.98	0.41	-0.46	1.60	0.42
White River	-0.89	0.18	0.09	-0.67	0.08	1.60	2.89
Williwakas Creek	-0.89	-0.49	2.17	-0.56	-0.66	1.60	-1.05
Wright Creek	-0.89	0.08	0.79	0.42	-0.58	1.60	-0.35

Table D 3. Iterations for combined regression. Bolded values are those removed from the analysis.

Regression 0		Regression 1		Regression 2		Regression 3	
Coef.	Wald	Coef.	Wald	Coef.	Wald	Coef.	Wald
β_1	0.095	β_1	0.096	β_2	0.548	β_3	1.523
β_2	0.407	β_2	0.579	β_3	1.678	β_4	0.618
β_3	1.726	β_3	1.750	β_4	0.552	β_6	9.179
β_4	0.629	β_4	0.638	β_6	8.911		
β_5	8.9E-5	β_6	8.862				
β_6	7.390						
R²	0.2385	R²	0.2385	R²	0.2375	R²	0.2318
Regression 4							
Coef.	Wald						
β_3	4.440						
β_6	8.637						
R²	0.2255						

Table D 4. Predictive model for combined regression. Bolded drainages are those that experienced a debris flow in 2006. Y values are either false positives or false negatives.

Mountain	Drainage	Y
St. Helens	Ape Canyon	0.63
	June Lake	0.57
	Shoestring Glacier	0.54
	Nelson Glacier	0.53
	Snowfield	0.52
	Swift Creek	0.51
	South Toutle	0.49
	Dryer Glacier	0.48
	Worm Flows	0.46
	Little Kalama	0.46
	Kalama	0.46
	Butte Camp Dome	0.46
	Sheep Creek	0.46
	Muddy River	0.46
Pine Creek	0.45	
Blue Lake	0.45	
Adams	Adams Creek	0.67
	Muddy Fork	0.67
	Big Muddy	0.65
	Salt Creek	0.63
	Lewis Creek	0.58
	East Fork	0.58
	Rush Creek	0.56
	Cascade Creek	0.53
	Hellroaring Creek	0.50
	Morrison Creek	0.49
	Horseshoe	0.48
	Riley Creek	0.48
	Gotchen Creek	0.47
	Crofton Creek	0.47
Killen Creek	0.47	
Little Muddy	0.45	
Bird Creek	0.38	
Trappers Creek	0.37	
Hood	Eliot	0.62
	Sandy	0.61
	Salmon	0.60
	Coe	0.59
	Newton	0.57
	White	0.57
Ladd	0.56	

Hood	Muddy	0.54
	Zigzag	0.54
	Clark	0.52
	Polallie	0.38
<hr/>		
	White River	0.75
	Fryingpan River	0.71
	Muddy Fork Cowlitz Ri.	0.67
	Basalt Creek	0.65
	North Mowich River	0.65
	South Puyallup River	0.61
	South Mowich River	0.61
	Carbon River	0.60
	Tahoma Creek	0.59
	Kautz Creek	0.59
	North Puyallup River	0.59
	Nisqually River	0.58
	Van Trump Fall Creek	0.57
	Ohanapecosh River	0.55
	West Fork of the White River	0.51
<hr/>		
	Pyramid Creek	0.49
Rainier	Williwakas Creek	0.45
	Wright Creek	0.45
	Boulder Creek	0.45
	Paradise River	0.43
	Inter Fork	0.41
	Grant and Spray Creek	0.40
	Stevens Creek	0.40
	Unicorn Creek	0.37
	Cataract and Marmot Creek	0.36
	Lodi Creek	0.36
	Crater Creek	0.33
	Sunbeam Creek	0.33
	Tatoosh River	0.31
	Lee Creek	0.30
	St Andrews Creek	0.29
	Rushing Water Creek	0.28
	Fish Creek	0.27
	Swift Creek	0.20
<hr/>		